Tu-Pos300

UNFOLDING OF YEAST PHOSPHOGLYCERATE KINASE MONITORED BY FLUORESCENCE INTENSITY AND ANISOTROPY DATA: FULL PICOSECOND DATA SETS OBTAINED ON THE MILLISECOND TIME SCALE. ((J. M. Beechem[1], M. A. Sherman[2], and M. T. Mas[2])) [1]Vanderbilt Univ., Nashville, TN, [2]Beckman Research Institute, City of Hope, Duarte CA.

Yeast Phosphoglycerate Kinase (PGK), is a well studied two domain hinge protein. Wild-type PGK (WT) contains two Trp residues (W308, W333) both in the carboxy-terminal domain. We are studying the WT, and a variety of single tryptophan containing mutants of PGK, in order to obtain a detailed understanding of the un-(re)folding kinetics of this enzyme. Single tryptophan mutants have been strategically placed within the amino-terminal domain (W48, W122), hinge region (W399, W194), and carboxyl domain (W308, W333). All of these mutants show large changes in the steady-state total-intensity and anisotropy upon unfolding. Stopped-flow studies of the amino terminal domain mutants, reveal that GuHCl concentrations could be found wherein almost a full change in steady-state total intensity could be obtained, with no corresponding anisotropy change. Combined analysis of the steady-state total-intensity and anisotropy stopped-flow data (Otto, Lillo, Beechem; Dec. 1994 *Biophys. J.*) reveal the presence of multiple unfolded intermediates. High resolution "double-kinetic" data, wherein picosecond anisotropy decays are obtained on the millisecond time-scale have now been collected. Utilizing a totally automated multiple-shot system, with enhanced high data rate capability, picosecond anisotropy decays with good signal to noise (>10,000 counts at the peak) can be obtained on the millisecond time-scale. New analysis programs are being developed to quantitatively analyze this data surface of: fluorescence vs. picoseconds vs. milliseconds vs. polarization state vs. emission wavelength in terms of internally consistent sets of folding models. This data allows one to directly address the photophysical origins of the complex signal changes which occur upon protein un(re)-folding. What is the origin of protein "dark-states," and partially folded "expanded-states?"

Tu-Pos301

PHOTOPHYSICAL AND HYDRODYNAMICS CHARACTERIZATION OF YEAST $p13^{suc1}$ BY TIME RESOLVED FLUORESCENCE SPECTROSCOPY. ((P. Neyroz, C. Menna, and L. Masotti)) Dipartimento di Biochimica *"G.Moruzzi"*, Università di Bologna, Italy.

The $p13^{suc1}$ acts in the fission yeast cell division cycle as a component of the $p34^{cdc2}$ protein kinase. It can suppress the catalytic defect of the mutant $p34^{cdc2}$ and inhibits $p34^{cdc2}$ tyrosine-15 dephosphorylation. p13 from *E.coli* has been purified and its intrinsic fluorescence parameters has been characterized. The protein has two tryptophans and seven tyrosines. In its native form, exciting at 295 nm, the $p13^{suc1}$ shows a fluorescence intensity maximum at 336 nm. The fluorescence decay of $p13^{suc1}$ is well described by three fluorescence lifetimes of 0.6 ns, 2.9 ns and 6.1 ns, respectively, with the longer component accounting for 64% of the total emitted flourescence. The medium and the long lifetime DAS are centered to 332 nm and 342 nm, respectively, corresponding to two different EDAS centered at 278 nm and 282 nm. Yet, time resolved and steady-state quenching experiments are consistent with the assignment of the predominant intrinsic emission to two distinct tryptophan rsidues. Upon acidic denaturation, the fluorescence intensity decreases of about 30% and its maximum is shifted to 355 nm. In addition, in the presence of increasing guanidine-HCl concentrations (0-0.4M) the relative amplitude of the shortest lifetime changes from 0.22 to 0.80. The decay of the fluorescence anisotropy of native $p13^{suc1}$ (at 20°C) revealed the contribution of two correlation times of 0.82 ns and 13 ns. This result is consistent with two rotational motions one due to the flexibility of the indole rings and one relative to the tumbling of the protein as a whole. SDS-PAGE and energy-transfer data obtained with FITC and lucifer yellow labelled p13, suggest that in solution the protein exists esclusively as a monomer. *Acknowledgment* This work was supported by C.N.R. Aimed Project A.C.R.O. n. 92.022 22 PF39 to L.M.. The *E.coli* [BL21(DE3)] p13-producing strain was generously provided by Dr. G.Draetta.

Tu-Pos302

MOBILITY AND POLARITY AT THE BOUNDARY OF BACTERIORHODOPSIN MEASURED BY TIME RESOLVED FLUORESCENCE ANISOTROPY OF SURFACE LABELS. ((H. Otto, H. Rosenhagen, U. Alexiev, T. Marti*, H.G. Khorana*, M.P. Heyn)). Biophysics Group, Freie Universität Berlin, D-14195 Berlin. *Dept. of Biology, MIT, Cambridge, MA 02139, USA.

Iodoacetamidofluorescein was selectively attached to a cysteine residue introduced by site directed mutagenesis at the extracellular side (T128C, V130C, S132C, Y133C, R134C, G72C) or at the cytoplasmic side (V101C, G231C) of bacteriorhodopsin (bR). The rotational correlation time (τ_R) of the fluorescein bound to the surface of bR-DMPC-CHAPS micelles and measured by the anisotropy r(t), increased from 50 ps for unbound fluorescein to more than 1 ns (e.g. a micro viscosity of up to 0.2 poise) and the rapid rotation is strongly hindered leading to a wobbling in-cone angle of 42-55 degrees. Both effects are explained by the DMPC and CHAPS molecules surrounding the protein partially also on the polar sides. The long τ_R-component (23 to 29 ns) corresponds to the rotation of a micelle containing a single bR molecule surrounded by a number of detergent and bound water molecules. Very different is the behaviour of fluorescein bound to the surface of native purple membranes. The hinderance is very small (fast $\tau_R \approx 200$ ps, $r(t \longrightarrow \infty) = 0$) leading to a viscosity of slightly more than for water and free rotation. The surface polarity was calculated from the spectral shift of the fluorescence and absorption maximum, comparing it with the spectral shift in mixtures of known polarity. While the surfaces of the micelles are more apolar than the water environment, the patch surfaces show comparable polarity.

Tu-Pos303

EXCITATION SPECTRA OF BIMANE-LABELED PROTEINS AS A NEW PROBE OF CONFORMATIONAL CHANGE. ((E.M.Kosower, M.Segev-Michael, S.Bachar and N.S.Kosower)) Biophys. Org. Chemistry Unit, School of Chemistry, Raymond & Beverly Sackler Faculty of Exact Sciences, and Department of Human Genetics, Sackler Faculty of Medicine, Tel-Aviv University, Tel-Aviv 69978 Israel

The excitation spectra for the strong fluorescence of bimanes in solution with the general formula [*syn*-(CH_3,Y)(CH_3,X)B] exhibit two broad maxima. These arise from an equilibrium mixture of two conformers, which differ in absorption maximum, quantum yield, and radiative rate. The ratio of conformers is solvent-sensitive; however, both conformers are present in solvents of both high and low polarity. Substituents also affect the conformer ratio. According to the relationship between dihedral angle and absorption maximum [D.Marciano, M.Baud'huin, B.Zinger, I.Goldberg, and E.M.Kosower, *J. Am. Chem. Soc.* 112, 7320-7328 (1990); E.M.Kosower, submitted], both conformers are non-planar, the short wavelength absorbing form designated as bent (B) and the long wavelength form as less bent (LB). The phenomenon creates the possibility of probing the conformation of proteins through measurement of the photophysical parameters, especially the excitation spectra. Bimane-labeled globin isolated from red blood cells treated with monobromobimane exhibits excitation spectra which vary with pH. At pH2, the long wavelength excitation maxima are at 372 (1)(em 470 nm) and 394 nm (1.36)(em 470 nm). At pH10, the maxima are at 359 (1)(em 442 nm) and 387 nm (0.97)(em 463 nm). Subtle changes in conformation may thus be followed. Binding of ligands may be followed with this new tool.

Tu-Pos304

EXTREMELY SLOW HYDROGEN-DEUTERIUM EXCHANGE IN *E. coli* ALKALINE PHOSPHATASE AS OBSERVED BY THE USE OF ROOM TEMPERATURE PHOSPHORESCENCE. ((Bruce D. Schlyer, Duncan G. Steel, Ari Gafni)) Institute of Gerontology, University of Michigan, Ann Arbor, MI 48109.

The room temperature phosphorescence of *E. coli* alkaline phosphatase Trp109 has been used to report on protein hydrogen-deuterium exchange. Upon dilution in D_2O the phosphorescence lifetime increases (at 20°C) in a biphasic manner with an immediate change (ca 30 seconds) followed by a slow change occurring on an extremely long timescale (days). At equilibrium the average phosphorescence lifetime is ca 20% larger in D_2O than in H_2O solutions. As the timescale of the initial lifetime change is long in comparison to established amide hydrogen-deuterium exchange rates in readily accessible protein regions, and since Trp109 is cloistered in the protein's core, the initial lifetime increase strongly suggests exchange-induced changes distant from the site of emission. On the other hand, the slow D_2O-induced growth in Trp109 lifetime exhibits first order kinetics (the rate of change being 0.012 min^{-1} at 66°C, for example) resulting from exchange reactions to highly protected protein groups. As the phosphorescence lifetime of Trp109 is dependent on local rigidity, the increase in apparent lifetime may reflect a change in alkaline phosphatase structure/stability or possibly be of a more fundamental nature. The observation of a two-fold decrease in the triplet state oxygen quenching constant with deuterium exchange is consistent with the former model. This first use of room temperature phosphorescence to monitor exchange shows promise as a sensitive and selective probe of protein core exchange dynamics. (Supported by NIA grant AG09761 and ONR contract N00014-91-J-1938.)

Tu-Pos305

THE USE OF TIME-RESOLVED CIRCULARLY POLARIZED FLUORESCENCE TO CHARACTERIZE EXCITED STATE DYNAMICS OF CAMPHORQUINONE COMPLEXED WITH METHYL-ETHYL KETONE ((J.A. Schauerte†§, T. Meade¶, B.D. Schlyer†, A. Gafni†§ & D.G. Steel†¶)) †Inst of Gerontology, §Dept of Biological Chemistry, ¶Dept of Physics and Electrical Engineering, Univ of Michigan, Ann Arbor, MI 48109

We have developed Time-Resolved Circularly Polarized Fluorescence (TR-CPF) instrumentation that allows us to observe the results of excited state dynamics of chromophores on the sub-nanosecond time scale. This technique provides additional information over existing steady-state excited state measurements which are complementary to ground state interactions probed by circular dichroism studies. In this work we utilized TR-CPF to demonstrate that the excited state optical activity of camphorquinone is highly dependent upon the ground state interactions of the chromophore. In the absence of ground state interactions, the enantomers of camphorquinone display time independent optical activity in their fluorescence that is approximately comparable to the ground state chirality measured by circular dichroism. In the presence of a ground state complex with non chiral methyl-ethyl ketone, formed by adding camphorquinone, the emission from the camphorquinone/methyl ethyl ketone complex shows a dramatic time dependent anisotropic emission that reverses sign during early times in the emission. The anisotropy is equal and opposite for the two camphorquinone enantomers. The ground state optical activity of free camphorquinone and camphorquinone complexed with methyl-ethyl ketone are not significantly different. The time dependent anisotropic emission is attributable to either induced optical activity of methyl-ethyl ketone luminscence or to altered excited state rearrangement of camphorquinone nuclear coordinates that reverses the sign of the emission chirality of the lowest singlet state. [NIA grant #AG09761 and ONR N00014-91-J-1938]

Tu-Pos306

EVIDENCE FOR THE INFLUENCE OF SOLVENT ON THE INTERNAL DYNAMICS OF E.COLI ALKALINE PHOSPHATASE FROM PHOSPHORESCENCE SPECTROSCOPY. **((L.Sun, *E.R. Kantrowitz and W.C. Galley)) Department of Chemistry, McGill University, Montreal, Quebec H3A 2K6, *Department of Chemistry, Boston College, Chestnut Hill, Mass. 02011.**

The phosphorescence of Trp 109 which lies buried below the active site in E.coli alkaline phosphatase decays exponentially at room temperature with a lifetime of about 2.0 seconds. With increasing temperature the decay remains exponential, but the lifetime shortens in an essentially linear manner. Interpreting these lifetimes in terms of a rate constant for internal fluctuations within the enzyme an Arrhenius plot can be contructed which is distinctly non-linear. The steeper slope observed at higher temperatures implies that the activation barrier for local fluctuations in the enzyme increases with temperature. Applying *transition-state theory* and assuming a larger Cp for the transition state than for the native state, results in both an activation ΔH and ΔS that are temperature dependent. The data can be readily accounted for with an activation ΔCp = 1300 J $mol^{-1}K^{-1}$. The parameters obtained from the fit are compared with those observed for the kinetics and thermodynamics of complete unfolding or denaturation. The comparison suggests that while hydrophobic hydration plays a less significant role in determining the dynamics of the protein interior, it is nonetheless involved.

Tu-Pos307

NOVEL EXCITED-STATE PHENOMENA AS FLUORESCENCE PROBES OF PROTEINS. ((A. Sytnik and M. Kasha)) Institute of Molecular Biophysics, Florida State University, Tallahassee, FL 32306-3015. (Spon. by R. Rill)

We employ molecules exhibiting three excited-state phenomena as fluorescence probes of proteins: (i) intramolecular proton transfer (PT); (ii) intramolecular charge transfer (CT) and (iii) R^{-3}-R^{-6} - coupled intermolecular energy transfer. PT in 4-hydroxy-5-azaphenanthrene (HAP) is followed by fluorescence observed in the 600 nm spectral region grossly wavelength-shifted from its UV absorption (onset at 400 nm). This chromophore has a fluorescence lifetime of 0.358 ns in cyclohexane and 0.497 ns in methanol. We have applied HAP as a PT-fluorescence probe of binding-site static polarity to human serum albumin and apo-myoglobin. Another molecule, diethylamino-3-hydroxyflavone (DHF), which combines CT and PT electronic transitions, extends the possibilities of fluorescence applications for biomolecules due to the existence of the two observable emissions from the S_1 and S_1' states. This offers the following additional determinations in comparison with commonly used probes: (i) fluorescence lifetime of the PT tautomer (nanoseconds); (ii) rate of the PT tautomer formation (subpicoseconds-picoseconds); (iii) rate of the back PT transfer (subpicoseconds-picoseconds); (iv) the ratio between the PT and CT exited state formation and their comparable fluorescence intensities. We have studied the fluorescence of DHF-rat serum albumin complex as an example of the PT, CT excitation competition. We have a special interest in expanding the *photon-antenna , energy-trap* strategy to the spectroscopic investigation of biopolymers (*antenna* molecules coupled by excitonic R^{-3} dependence, with a final trapping step with R^{-6} dependence in a covalently-bonded *antenna* molecule, acceptor molecule pair - which acts as the *antenna-trap* coupler). We have applied this approach to the complexes of serum albumins with dansyl-tryptophan as the *probe-antenna pair,* for tryptophans as the antenna molecules.

Tu-Pos308

ON THE CONTRIBUTION OF ELECTRON TRANSFER REACTION TO THE QUENCHING OF TRYPTOPHAN FLUORESCENCE. (Carla Goldman, Pedro Pascutti, Paulo Piquini and Amando Ito) Inst. Física, Universidade de São Paulo, CP 20516, CEP 01452-990, SP, Brasil.

Within the Born-Oppenheimer approximation, a theoretical calculation of electron transfer (e.t.) reactions rates for excited state of zwitterionic Trp is presented for each of its six rotameric forms. For the electronic part, analytical expressions of the relevant transition matrix element are obtained using the Renormalized Perturbation Expansion[1]. The vibrational part is fitted on experimental data, assuming that measures of fluorescence intensity decay are averages over two competing populations: one in which fluorescence have been accompained by e.t. and one that have been not. Complementary data, namely, ionization potentials and charge distributions are obtained using an *ab-initio* numerical calculation of molecular orbitals. Our results indicate that conformer anti$\chi_2 g^-$ gives the main contribution to e.t. in the time scale of fluorescence. Ref.: C.Goldman, Phys. Rev. A43, 4500 (1991).

Financial support: FAPESP, CNPq and FINEP.

Tu-Pos309

TFE QUENCHES TRYPTOPHAN FLUORESCENCE BY EXCITED-STATE PROTON TRANSFER. ((Yu Chen, Bo Liu, and Mary D. Barkley)) Department of Chemistry, Louisiana State University, Baton Rouge, LA 70803-1804. (Spon. by J. Nelson)

2, 2, 2- Trifluoroethanol (TFE) is best known as a structure-promoting solvent for peptides. The pure solvent has a large quenching effect on indole fluorescence. Fluorescence quantum yields of 3-methylindole, indole, and NATA in TFE are 0.022, 0.033, and 0.029, an order of magnitude less than in water. Lifetimes of these compounds in TFE drop proportionally. Solvent quenching by TFE is much less temperature-dependent compared to water. The activation energies in TFE are about 1.4 kcal/mol with frequency factors in the range of 10^{10} s^{-1}. A 3-fold deuterium isotope effect on fluorescence quantum yield and lifetime was found in TFE, suggesting a proton transfer reaction in the excited-state which was confirmed by photochemical H-D exchange experiments. H-D exchange was readily observed for all aromatic carbon hydrogens except positions 5 and 6 of the indole ring. The reaction quantum yield of deuterium exchange was 0.47 ± 0.11. The proton transfer yield in TFE was estimated from this value to be 0.71 ± 0.18. The proton transfer rate is discussed in terms of proton donation ability of solvent. The implications for TFE as a solvent probe of tryptophans in proteins are also discussed.
(Supported by NIH Grant GM 42101)

Tu-Pos310

EFFECT OF PROTON-TRANSFER AND PACKING ON THE STABILITY OF THIOREDOXIN: FLUORESCENCE AND MINIMUM PERTURBATION MAPPING STUDIES ((Christopher Haydock, Norberto D. Silva, Jr. and Franklyn G. Prendergast)) Department of Pharmacology, Mayo Foundation, Rochester, Minnesota 55905.

Time resolved fluorescence intensity decay spectra of oxidized and reduced *Escherichia coli* thioredoxin suggest that the active-site side chains aspartate-26, tryptophan-28, and lysine-57 may be conformationally disordered. Hydrogen exchange and near-UV circular dichroism measurements hint that reduced thioredoxin is in a highly-ordered molten globule state. Aspartate-26 has an unusually high pK_a of around 7.5, which seems to explain the stability as a function of pH of oxidized thioredoxin. In reduced form redox-active cysteine-32 has a somewhat low pK_a of around 7.0. A quantitative atomic level model of the stability of oxidized and reduced thioredoxin evidently must include multiple conformations of side chains in various states of ionization. We present such a model by minimum perturbation mapping of selected active-site side chains. Ionization effects are included with the inducible multipole solvation model. Our results also offer a method of modeling the pH dependence of the lifetimes and preexponential factors in the intensity decay spectra. This work is supported in part by GM 34847.

Tu-Pos311

RESOLUTION OF THE PROPERTIES OF HYDROGEN-BONDED TYROSINE USING A TRILINEAR MODEL OF FLUORESCENCE ((Jinkeun Lee and Robert T. Ross)) Biophysics Program and Department of Biochemistry, The Ohio State University, Columbus, OH 43210.

The fluorescence of any dilute specimen is separately linear in functions of each of the independent variables excitation wavelength, emission wavelength, and any treatment which alters concentration or fluorescence quantum yield. The resulting trilinear models have a structure that permits the mathematical dissection of spectra from complex specimens without the use of any other information about the properties of the specimen. Using this technique, the steady-state fluorescence of aqueous N-acetyl-L-tyrosinamide(NAYA) in the presence of eight ligands was resolved into three components, corresponding to normally solvated side chain, side chain hydrogen-bonded to the added ligand, and impurity. The ligands were acetate(Ac), imidazole(Im), tris[hydroxymethyl]aminomethane(Tris), phosphate monoanion(P1), phosphatedianion(P2), N-methylacetamide(MA), N,N-dimethylacetamide(DMA), and urea. The excitation spectrum of the hydrogen-bonded complex is red-shifted about 2 nm except 3 nm for MA and 5 nm for DMA. The emission maximum of the complex is 300 nm for MA, DMA, and urea, 310 nm for P1, 320 nm for Ac, 330 nm for P2, and 335 nm for Im and Tris. The dissociation constants in aqueous solution are 0.2~0.3 M for Ac, P2, Im, and Tris, 3.3 M for P1, 2.7 M for urea, 3.5 M for MA, and 5.5 M for DMA. Nonaqueous NAYA in the presence of urea, MA, and DMA shows further red-shifts of the excitation spectra, but no emission spectral shift. The dissociation constants decrease to 0.3~0.9 M in nonaqueous solution. The temperature dependence of the dissociation constants is small, giving a ΔH for complex dissociation between -0.8 and 0.0 kcal/mol.

Tu-Pos312

THE *TRUE* ^1L_a ORIGIN OF INDOLE DEDUCED FROM JET SPECTRA OF COMPLEXES, AR MATRIX SPECTRA AND CALCULATED VIBRONIC SPECTRA. **((Pedro L. Muiño, Bruce Fender, James Vivian, Lee S. Slater and Patrik Callis*)) Department of Chemistry and Biochemistry, Montana State University, Bozeman, MT 59717.**

Of the several ^1L_a lines interspersed in the ^1L_b manifold of jet-cooled indole, identified using polarized two-photon fluorescence excitation, the lowest two (at 455 and 480 cm^{-1} above the dominant ^1L_b origin) now appear to be a false origin, split by Fermi resonance. Complexing with methanol collapses the pair, but does not cause a shift relative to known ^1L_b lines, as would be expected for a ^1L_a line. Site selective fluorescence excitation spectra in Ar at 20 K also show only one line at 470 cm^{-1} and all other ^1L_b lines retain their vacuum frequencies. Polarized fluorescence measurements on this line in emission confirm that this vibration is Herzberg-Teller active, giving the ^1L_a properties. Furthermore, the strong ^1L_a lines at 1410-1460 cm^{-1} in jet are shifted to 1200 - 1270 cm^{-1} in Ar, indicating that they are associated with the true origin, split by interaction with the ^1L_b manifold. Calculated vibronic spectra based on ab initio (CIS/3-21G) ground and excited state geometries and MP2/6-31G* ground state frequencies are in excellent agreement with experiment. They predict the origin to be the most intense ^1L_a line!

Tu-Pos313

CONFIGURATIONAL RELAXATION OF THE SOLVENT SHELL OF THE INDOLE FLUOROPHORE IN SOLUTION AND IN A PROTEIN. ((A.S. Ladokhin)) McCollum-Pratt Institute, Department of Biology, The Johns Hopkins University, Baltimore, MD 21218 and Palladin Institute of Biochemistry, Ukrainian Academy of Sciences, Kiev 252030, Ukraine.

Proteins are known to be heterogeneous systems with a hierarchy of internal motions. However, those properties are often ignored when the complex fluorescence decay of tryptophan residues is compared to model studies with indole derivatives in solution. We report here the substantial dependence of fluorescence decay of indole in viscous media on the excitation wavelength and suggest that this is due to slow configurational relaxation in solvate (defined as a chromophore and its solvent shell). In contrast, decay of tryptophan zwitterion in aqueous solution shows very little dependence on the excitation wavelength. The excitation dependence of fluorescence decay, observed in bee venom melittin, is attributed to the preferential excitation of molecules with different energies of interaction in solvate. Such photoselection is achieved due to the rigidity of the environment of tryptophan residue, which is altered by conformational changes in the protein. The criterion is introduced to differentiate the heterogeneity of fluorescence decay in proteins introduced by conformers (multiexponentiality), versus the one introduced by inhomogeneous broadening of electronic spectra of single species (nonexponentiality).

Tu-Pos314

CONFORMATIONAL HETEROGENEITY OF TRYPTOPHAN IN CRYSTALLINE PROTEINS: A Review of Time-Resolved Fluorescence Studies. ((T. E. S. Dahms* and A. G. Szabo†)) *University of Ottawa, Ottawa, Ont. CA K1H 8M5 †University of Windsor, Windsor, Ont. CA N9B 3P4.

Erabutoxin b was the first single Trp protein reported to have multi-exponential fluorescence decay kinetics in the crystalline state. Crystal orientation experiments confirmed the presence of alternate Trp side chain conformations, verifying the rotamer hypothesis of Trp photophysics. Calculations, which simulated the orientational dependence of the fluorescence decay-time relative proportions, generated curves similar to those obtained experimentally. Previous experiments from this laboratory had shown that single and double exponential fluorescence decays (on the order of 10-120 picoseconds) could be resolved from the fluorescence of myoglobin single crystals . Ergo, the triple-exponential decay kinetics observed for erabutoxin b was not a fortuitous consequence of data analysis.
In order to further confirm that the orientational dependence of the fluorescence decay normalized pre-exponential terms for erabutoxin b was not an experimental artifact, crotonase (which also displays triple exponential decay in solution) was studied in the crystalline state. As expected, the relative proportions of three decay components showed no orientational dependence owing to the large number (dimer of hexamers) of protein molecules in the crystallographic unit cell.
Pseudomonas fluorescens holo and apoazurin as well as ribonuclease T1 in the presence and absence of inhibitor (2'-GMP) will provide additional examples of protein crystal fluorescence and Trp side chain conformational heterogeneity.

Tu-Pos315

STUDIES OF CONFOMATIONAL SUBSTATES IN GLASSES WITH FLUORESCENCE DISTRIBUTION OF LIFETIMES. ((J.D.B. Sutin, P.T.C. So, and E. Gratton)) Laboratory for Fluorescence Dynamics, Dept. of Physics, Univ. of Illinois at Urbana-Champaign, Urbana, IL 61801.

Previous work has demonstrated that a single distribution of lifetimes model of fluorescence decay cannot be resolved from a multiple discrete exponentials model (Alcala, et al.; *Biophys J 56*: 587). In proteins, a distribution of lifetimes can be physically justified by the conformational substates model, where the width of the distribution arises from a heterogeneous conformational energy landscape. The temperature dependence of this model allows the distribution and discrete models to be distinguished. The conformational substates model also suggests proteins share some essential characteristics with glassy systems since both have heterogeneous landscapes (Silva, et al.; *Biophys J*: to be published). In this study, we are using N-acetyl-tryptophanamide (NATA) in glass forming glycerol:buffer solutions to investigate the dependence of the fluorescence decay on conformational substates. The measured width of the lifetime distribution increased with decreasing temperature but reached a plateau at a certain "critical" temperature, in agreement with the conformational substate model. In addition, the temperature dependence of the lifetime distribution has been measured for solutions of NATA with glycerol concentrations ranging from 60 to 98 percent. Similar temperature dependence is observed at these concentrations, but the critical temperatures are shifted in the same direction as the shift in the glass transition temperatures of the solutions. Although the critical temperatures correlate with the glass transition temperatures, the critical temperatures are much higher than the glass transition temperatures. We believe this occurs because the fluorophores become "frozen" in the solution depending on the hindrance of the fluorophore by the viscous solution. If this model is correct, the critical hindrance should occur at the same solution "viscosity" as seen by the fluorophore. When the lifetime parameters were plotted against viscosity measured by the fluorescence anisotropy decay, the transition for different glass forming solutions indeed occurred at a common viscosity.
Supported by NIH grant RR03155 and a grant from the Colgate-Palmolive Company.

Tu-Pos316

GENETIC ALGORITHMS FOR "MODEL-FREE" FLUORESCENCE DECAY ANALYSES WITH DIVERSITY FEATURES.
((J. R. KNUTSON)) LCB, NHLBI, NIH, Bethesda, MD 20892.

The sophistication of analysis programs for time and/or phase-resolved intensity decay and depolarization has grown enormously in the last dozen years. Nevertheless, a number of systems (e.g., certain protein decays) can still be fit equally well by competing models (e.g., distributed vs. discrete) for single curves. Global analysis can quickly select among such models, but some are reluctant to use wavelength links.

We have developed genetic algorithms[1] for such problems. The values of amplitudes (e.g., "alpha, beta") on a lifetime (or correlation time) mesh constitute a genotype, yielding an appropriate decay curve (phenotype) to fit data. "Survival of the fittest", reproduction, mutation and sex among a population of these curves eventually leads to both fit optimization and a new view of how much diversity in parameters is tolerable.

Applications to difficult problems and incorporation of multiple fitness criteria (i.e., "partial globals"[2]) will be discussed.

1. Science v261, p872. 2. Methods in Enzymology v210, p365.

Tu-Pos317

NEAR NEIGHBORS OF TRP-102 IN RAT F102W PARVALBUMIN MUTATED TO RESIDUES OF ONCOMODULIN. WHY IS THE MULTI-EXPONENTIAL FLUORESCENCE DECAY OF ONCOMODULIN NOT EXHIBITED IN THIS MUTANT? **((I.D. Clark[1], C.W.V. Hogue[2], D. Dufor[2], T.L. Pauls[4], J.A. Cox[3], M.W. Berchtold[4], and A.G. Szabo[5])) [1]IBS-NRC, Ottawa, ON, Canada K1A 0R6. [2]Dept. of Biochem. U. of Ottawa, ON, Canada K1H 8M5; [3]Inst. of Vet. Biochem. U. of Zürich-Irchel, 8057 Zürich Switzerland; [4]Dept. of Biochem. U. of Geneva, 1211 Geneva 4 Switzerland; [5]Dept. of Chem. & Biochem. U. of Windsor, ON Canada N9B 3P4.**

Rat parvalbumin (PV) F102W is one of very few single-Trp proteins which has single-exponential fluorescence decay (ca. 4 ns; Pauls et al., 1993, J. Biol. Chem. 268:20897). The structurally isomorphous rat F102W oncomodulin (OM) has non-exponential Trp-102 fluorescence decay. Of 11 near-neighbor residues to Trp-102 within 6 Å, there are only 4 different residues between these two proteins. These were mutated in rat PV to match those of rat OM, forming the rat PV 5x mutant: V46I, L50I, I58L, I66F, and F102W. Rat OM exhibits dual-exponential fluorescence decay in the holo- (Ca^{2+} filled) form, and triple-exponential decay in the apo- (Ca^{2+} free) form. The 5x PV mutant retained single-exponential fluorescence decay in both apo and holo states. Residues other than the Trp-102 near-neighbors must be responsible for the different fluorescence decay behavior observed in rat OM F102W. If in the oncomodulin case the multi-exponential decay behavior are interpreted in terms of different conformational states or rotamers, then it can be concluded that structural elements other than the hydrophobic core residues influence the conformational heterogeneity of the core. Most of the amino acid differences between OM and PV lie on the surfaces of these two proteins. Perhaps mutations of other exposed residues may indicate a basis for the observed fluorescence differences in these isomorphous calcium-binding proteins.

Tu-Pos318

PHOTOPHYSICS OF 7-AZAINDOLE IN PROTON DONATING AND ACCEPTING SOLVENTS. ((John D. Brennan and Arthur G. Szabo*)) Department of Chemistry and Biochemistry, University of Windsor, Windsor, Ontario, N9B 3P4, Canada.

7-azatryptophan (7AW) is a non-natural amino acid which may be used as an intrinsic probe of protein structure and function [Négrerie *et al., J. Phys. Chem.*, 95 (1991) 8663]. The interpretation of fluorescence signals from proteins and their relationship to protein structure requires that the photophysics of the intrinsic probes be fully understood. This has prompted a number of investigations of the excited-state behaviour of 7AW and its substituent chromophore 7-azaindole (7AI) over the past few years [Chen *et al., J. Phys. Chem.*, 97 (1993) 1770]. There appears to be some confusion in the literature regarding the mechanism of the fluorescence decay of 7AW and the origin of the changes in decay kinetics as a function of wavelength. In another work from this lab [Houge and Szabo, *Biol. Chem.*, 48 (1993) 169] 7AW in a protein was shown to have a very long decay time, on the order of 10 ns. In the present study, the fluorescence spectra, intensity and decay behaviour of 7AI were investigated. The effect of parameters such as pH, hydrogen bonding capacity of the solvent, proton donating and accepting ability of the solvent and deuteration of the solvent were examined to gain a more complete understanding of the photophysics of 7AI. These studies revealed several interesting results which have not been reported previously. There is a clear observation that 7AI shows a double exponential decay wherein the pre-exponential term of the shorter decay component becomes negative at wavelengths above 420 nm in H_2O, or 440 nm in D_2O. This result suggests that proton transfer occurs between the excited 7AI and water, and that this interaction significantly reduces both the fluorescence lifetime and intensity of 7AW. Decreases in solvent polarity (moving from water to hydrophobic solvents) resulted in increases in both fluorescence intensity and lifetime. These results provide a basis for the rationalization of 7AW fluorescence data from proteins.

Tu-Pos319

EFFICIENT INCORPORATION OF TRYPTOPHAN ANALOGS IN RECOMBINANT RAT F102W PARVALBUMIN FOR FLUORESCENCE AND ^{19}F NMR STUDIES. ((C.W.V. Hogue[1,2], S. Cyr[2], J.D. Brennan[2], T.L. Pauls[3], J.A. Cox[4], M.W. Berchtold[3], and A.G. Szabo[2])) [1]NCBI, NIH Bethesda MD 20894; [2]Dept. of Chem. & Biochem., U. of Windsor, ON, Canada N9B 3P4; [3]Inst. of Vet. Biochem. U. of Zürich-Irchel, 8057 Zürich Switzerland; [4]Dept. of Biochem. U. of Geneva, 1211 Geneva 4 Switzerland.

An expression system for rat F102W parvalbumin was created in an *E. coli* Trp auxotroph modified for use with the T7 polymerase promoter and the pLysE plasmid for limiting promoter leakage. Difficulties were encountered with these strains that precluded centrifugation steps to exchange growth media. These were overcome by alterations to the analog incorporation procedure. The Trp analogs incorporated were 7-azatryptophan (7AW), 5-hydroxytryptophan (5HW), 4-, 5-, and 6-fluorotryptophan (nFW, n=4,5,6). A -43.6 ppm ^{19}F NMR peak was consistent with burial of 6FW in a hydrophobic region. Substantial amounts of analog incorporated protein were accumulated, but Trp leakage was not entirely abolished with this expression system. 5HW substitution at position 102 rendered the protein unstable and attempts at its further purification were unsuccessful, suggesting that 5HW is incompatible with the hydrophobic pocket accommodating residue 102. 7AW has unique fluorescence characteristics for use as an intrinsic fluorescence probe. 10-fold changes in quantum yield and lifetime have been observed upon sequestering 7AW into a hydrophobic binding site (Hogue & Szabo, 1993 Biophys. Chem. 48:159). Fluorescence of the 7AW incorporated holoprotein exhibited a two-exponential decay at 295 nm, one of which was assigned to leakage product, the other to 7AW-102. Fluorescence studies further demonstrate the extreme sensitivity of 7AW fluorescence to environment, as 7AW-102 exhibits very intense and blue-shifted fluorescence relative to 7AW in water.

Tu-Pos320

COMPARISON OF TRYPTOPHAN AND 5-HYDROXYTRYPTOPHAN FOR DETERMINING THE SHAPE AND DYNAMICS OF INSULIN: TIME-RESOLVED FLUORESCENCE ANISOTROPY. ((W.R. Laws, E. Rusinova, G. Schwartz, P.G. Katsoyannis, & J.B.A. Ross)) Dept. of Biochemistry, Mt. Sinai School of Medicine, New York, NY 10029.

We have previously shown the usefulness of Trp analogues, such as 5-hydroxytryptophan (5OH-Trp), to generate spectrally-enhanced proteins for the study of macromolecular complexes. To assess 5OH-Trp as a probe of macromolecular shape and dynamics, we have synthesized insulins in which tyrosine at position A14 is replaced either with Trp or 5OH-Trp and performed time-resolved fluorescence anisotropy. The A14-Trp and the A14-5-OH-Trp insulins were excited at 295 and 315 nm, respectively, while emission was observed at 340 nm for both. Three probe-independent rotational correlation times are found for these biologically-active insulins: 1) a subnanosecond term reflecting the contributions from segmental motions; 2) a 3 ns term corresponding to the expected rotational time of monomeric insulin; and 3) a 50-55 ns term representing the rotation of an insulin aggregate(s). Thus, 5OH-Trp is capable of providing the same information about a macromolecular system as Trp, regardless of the fluorescence property being measured. Supported by NIH grants GM-39750 (JBAR) and DK-12925 (PGK).

Tu-Pos321

GENERATION OF SPECTRALLY ENHANCED SOLUBLE HUMAN TISSUE FACTOR BY INCORPORATION OF TRYPTOPHAN ANALOGS ((E. Rusinova, C.A. Hasselbacher, R. Rusinova, and J.B.A. Ross)) Biochem. Dept, Mount Sinai School of Medicine, New York, NY 10029.

The critical step in blood coagulation is complexation of tissue factor (TF) with factor VIIa. To study function and structure of TF, we have constructed a soluble TF (extracellular soluble domain of TF, sTF; sTF has four Trp residues. Our goal is a molecular description of the TF interaction with blood coagulation factors VIIa and X. For this purpose, we have attempted to generate spectrally enhanced sTF by *in vivo* incorporation of the Trp analogs 5-hydroxytryptophan and 7-azatryptophan. This would provide an sTF analog with absorbance and fluorescence properties distinguishable from those of VIIa and X, both of which contain Trp. Replacement of all of the Trp residues by the Trp analogs results in low yields of labelled protein. To help identify the functionally critical Trp residues, we have generated four single Trp-replacement mutants of sTF. All of these mutants retain their procoagulant activity. We have used difference absorbance and fluorescence techniques to analyze the environment of each individual Trp. Iodide quenching shows that the two fluorescent Trps, W14 and W45, are partially buried. The difference absorption spectra indicate that the side chains of W14 and W25 are more conformationally restricted than those of W45 and W158. W158F and W14F are promising mutants for analog incorporation. Supported by NIH Grants GM-39750 and HL-29019.

Tu-Pos322

SPONTANEOUS RECOVERY OF FLUORESCENCE BY PHOTOBLEACHED SURFACE-ADSORBED PROTEINS. ((A. L. Stout* and D. Axelrod+)) *School of Applied and Engineering Physics, Cornell University, Ithaca, NY 14853 and +Biophysics Research Division, University of Michigan, Ann Arbor, MI 48109.

Fluorescence photobleaching of a carboxyfluorescein-labeled protein (erythrocyte cytoskeletal protein 4.1) immobilized on bare glass is found to be reversible, provided that the sample is deoxygenated. After a short (hundredths of seconds) photobleaching laser flash, the subsequent fluorescence excited by a dim probe beam partly recovers on a long (tenths of second) time scale, even in the absence of chemical exchange or diffusion processes. Neither the fraction of the fluorescence that bleaches reversibly nor its recovery rate is a strong function of fluorophore surface concentration. At a fixed surface concentration, the reversibly photobleached fraction and its recovery rate decreases with increasing duration or intensity of the bleaching flash. On the other hand, non-deoxygenated, air-equilibrated samples exhibit almost total irreversible bleaching on this time scale. These observations indicate that fluorescence recovery after photobleaching (FRAP) experiments performed under deoxygenated conditions for measuring diffusion or chemical kinetics should be interpreted with caution: fluorescence recoveries may be due to intrinsic photochemical processes rather than fluorophore mobility. The recovery effect appears too slow to be ascribed simply to a relaxation of a triplet state; other possible explanations are offered. Supported by NSF DMB 8805296 (to D. A.).

Tu-Pos323

SOLVATOCHROMIC/THERMOCHROMIC STUDIES OF THE PROTEIN PROBE NILE RED ((Christina Golini and Brian Wesley Williams)) Chem. Dept. Bucknell Univ. Lewisburg, PA 17837

Recently, the long wavelength, solvent-sensitive dye Nile Red has been proposed as a probe of protein binding sites [1], [2]. To better characterize the response and physical properties of this probe, solvatochromic and thermochromic spectral studies were undertaken in a variety of aprotic solvents. In addition, some decay lifetime data was taken in a more limited range of solvents. The thermochromic data obtained for Nile Red also permits comparison of two alternative descriptions of observed thermochromic "blue shifts" in emission [3], [4]. (Supported by ACS-PRF #27003-B4 and Ethel Ward Grant-Bucknell University)

[1] M. B. Brown,T. E. Edmonds,J. N. Miller D. P. Riley and N. J. Seare, Analyst 118 407 (1993)
[2] M. B. Brown,T. E. Edmonds,J. N. Miller and N. J. Seare, J. Fluor. 3 129 (1993)
[3] R. B. Macgregor, Jr., G. Weber, Ann. NY Acad. Sci. 366 140 (1981)
[4] T. Hagan, D. Pilloud and P. Suppan, Chem. Phys. Lett. 139 499 (1987)

Tu-Pos324

THE EMISSION AND POLARIZATION ANISOTROPY OF RHODAMINE DIMERS. ((Thomas P. Burghardt and James E. Lyke)) Department of Biochemistry and Molecular Biology, Mayo Foundation, Rochester, MN 55905.

The absorption, emission, and excitation polarization anisotropy spectra of a rhodamine dye in a water/glycerol solution at high concentration was investigated to determine spectroscopic properties of the ground state dimer. The combination of data from these spectra measured at several dye concentrations contained sufficient constraints on the model for dimer association to permit the estimation of the association constant, the relative quantum yield of the monomer and dimer species, and the representation of these spectra in terms of a linear combination of the separate monomer and dimer spectra. The polarization anisotropy of the pure dimer is larger than or equal to that of the pure monomer species over the range of wavelengths covering both of the longest wavelength transitions of the dimer indicating unique qualitative properties of the dimer conformation. Supported by NIH (R01 AR 39288), the American Heart Association (930 06610), and the Mayo Foundation.

Tu-Pos325

POLYMERIC TERBIUM CHELATES FOR TIME RESOLVED LUMINESCENCE DETECTION OF SPECIFIC MACROMOLECULES ((Theodore G. Wensel, & Jagannath B. Lamture)) Verna & Marrs McLean Department of Biochemistry, Baylor College of Medicine, Houston, TX 77030

Time gated measurements of millisecond lanthanide luminescence can lead to very efficient rejection of background fluorescence and scattering signals in detection schemes for specific macromolecules. While certain organic ligands form luminescent complexes with Tb(III) or Eu(III) that have detection sensitivities comparable to those of common organic fluorophores, previously available reagents for coupling Tb(III) or Eu(III) to macromolecules have either lacked sensitizing ability, or suffered from poor stability. We have developed polymeric Tb(III) chelates containing multiple Tb(III) ions complexed to an analogue of the highly efficient sensitizing ligand, dipicolinic acid. The resulting complexes have greater stability than $TbEDTA^-$ ($K_a > 10^{18}\ M^{-1}$), intense visible emission, and millisecond luminescence lifetimes. We have coupled them to proteins under conditions that allow retention of specific binding properties for use in immunoassays.

Tu-Pos326

HIGHLY LUMINESCENT EUROPIUM AND TERBIUM CHELATES. ((Min Li, Zakir Murtaza, John S. Mills*, John E. Hearst and Paul R. Selvin))

Department of Chemistry, University of California, Berkeley, Berkeley CA 94720 and *University of Illinois — Chicago, Chicago Ill. 60808

Luminescent lanthanide (terbium and europium) chelates have millisecond lifetime, sharply spiked emission spectrum (10nm fwhm), huge Stokes shifts (>150nm), high quantum yield (~1) and excellent solubility. These characteristics makes them useful alternatives to fluorescent dyes, particularly for overcoming problems of autofluorescence, for two-color detection (with *no* spectral overlap), and as donors in energy transfer experiments. We have developed a series of new chelates with a variety of characteristics, including: binding constants in excess of $10^{20}\ M^{-1}$; exclusion of all water from inner coordination sphere of lanthanide; net charge ranging from -2 to +1; thiol and amine-reactive forms; absorbances of $>10{,}000\ M^{-1}cm^{-1}$ around 337nm. The compounds consist of a polyaminocarboxylate chelate covalently coupled to a coumarin or carbostyril "sensitizer" and a reactive group.

Tu-Pos327

FLUORESCENCE STUDIES OF CALMODULIN COMPLEXES WITH TARGET PROTEINS AND PEPTIDES ((P.B. O'Hara, M.A. Rahman, A. Chandani, and M.J. Lee)) Department of Chemistry, Amherst College, Amherst, MA, 01002

Multifrequency Phase Fluorometry has been used to study the binding of the calcium regulatory protein calmodulin CaM to two different target proteins. Calmodulin's conformational sensitivity was optically probed by positioning fluorescent donors and acceptors at site specifically mutated positions 34 and 110. By replacing threonines in these two positions with cysteines, each calmodulin molecule could be selectively labelled with one AEDANS donors and one of two different acceptors. The interaction between CaM and M13, a peptide derived from the binding domain of myosin light chain kinase, was examined by fluorescence energy transfer. In the absence of target peptide, Forster theory is used to calculate a 56 A donor-acceptor distance consistent with the X-ray crystal structure (Babu et al. Nature 315, 37-40, 1985). The target peptide induces a compaction of the entire protein and a quenching of the donor fluorescence. The new 16 A donor-acceptor distance calculated from this quenching is consistent with the NMR structure of the calmodulin-peptide complex (Ikura et al, Science, 256, 632, 1992). In a further demonstration of the tremendous flexibility of calmodulin, the two cysteines can be successfully crosslinked with a 10 A crosslinker in the absence of target peptide. Surprisingly, the crosslinked protein retains its ability to bind to target peptide. The complex between the peptide and the crosslinked protein was studied by the fluorescence of the single Trp in the 4th position of the peptide. The interaction between CaM and an intact target protein, phosphodiesterase (PDE) was also examined. The mutant CaM was shown to activate PDE at least as effectively as wild type calmodulin. Energy transfer studies will determine the distance between donors and acceptors positioned at position 34 and 110.

Tu-Pos328

EFFECTS OF SR-Ca^{2+}-ATPASE INHIBITOR ON CYTOSOLIC CALCIUM AND ISOVOLUMIC RELAXATION ((J.M. Halow, J.S. Schreur, S.A. Camacho)) Dept. of Med., UCSF, CA (Spon. by Edmund Keung)

The hypothesis that the cytosolic $[Ca^{2+}]$ ($[Ca^{2+}]_c$) decline determines isovolumic relaxation (i.e. left ventricular pressure (LVP) decline) has not been adequately tested. We used cyclopiazonic acid (CPA) to inhibit the sarcoplasmic reticulum-Ca^{2+}-ATPase (SR--Ca^{2+}-ATPase) in isovolumic rat hearts. The goals were to 1) determine the effects of CPA on the $[Ca^{2+}]_c$ transient and 2) to determine the relationship between the exponential time constants of $[Ca^{2+}]_c$ transient decline (τ_{Ca}) and LVP decline (τ_P). $[Ca^{2+}]_c$ was determined using indo-1 fluorescence and LVP was measured with a solid state transducer. With 9μM CPA, diastolic $[Ca^{2+}]_c$ increased from 150±20 nM to 340±56 nM, while systolic $[Ca^{2+}]_c$ decreased from 741±190 nM to 557±175 nM (n=7). Diastolic LVP increased from 12±2 mmHg to 31±4 mmHg, while systolic LVP decreased from 93±8 mmHg to 71±5 mmHg. There was a relationship between the τ_P and τ_{Ca} (figure). **Conclusions:** 1) CPA increased both diastolic $[Ca^{2+}]_c$ and τ_{Ca} which is consistent with inhibition of the SR-Ca^{2+}-ATPase. The decrease of systolic $[Ca^{2+}]_c$ is likely caused by a decrease in SR-Ca^{2+}-loading. 2) The relationship, which shows an increase in τ_P with τ_{Ca}, is consistent with the hypothesis that $[Ca^{2+}]_c$ decline determines relaxation.

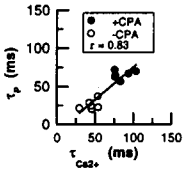

Tu-Pos329

CYTOSOLIC CALCIUM TRANSIENTS FROM WHOLE HEARTS USING INDO-1 AM: CORRECTION FOR NON-CYTOSOLIC FLUORESCENCE ((Joop H. M. Schreur, Vincent M. Figueredo, David M. Shames, S. Albert Camacho)) VAMC, UCSF, San Francisco, CA.

Previous studies using indo-1 AM in whole hearts have ignored the contribution of non-cytosolic fluorescence (NCF). However, NCF may greatly affect the derived cytosolic $[Ca^{2+}]$ ($[Ca^{2+}]_c$). To more accurately derive $[Ca^{2+}]_c$, we sought to determine the non-cytosolic contribution to total indo-1 fluorescence. Because NCF is believed to primarily represent mitochondrial $[Ca^{2+}]$ ($[Ca^{2+}]_m$), we also sought to estimate $[Ca^{2+}]_m$. Isolated rat hearts, paced at 5 Hz, were loaded with indo-1 AM at 37°C. Hearts were then perfused with Mn^{2+} (15 mM) until fluorescence transients disappeared (pressure transients remained unchanged). Residual fluorescence was presumed to be NCF. The non-cytosolic contribution was 61 ± 6% and 56 ± 7% of total fluorescence at emission λ 385 and 456 nm, respectively. The effect of correcting for NCF on the total indo-1 transient is shown. After correction, the diastolic and systolic $[Ca^{2+}]_c$ were 131 ± 9 and 707 ±48 nM (n=17). $[Ca^{2+}]_m$ was estimated to be 183 ± 36 nM. Conclusions: 1) In hearts loaded with indo-1 AM, correction for NCF is essential for calculating $[Ca^{2+}]_c$. 2) Estimated $[Ca^{2+}]_m$ is comparable to diastolic $[Ca^{2+}]_c$ levels.

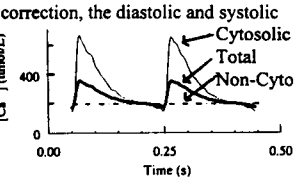

Tu-Pos330

FLUORESCENCE ENERGY TRANSFER (FET) BETWEEN FLUO-3 AND SNARF-1, AFFECTS THE ACCURACY OF ION MEASUREMENTS WHEN USING THESE PROBES SIMULTANEOUSLY. ((R. Martínez-Zaguilán, G. Parnami, and R.M. Lynch)). Dept.Physiol. U. Arizona. Tucson, AZ 85724.

Studies using fluorescent probes have demonstrated that intracellular Ca^{2+} ($[Ca^{2+}]^{in}$) is involved in signal transduction mediating cell growth, secretion, motility, and contraction. However, all Ca^{2+} indicators are affected by pH, necessitating simultaneous measurements of these two ions for accurate determination of $[Ca^{2+}]^{in}$. We have used SNARF-1 and Fluo-3 to simultaneously monitor pH^{in} and $[Ca^{2+}]^{in}$ in single cells. Although expected experimental results can be obtained, discrepancies from predicted responses are observed. FET is maximal when the emission spectrum of one fluoroprobe overlaps the excitation spectrum of the other, and when the probes are <100 apart. Since maximal emission of Fluo-3 (530 nm) and excitation of SNARF-1 (534 nm) overlap, we determined whether FET could account for the discrepancies. Increasing the concentration of Fluo-3 at constant [SNARF-1] decreased the absolute emission of Fluo-3 and increased the intensity of the SNARF-1 emission spectra, with the effect larger at 584 nm than at 644 nm. Further, increasing Ca^{2+} at constant pH resulted in decreases in the 644/584 SNARF-1 pH-sensitive ratio, supporting our contention that FET affects Ca^{2+} and pH measurements. The magnitude of these effects is dependent on ion and dye concentration, and compartmentalization of dyes within the cells. Thus, to accurately determine $[Ca^{2+}]$ not only must pH be considered, but also interactions between the probes used to monitor these ions.

Tu-Pos331

CHARACTERIZATION OF Mg^{2+}-DEPENDENT ENDONUCLEOLYTIC ACTIVITY AND DEVELOPMENT OF A FLUORESCENCE ASSAY FOR HIV-1 INTEGRASE *IN VITRO*. ((S.P. Lee[1], H.G. Kim[1], M.L. Censullo[1], J.R. Knutson[2], and M.K. Han[1])) [1]Georgetown University Medical Center, Department of Biochemistry, Washington, DC 20007 and [2]NHLBI, NIH, Bethesda, MD 20892.

In vitro reactions of Human Immunodeficiency Virus-1 Integrase (HIV-IN) performed with short oligonucleotide substrates show a preference for Mn^{2+} as the catalytic cofactor. In contrast, studies with infected cell extracts show that viral DNA integration occurs in the presence of Mg^{2+}. We report that changes in the structure and length of the oligonucleotide substrates alter the donor processing activity of HIV-IN to a Mg^{2+}-dependent activity, thereby bringing both the *in vivo* and *in vitro* reactions into agreement. Furthermore, a novel mechanism (alternative disintegration) catalyzed by the endonuclease activity of HIV-IN is responsible for cleaving the junction between the viral and target sequences of the intermediate without rejoining the target strands.

The Mg^{2+}-dependent donor processing activity allows for the development of a rapid and continuous fluorescence assay for HIV-IN based on fluorescence resonance energy transfer (FRET). Steady-state fluorescence studies indicate the fluorescence cleavage assay monitored by the enhancement of the donor fluorescence is consistent with data obtained from the radioactive assay. This fluorescence assay will facilitate both detailed kinetic studies and rapid screening of HIV-1 integrase inhibitors.

Tu-Pos332

IMMUNOSUPPRESSANT LIGAND BINDING TO FKBP12: A TIME-RESOLVED FLUORESCENCE STUDY. ((Norberto Silva, Jr., and Franklyn Prendergast)) Mayo Clinic, Guggenheim 14, 200 First St. SW, Rochester, MN 55905. Supported by GM34847 and the Damon Runyon-Walter Winchell Fellowship Foundation, DRG-1289.

The immunosuppressants tacrolimus (FK506) and rapamycin have had a tremendous impact on the effectiveness of organ transplants over the past decade. Immunosuppression is ultimately achieved after either drug is bound by a peptidyl-prolyl cis-trans isomerase called FK506 binding protein (FKBP12). Presently, the interpretation of drug interaction with FKBP12 is based on X-ray and NMR structural studies as well as NMR backbone relaxation experiments. However, it has been noted that FKBP12 loses its function when its single Trp residue (W59) is mutated. Since W59 is at the center of the FKBP12 binding site we have undertaken a study to investigate the pertinence of W59 side chain dynamics in the association of FK506 and rapamycin to FKBP12. In particular, the time-resolved fluorescence anisotropy decay $r(t)$ of W59 in FKBP12, with and without drug, is considered. In addition, our experimental measurements are interpreted through minimum perturbation mapping calculations of W59 in the FKBP12 system using CHARMM 22. Minimum perturbation maps of W59 yields the energy landscape of W59 as a function of its χ_1,χ_2 dihedral angles from which order parameters and isomer interconversion rates can be calculated. Preliminary measurements of $r(t)$ for W59 show that the system is best described by a single rotational correlation time and a low initial anisotropy r_o (less than 0.2). Low temperature-high viscosity measurements of the steady state anisotropy of W59 yield a value significantly higher than r_o but less than that of free tryptophan. The experimental measurements suggest that W59 displays rapid motions and the theoretical calculations suggest that these motions are isomerizations of W59 about its χ_2 dihedral. Experimental measurements and theoretical calculations of FKBP12 with the immunosuppressant drugs are also discussed.

Tu-Pos333

TWO NEW FLUORESCENT REAGENTS FOR DETECTION AND QUANTITATION OF PICOGRAM LEVELS OF DOUBLE-STRANDED DNA AND OLIGONUCLEOTIDES IN SOLUTION. ((L.J. Jones, S.T. Yue, Z. Huang, V.L. Singer)) Molecular Probes, Inc., Eugene, OR 97402.

We have developed two new fluorescence-based assays for the sensitive detection and quantitation of nucleic acids in solution. These assays rely on the use of two novel reagents, PicoGreen™ dsDNA Quantitation Reagent and OliGreen™ Oligonucleotide Quantitation Reagent for ssDNA. These dyes are essentially nonfluorescent in the absence of nucleic acids and have fluorescence enhancements of over 1000-fold. Both dyes are optimally excited at about 490 nm and have emission maxima at about 520 nm. The dsDNA assay allows the detection of as little as 25 pg/ml linear or supercoiled double-stranded DNA in solution. This sensitivity is 400 times better than can be achieved using Hoechst dyes and more than 10 times that provided by YOYO®-1. The assay is linear over four orders of magnitude in DNA concentration — from 25 pg/ml to 1 μg/ml — using a single concentration of dye. In contrast, Hoechst-based assays require the use of two different dye concentrations to achieve even three orders of magnitude in DNA concentration. Single-stranded DNA and RNA have essentially no contribution to the signal, except at very high concentrations. The OliGreen™ assay allows the detection of as little as 100 pg/ml of synthetic oligonucleotides ranging in size from 10 bases to at least 50 bases. This sensitivity is 10-fold greater than can be achieved on electrophoretic gels using SYBR™ Green I Nucleic Acid Gel Stain and 50-to 100-fold better than can be achieved using ethidium bromide in the same application. The assay is linear over four orders of magnitude in oligonucleotide concentration and shows some sequence selectivity.

Tu-Pos334

ORIENTATIONAL EXCHANGE THEORY FOR FLUORESCENCE ANISOTROPY FROM FLAT MEMBRANE PROBES

((B. Wieb Van Der Meer and S.-Y. Simon Chen)) Department of Physics and Astronomy, Western Kentucky University, Bowling Green, KY 42101

A model is proposed in which a membrane probe is represented by a flat disk with its transition moments along the long and short symmetry axes. Six possible orientations are considered with respect to an XYZ coordinate system with the Z-axis along the membrane normal: the disk has its long and short axes along the Z- and X-, Z- and Y-, X- and Z-, Y- and Z-, X- and Y-, or Y- and X- axes, respectively. The reorientational dynamics in an isotropic suspension of uniaxial membranes, is described by 2 order parameters and 9 rotational rates, of which 4 are independent. The anisotropy has, therefore, 6 independent molecular parameters, and contains 5 exponentials. In the limit of a cylindrically symmetric probe the anisotropy has only 2 exponentials and an r_∞-term containing 3 independent parameters: 1 order parameter and 2 rotational rates. Only in this special case are the following statements true: 1) the normalized one-photon anisotropy decay is independent of excitation wavelength 2) the ratio of 2-photon over 1-photon anisotropy is independent of time and temperature. This work is supported by the National Science Foundation EPSCoR program (EHR-9108764).

Tu-Pos335

CO-OPERATIVE INSERTION OF THE ANTIBIOTIC NYSTATIN IN A LIPID BILAYER. A FLUORESCENCE STUDY. ((A.Coutinho and M.Prieto)) Centro Quimica-Fisica Molecular, I.S.T., Lisbon, Portugal

Nystatin is a member of the polyene macrolide antibiotics family that acts by permeablizing the cell membranes of fungi which are its main cellular target. We have taken advantage of the intrinsic fluorescence properties of its tetraene chromophore to study its interaction with small unilamellar vesicles of DPPC. Nystatin has a complex fluorescence decay described by 3 and 2 exponentials when interacting with lipid vesicles in the gel and liquid-crystalline states, respectively. Its mean lifetime, $\langle\tau\rangle$, is a sigmoidal function of antibiotic concentration when the lipid vesicles are in the gel state (a sharp transition in $\langle\tau\rangle$ (from 11 ns to 32 ns) is observed around $5<[Nys],\mu M<8$). On the other hand, above the lipid phase transition temperature a constant value of $\langle\tau\rangle = 2.8$ ns was measured. To further investigate Nystatin behaviour, we have performed a time-resolved and steady-state fluorescence quenching study of Nystatin by DOXYL-stearic acids, *n*-DS (n= 5 and 16). The spin-labelled surface probe 5-DS shows a higher quenching efficiency than 16-DS (a inner-membrane probe) for the short-lived antibiotic species. The quenching efficiency by the 5-DS probe decreases for the long-lived species, becoming almost identical to the one measured with 16-DS. These results suggest that Nystatin chromophore undergoes a change in its position towards the centre of the bilayer upon increasing its concentration in the membrane; this transition is highly co-operative.(Supported by JNICT, Portugal)

Tu-Pos336

THERMODYNAMICS OF (1,8)ANS BINDING TO INTESTINAL FATTY ACID BINDING PROTEIN (IFABP) ((*W. R. Kirk, S. Kurian & F.G. Prendergast*))Mayo Foundation, Rochester MN, 55905 (Sponsored by W.R. Kirk).

We have monitored the interaction of (1,8)Anilinonaphthalenesulfonate with IFABP by means of the large enhancement of ANS fluorescence upon binding. The binding constant was determined at a variety of temperatures, allowing us to determine the effective enthalpy and entropy of binding (~ -6.3 kcal/mol and ~ -1.0 cal/deg-mol, respectively). This remarkably small entropy is compared with that of a model system (poly-β-cyclodextrin). The solvent isotope effects on binding were also measured and correspond roughly to the small (inverse) isotope effect of removing a hydrophobic solute from aqueous solution. Fluorescence lifetime analyses were also employed to study the enhancement of the quantum yield upon binding, comparing these data to that obtained with a model solvent consisting of 10M dioxane (X=0.67) with 4.9 M H_2O, which closely reproduces the spectral properties of the bound species. From these studies we hope to disentangle the various contributions to the binding which may be due to desolvation, cratic and configurational entropy and enthalpy which may be peculiar to protein-ligand interaction. In addition, we can now more easily measure the affinity of [illegible] for particular fatty acids by competition assays against ANS. Supported by GM-34847-10

Tu-Pos337

THE ROLE OF A FREE SULFHYDRYL GROUP IN THE ACTIVITY OF CHOLESTERYL ESTER TRANSFER PROTEIN (LIPID TRANSFER PROTEIN). ((D.E. Epps, G.W. Melchior, K.A. Greenlee, J.S. Harris, J. F. Fisher, E.W. Thomas, C.K. Castle, and F.J. Kezdy)). Upjohn Laboratories, The Upjohn Company, Kalamazoo, MI 49001.

Human, cynomolgus, and rabbit cholesteryl ester transfer proteins (CETP) all contain an odd number of Cys's which implies that CETP contains at least one free sulfhydryl group. The presence of —SH in an exocellular protein usually indicates that the thiol group is required for catalytic activity. A —SH-specific fluorescent reagent does, in fact, react with cynomolgus-CETP in a *pseudo*first-order manner to yield a mono-derivatized protein which is inactive in our cholesteryl ester (CE) transfer assay. Although $HgCl_2$ is only weakly inhibitory toward CETP, an organomercurial derivative of cholesterol (U-617) is an excellent inhibitor of the CETP-catalyzed CE transfer and of the —SH labelling of CETP. In contrast, the corresponding amino derivative of cholesterol is only mildly inhibitory. Inhibition of CETP by U-617 is biphasic and at the end of the slow phase the inhibition has a K_i in the nanomolar range. We propose that the free —SH group of CETP is located in a hydrophobic environment close to, but not within, the substrate-binding site of CETP. The presence of this unique —SH group on CETP may provide an ideal target for the design of specific CETP inhibitors.

Tu-Pos338

AN IMPROVED FLUORESCENCE METHOD FOR MEASURING THE ACTIVITY OF CHOLESTERYL ESTER TRANSFER PROTEIN (LIPID TRANSFER PROTEIN). ((D.E.. Epps, J.S. Harris, K.A. Greenlee, J.F. Fisher, C.K. Marschke, C.K. Castle, R.G. Ulrich, T.S. Moll, G.W. Melchior and F.J. Kezdy)) Upjohn Laboratories, The Upjohn Company, Kalamazoo, MI 49001.

A rapid and extremely sensitive fluorescence assay of cholesteryl ester (CE) transfer protein (CETP) was developed from a previously described procedure [Bisgaier *et al., J. Lipid Research* **34**, 1625-1634, 1993]: With the new assay, we can measure accurately as little as 50 ng of CETP. The increase in sensitivity is due mostly to the addition of apoproteins before sonication of the donor and acceptor lipids and to the reduced particle size obtained by efficient sonication. With this method the full time course of the reaction can be recorded. Donor particles contained hexabromotriolein for easy separation from acceptor particles. We showed that the increase in fluorescence was linearly related to the transfer of labelled CE. We have also synthesized a fluorescently labelled triglyceride (TG) and incorporated it into donor emulsion particles. The CETP-catalyzed transfer of TG was some sixfold slower than that of CE. The kinetics of the exchange fully support a mechanism of adsorption-exchange-desorption-diffusion. Experimental conditions were optimized for detecting CETP inhibitors and defining their mode of action.

Tu-Pos339

SINGLE PHOTON RADIOLUMINESCENCE (SPR) MEASUREMENT OF THE DISTANCE BETWEEN CYS-201 IN ERYTHROCYTE BAND 3 AND THE BILAYER. ((B.J.-M. Thevenin, S.E. Bicknese, J. Park, A.S. Verkman and S.B. Shohet)) U.C.S.F., San Francisco, CA 94143.

SPR is a new technique based on excitation of fluorescence by short range β-decay electrons which is suitable for the measurement of molecular distances up to 0.1 μm (Biophys. J. **63**, 1256-79). The cytoplasmic domain of band 3 (cdb3) is the major anchorage for the erythrocyte membrane skeleton. Because of the high axial asymmetry of cdb3, we used SPR to measure the distance between cdb3 Cys-201 (labeled with fluorescein) and the bilayer (labeled with [9,10(n)]^{3}H-oleic acid). Cdb3 in KI-stripped inside-out membranes was stoichiometrically labeled with fluorescein maleimide. Nonspecific labeling was corrected for by subtracting the SPR signal from trypsin-cleaved samples in which cdb3 was removed. Bremsstrahlung (stopping radiation) background signal was measured in ^{3}H-labeled, non-fluorescent membranes and subtracted. The intrinsic efficiency for excitation of fluorescein on cdb3 was measured using a fluorescent sample in which ^{3}H-oleic acid was replaced by ^3H_2O. The corrected SPR signal at pH 7.4 was 0.62 +/- 0.02 cps/mCi ^{3}H/ml of 15.6 nM band 3 sample. Assuming that the ^{3}H in oleic acid formed two "donor" planes 11 and 33 Å below the bilayer surface, a Cys-201-to-bilayer separation of 43 +/- 4 Å was calculated. This relatively short distance was confirmed by fluorescence energy transfer between fluorescein on Cys-201 and the "acceptors" eosin and rhodamine B anchored at the membrane surface with lipophilic tails (41 and 49 +/- 4 Å, respectively). These results demonstrate the utility of SPR for measuring submicroscopic distances in biological membranes.

Tu-Pos340

INTERACTIONS OF COMPONENTS OF COMPLEMENT MEMBRANE ATTACK COMPLEX AS MEASURED BY FLUORESCENCE RESONANCE ENERGY TRANSFER. ((J.F. McDonald and G. Nelsestuen)) Dept. of Biochemistry, U. of Minnesota, St. Paul, MN 55108.

The sequential membrane-associated interactions of the complement proteins C5b, C6, C7, and C8 result in activation of several C9 molecules that insert and form a cytolytic channel known as the membrane attack complex(MAC), which in ultrastructural studies resembles a circle or "doughnut". The proteins C7, C8 and C9 were labeled with FITC and TRITC as donor and acceptor probes in order to utilize resonance energy transfer effects to study the mechanism of assembly in vitro on phospholipid vesicles. Light scattering was employed to determine the stoichiometry of C9 assembly, and correlated with fluorescence changes associated with protein assembly. Insertion of variable equivalents of C9 between donor- and acceptor-labeled proteins allowed the distance dependence of the resonance energy transfer to be utilized to discern modes of assembly of the C9 channel, and to identify the roles of MAC components. It was found that C9 assembles in an ordered, sequential manner in which incoming subunits are progressively displaced from C8 and the initial C9 molecule. Completion of the C9 polymer occured at a site remote from either of these molecules as evidenced by lack of energy transfer. This was consistent with models of assembly characterized by closure at a distant site on C5b-7, or alternatively by a "corkscrew"-like process in which the two ends are displaced from each other.(Supported in part by grant HL15728 from NIH).

Tu-Pos341

NEW PENTAENE FLUORESCENT SINGLE-CHAIN LIPIDS AS PROBES OF MEMBRANE PROPERTIES AND OF TRYPTOPHAN ENERGY TRANSFER. ((A.A.Souto, C.R.Mateo, F.Amat-Guerri* and A.U.Acuña)) Insts. of Physical Chemistry and *Organic Chemistry, CSIC, 28006-Madrid, Spain.

We have synthesized[1] a new set of linear, fluorescent lipid analogs that contain a five-double-bond conjugated system. A representative member is the *all-trans* octadecapentaenoic acid (TPT), which is characterized by a large absorption coefficient (~$10^5 M^{-1}cm^{-1}$ at 350 nm) and a long-wavelength (470 nm), highly polarized (r_0=0.39) fluorescence, with a major lifetime of 20 ns, both in fluid solution and in lipid bilayers. Since TPT aligns parallel to the bilayer lipids (as determined by quenching techniques) and shows a non-selective homogeneous lateral distribution between fluid and gel domains, it was used with success to determine changes in the apparent viscosity and long-range order of the bilayer. These probes are also efficient acceptors of protein tryptophan fluorescence (R_0 ~ 34 Å), facilitating the study of lipid/protein interactions. Supported by the Spanish Comis.Interm. Ciencia y Tecnolog. Grants PB 90-102/93-126.

1.-A.A.Souto, A.U.Acuña, F.Amat-Guerri, Tetrahedon Lett. 35 (1994) 5907.

Tu-Pos342

LIPID DOMAINS IN BIOLOGICAL MEMBRANES STUDIED BY USING A TWO-PHOTON MICROSCOPE. (W.M. Yu, P.T.C. So, T. French and E. Gratton) LFD, University of Illinois at Urbana-Champaign, Urbana, IL 61801

We have investigated lipid domains in biological membranes using LAURDAN (2-dimethylamino-6-lauroyl-naphthalene) generalized polarization obtained from a scanning two-photon fluorescence microscope. The lipophilic fluorescence probe LAURDAN is sensitive to the polarity of its environment and its fluorescence spectra change with variations in membrane lipid composition as well as in the membrane phase state. The generalized polarization function(GP) is useful in exploring the existence of lipid micro-domains in biological membranes. In conventional confocal microscopy, fluorescence imaging of a single cell stained with LAURDAN has been unsuccessful, primarily due to the probe's susceptibility to photobleaching. By taking advantages of two photon scanning fluorescence microscopy photo bleaching is localized and reduced to a minimum. We have obtained single cell three dimensional images of both fluorescence intensity and generalized polarization by the two photon scanning approach. From these images, regions characterized by different fluorescence intensities for the blue and red edge of the LAURDAN emission spectra are observed on the cell membrane. The corresponding GP values cover broad ranges. These results point to the heterogeneity of cellular membrane. We have searched for a pixel by pixel correlation between the distribution of intensity and GP with the goal of obtaining a 3D correlation image. The intensity and GP distribution could be an indication of the coexistence of lipid gel and liquid-crystalline phase domains. More likely, the inhomogenous distribution of lipid components, such as cholesterol that leads to regions with differing degrees of solvent accessibility contribute to the observed intensity and GP distribution. This latter lipid composition variation may be of paramount importance in fulfilling functions of biological membranes.

This work was supported by NIH grant RR03155.

Tu-Pos343

VOLUMETRIC PHOTOACOUSTIC ANALYSIS OF PROTEIN FLUORESCENCE: DETERMINATION OF FLUORESCENT QUANTUM YIELDS AND MEASUREMENT OF VOLUME CHANGES OCCURRING UPON PHOTOEXCITATION.

((E. Kurian, F.G. Prendergast, L.J. Libertini, E.W. Small, S.T. Daniels and J.R. Small)) Mayo Clinic and Foundation, Rochester, MN 55905; Quantum Northwest, Inc., Spokane, WA 99207; Eastern Washington University, Cheney, WA 99004 (kurian@mayo.edu, jsmall@ewu.edu).

A series of proteins containing either an intrinsic or extrinsic fluorophore have been examined using the time-resolved, pulsed-laser volumetric photoacoustic technique. Different temperature ranges were used to recover enthalpic (15 to 35 °C) and volumetric (0 to 4 °C) changes due to photoexcitation. The enthalpic data are used to estimate fluorescent quantum yields, which are compared to fluorescent quantum yields determined by conventional methods. The volumetric data, obtained at temperatures for which heat release does not contribute to photoacoustic signals, provide insights into how a protein in solution responds to photoexcitation and the release of absorbed light energy. The proteins studied include the Green Fluorescent Protein (GFP); papain, intestinal fatty acid binding protein (I-FABP), and adipocyte lipid binding protein (ALBP), each labeled with acrylodan; I-FABP and ALBP, both labeled with 1,8-ANS; and I-FABP and ALBP, both labeled with 2,6-TNS. Supported by GM-34847 (FGP), GM-51147 and DMI-9362206 (EWS), and GM-41415 (JRS).

Tu-Pos344

MULTIPHOTON PUMP-PROBE FLUORESCENCE SPECTROSCOPY BY STIMULATED EMISSION FOLLOWING EXCITATION ((C. Y. Dong, P. T. C. So, and E. Gratton)) Department of Physics, University of Illinois at Urbana-Champaign, Urbana, IL. 61801.

We are developing the technique of pump-probe fluorescence spectroscopy by stimulated emission following excitation. This method involves spatially overlapping two pulse laser sources at the sample. One beam (pump) is used to excite the molecules under study and a second beam (probe) is used to induce stimulated emission from the molecules still in the excited state. The two pulse trains are offset in frequency by an amount small compared to the laser repetition frequency. The presence of a probe beam at a different frequency means that the fluorescence from excited state molecules contains a component at the difference frequency and corresponding harmonics. The lower frequency cross-correlation signal gives us picosecond information about the response of the chromophores at high laser frequency harmonics. For spectroscopic applications, the main advantage of this sample heterodyning technique is that we can study ultra-fast phenomena at higher frequencies using the same optical detector.

In this version of pump-probe method, we propose to combine two-photon excitation and one-photon stimulated emission approach. The advantage of using two-photon excitation is superior signal to background ratio. We plan to implement this form of pump-probe spectroscopy to measure lifetime of near-UV dye DAPI. Applications to UV excitable amino acids will be discussed. This work is supported by the NIH (RR03155).

Tu-Pos345

Two-photon Excitation Cross-sections for Commonly Used Biological Fluorophores. ((Chris Xu, Jeffrey Guild and Watt W. Webb)) Applied and Engineering Physics, Cornell University, Ithaca, NY 14853

The recent development of two-photon fluorescence laser scanning microscopy for 3-D resolved real time imaging of living cells imposes an urgent need to understand the physics of two-photon excitation of fluorescent dyes. We discuss here two important aspects of two-photon fluorescence excitation. First, we report two-photon fluorescence excitation spectra and cross-sections of some commonly used biological fluorophores, such as fluorescein, rhodamine, indo-1 etc. from 690 nm to 990 nm. Several experimental approaches to measure two-photon cross-sections will be discussed. Two-photon excited fluorescence emission spectra are being measured for precise comparison with one-photon excitation. Second, fluorophore saturation is an important consideration in two-photon excitation, especially when femto-second laser pulses and high NA lenses are used because such saturation results in an expanded excitation volume, degrading image resolution by accentuating the lower intensity values of the optical point spread function relative to the peak. We have observed and are measuring two-photon saturation under femto-second pulse excitation. Its potential applications for measuring absolute values of two-photon absorption cross-section and two-photon excited fluorescence quantum efficiency are currently under investigation.

Supported by the Developmental Resource for Biophysical Imaging and Opto-electronics funded by NSF(DIR8800278), NIH(RR04224) and NIH(RR07719).

Tu-Pos346

TWO-PHOTON INDUCED FLUORESCENCE OF ALKANES. ((J.R. Lakowicz and I. Gryczynski)) Center for Fluorescence Spectroscopy, Dept. Biol. Chem., Univ. MD, Sch. of Med., 108 N. Greene St., Baltimore, MD 21201. (Spon. by M.L. Johnson).

We observed fluorescence emission from cyclohexane (CH) and methylcyclohexane (MCH) using picosecond pulses at 298-300 nm from a frequency-doubled cavity-dumped R6G dye laser. The emission maxima for CH and MCH are 209 and 215 nm, respectively, which agree with previous studies using vacuum ultra-violet (VUV) excitation near 150 nm. The fluorescence intensities depended quadratically on peak laser intensity indicating two-photon excitation. The intensity decays resulting from two-photon excitation were measured using frequency-domain fluorometry and were found to be nearly singly exponential ranging from 0.59 to 0.80 ns. We found that two-photon induced fluorescence (TPIF) of alkanes is strongly quenched by alcohol. The use of two-photon excitation circumvents the need for VUV conditions, which are not readily compatible with biochemical research. Two-photon induced fluorescence of cyclic and linear alkanes many provide new intrinsic spectroscopic probes of biological molecules.

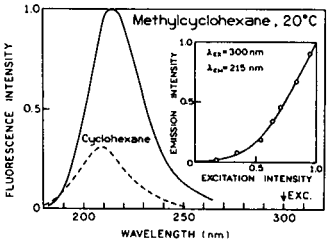

Tu-Pos347

LIGHT QUENCHING OF FLUORESCENCE USING TIME-DELAYED LASER PULSES. ((J.R. LAKOWICZ, I. Gryczynski, and J. Kuśba)) Center for Fluorescence Spectroscopy, Dept. Biol. Chem., Univ. MD, Sch. of Med., 108 N. Greene St., Baltimore, MD 21201. (Spon. by J.R. Lakowicz).

We describe experimental observations of fluorescence quenching by time-delayed light pulses whose wavelength overlaps the emission spectrum of 4-dimethylamino-4'-cyanostilbene (DCS). The relative cross sections for light quenching were proportional to the amplitude of the emission spectra at the light quenching wavelength. The frequency-domain intensity and anisotropy decays showed oscillations resulting from time-delayed light quenching. The amplitude of the oscillations depends upon the amount of light quenching. The frequency of the oscillations depends upon the delay between the excitation and quenching pulses. We also examined the emission spectra and wavelength-dependent anisotropies of DCS, a solvent sensitive fluorophore, under condition of light quenching. Illumination on the long-wavelength side of the emission spectrum with a time-delayed quenching pulse resulted in a blue shift of the emission spectrum, and a progressive decrease of the emission anisotropy as the observed wavelength approached the quenching wavelength. Spectral shifts and wavelength-dependent anisotropies of DCS are more pronounced in solvents where spectral relaxation is incomplete during the excited state lifetime. Light quenching of fluorescence is thus shown to provide a means to control the number and orientation of the excited fluorophores. The use of multiple light pulses for excitation and quenching can have far reaching applications in the use of time-resolved fluorescence in physical chemistry and biophysics.

Tu-Pos348

A MULTILENGTH, DUAL POLARIZATION FLUORESCENCE DECAY INSTRUMENT WITH BOTH TCSPC AND ANALOG CHANNELS.
((J. XIAO)) LCB, NHLBI, NIH, BETHESDA, MD 20892.

Collection of multiple decay curves for global analysis of DAS (decay associated spectra) and anisotropy parameters during biochemical reactions, beginning with 'KINDK' experiments in the Brand lab, has become a powerful tool for biochemistry. To reduce cost/channel and extend such instruments, we have built a system based on a fast CAMAC time-to-digital converter (TDC) capable of simultaneous 16 channel acquisition (Phillips 7186). Excitation is by frequency doubled pulses from a synch-pumped, cavity-dumped dye laser (S/P 3520) coupled into a Biologic SFM-3 stopped-flow cuvette. Emission is split by a Rochon prism according to polarization and introduced into an imaging spectrometer (SPEX 270M).

Currently, a multianode microchannel plate PMT (HR R3841-07) detects 8 channels (wavelengths) for each polarization. Each anode event is amplified and discriminated into a TDC start channel. Stop rate reduction logic is assembled from NIM modules. The maximum count rate per TDC/list-sequencer is ca. 35Khz. To achieve single 'shot' monitoring of very fast (sub 100 ms) reactions, we have added two fast gated integrators to collect broadband decays of both polarizations. Application to protein-protein, protein-DNA and folding problems will be discussed.

Tu-Pos349

CONSTRUCTION AND PERFORMANCE OF A FRAP INSTRUMENT WITH MICROSECOND TIME RESOLUTION: APPLICATION TO DEXTRAN DIFFUSION IN CYTOPLASM. ((H. Pin Kao and A.S. Verkman)), U.C.S.F., San Francisco, CA.

Fluorescence recovery after photobleaching (FRAP) is a well established method to measure the diffusive and directed mobilities of ensembles of fluorescent particles in biological systems. In systems where particle mobility is high or the measured region size is small, rapid recoveries are expected, with recovery half times of < 500 μs. A FRAP apparatus was constructed to measure recoveries of ≥ 50 μs. The probe beam and photobleaching pulse were formed by modulating the intensity of a 488 nm laser using two acousto-optic modulators in series. The maximum intensity modulation was $> 10^6$:1 with a rise time of < 1 μs and a minimum pulse width of 6 μs. The signal was detected by a photomultiplier, amplified by a transimpedance amplifier and digitized at 1 MHz. During the photobleaching pulse, the photomultiplier gain was reduced by ≈ 1600 by switching the second dynode to the cathode voltage by computer control of 2 bidirectional MOSFET optoisolators. This apparatus was applied to examine the dependence of dextran diffusion in cytoplasm on photobleaching spot size. The diffusion of FITC labeled dextrans (10, 150, 500 kD) in the cytoplasm of Swiss 3T3 fibroblasts was measured with laser spot diameters of 0.96, 1.6 and 2.4 μm. Diffusion was strongly dependent on dextran size, but independent of laser spot size, indicating that any cytoplasmic domains which hinder dextran mobility must exist on a scale of < 1 μm.

Tu-Pos350

PHOSPHORESCENCE QUENCHING AS A METHOD FOR STUDYING OXYGENATION OF HETEROGENEOUS OBJECTS. **((S.A.Vinogradov and D.F.Wilson)) Department of Biochemistry and Biophysics, School of Medicine, University of Pennsylvania, Philadelphia, PA 19104.**

Pd, Pt and lanthanide porphyrins phosphores with high quantum yields and lifetimes long enough to allow quantitative measurements of oxygen pressure by the oxygen dependent quenching of phosphorescence. The application of this method to measurements of oxygen in living tissue has recently been extended through synthesis of porphyrins which have strong absorption and emission in the near infra red, making possible measurements through *cm* thickness of tissue. Further chemical modification of these porphyrins has provided water soluble phosphorescent probes which can readily be introduced into biological systems and are not toxic to the tissue.
For homogeneous samples, the phosphorescence emission following a flash of excitation light decays exponentially and its characteristic lifetime is reciprocally related to the concentration of quencher (Stern-Volmer relationship). For heterogeneous samples, such as tissue *in vivo*, the phosphorescence decay law is a convolution of many single exponentials, each representing a tissue volume with a specific oxygen concentration. Thus the phosphorescence decay contains information on the oxygen pressures in all regions of the tissue measured and the relative fraction of the tissue with each oxygen pressure. Deconvolution of the phosphorescence decay can, in theory, provide a complete histograms of the distribution of oxygen pressures within the tissue. We have used quadratic programming principles to obtain a robust, computationally fast and efficient algorithm which can correctly recover the tissue oxygen distribution (histogram). This method can provide important new insight into the function and regulation of the microvascular system. (Supported by grants 2R44-NS30265 and PO1-CA56679 from NIH).

Tu-Pos351

THE SPECTROSCOPY OF THE SKIN'S ULTRAVIOLET CHROMOPHORE UROCANIC ACID. ((Kerry M. Hanson, Bulang Li, Cynthia Hayne and John D. Simon)). Department of Chemistry and Biochemistry, University of California San Diego, La Jolla, CA 92037-0341.

Because of an absence of epidermal urocanase, histidase acting upon histidine leads to the accumulation of urocanic acid (UA) in the stratum corneum.

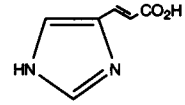

This molecule behaves as an ultraviolet chromophore, where the naturally occuring *trans*-UA isomerizes to its *cis* form upon photolysis with ultraviolet B (UVB) radiation. Although this isomerization has led to conjecture over whether or not photolysis of UA has either protective or immunosuppressive effects, the wavelength dependent photodynamics are not well understood. Fluorescence, resonance Raman and time-resolved laser experiments will be presented on *in vitro* samples of UA. Progress toward the development of a comprehensive model of the photodynamics of UA will be discussed.
Supported by NIH Grant GM41942.

Tu-Pos352

DETECTION OF CONFORMATIONAL CHANGES IN THE LOW MOLECULAR WEIGHT GTP-BINDING PROTEIN CDC42HS BY FLUORESCENCE SPECTROSCOPY. ((David A. Leonard, Richard A. Cerione, and Danny Manor)) Department of Pharmacology, Cornell University, Ithaca, NY 14853 (Spon. by J.W.Erickson)

Cdc42Hs is a low molecular weight GTP-binding protein of the ras superfamily, and has been implicated in cell growth regulation. We have shown that the fluorescence of the single tryptophan of Cdc42Hs (W97) is sensitive to the nucleotide state of the protein. The GTP-bound form of this G-protein shows a slow exponential increase in fluorescence to a level that is equivalent to the fluorescence emission of the GDP-bound form. Neither the GDP- or GMP-PCP-bound forms exhibit any change in fluorescence over time, indicating that the change seen when GTP is bound may represent a conformational change that occurs during the hydrolysis of GTP to GDP.

Comparisons of the fluorescence increase with radioactive GTP-hydrolysis filter assays indicate that this conformational change follows the release of inorganic phosphate from the active site. The coupling of a hydrolysis-dependent conformational change to a spectroscopic assay allows us to follow both intrinsic and GAP (GTPase Activating Protein)-accelerated hydrolysis in real time. We have used this assay combined with molecular deletion analysis to determine a 22 kDa limit catalytic domain for Cdc42-GAP.

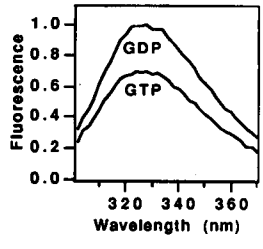

Tu-Pos353

PURIFICATION AND CHARACTERIZATION OF BOVINE CERULOPLASMIN ((C.A. Goode, K.A. Kantardjieff, K. Letson, C.Bula, R. Igarashi, M. MacMurray, Q. Truong and S. Sedighi)) Department of Chemistry, California State University, Fullerton, CA 92634. NSF MBC-9317963 and NIH GM08258. (Spon. by K.A. Kantardjieff)

Purification of bovine ceruloplasmin (Cp), a serum protein implicated in copper transport, results in several different isoforms. The *in vivo* relevance of these various forms is unclear, although it is probable that at least one of these various forms is the result of delivery of copper to cells. A homogeneous, well-characterized protein is essential to our study of Cp-receptor interaction, circular dichroism analysis (CD) and structure determination by x-ray diffraction. Satisfactory purification has been achieved using FPLC with DEAE column and potassium phosphate gradient, followed by high resolution gel permeation chromatography or fractionation with ammonium sulfate. Capillary electrophoresis has been a powerful tool for rapid analysis and quantitation during purification. Proteins with apparent molecular weights of 130 kDA and 115 kDA have been identified as Cp, based on blue color, absorbance at 610 nm and oxidase activity. These proteins have been found to be rich in β structure by far ultraviolet CD and have visible CD spectra characteristic of blue copper proteins, due to the presence of Type I and Type III copper. Small crystals for diffraction analysis have been produced by vapor diffusion.

Tu-Pos354

HUMAN HEART (R)-3-HYDROXYBUTYRATE DEHYDROGENASE EXPRESSED IN INSECT CELLS ((Johannes Moeller[#], David Green[+], Roy Jensen[**], Wolfgang E. Trommer[#], Andrew R. Marks[+], Sidney Fleischer[#] and J. Oliver McIntyre[#])) Dept. of Mol. Biol, Vanderbilt Univ., Nashville TN 37235, [+]Memorial Sloan-Kettering Cancer Center, New York, NY, [#]Univ. of Kaiserslautern, Kaiserslautern, Germany, [+]Mt. Sinai School of Medicine, New York, NY and [**]Vanderbilt School of Medicine, Nashville TN.

(R)-3-Hydroxybutyrate dehydrogenase (BDH) is a lipid-requiring mitochondrial enzyme with an absolute requirement of phosphatidylcholine (PC) for function. PC serves as an allosteric activator to enhance NAD(H) binding to BDH. We have previously reported expression of catalytically active human heart (HH) BDH in insect cells (Sf9, *Spodoptera frugiperda*) transfected with BDH-cDNA in baculovirus [Green et al., Biophys. J. 66, A267 (1994)]. The mature form of BDH is expressed to about 1% of total cell protein and is localized in the particulate fraction of the Sf9 cells. Expressed HH-BDH is active and can be solubilized from the Sf9 cell membrane fraction using phospholipase A_2 digestion; ~50% activity was recovered in the supernatant after reconstitution with phospholipid vesicles containing PC. Significant purification of HH-BDH has been achieved using methodology similar to that developed for bovine heart BDH including adsorption chromatography on controlled pore glass. Studies to complete the purification and characterization of expressed HH-BDH are in progress. (NIH HL 32711)

Tu-Pos355

ADENOSINE DEAMINASE COMPLEXING PROTEIN EXHIBITS A REGULATORY ROLE ON ADA ACTIVITY. ((S. Ra've, Y. Roth, M. Zamai, R. Cohen-Luria, N. Porat, A.H. Parola)) Department of Chemistry, Ben-Gurion University of the Negev, P.O. Box 653, Beer-Sheva, 84105, Israel.

Adenosine deaminase (ADA) catalyzes the irreversible hydrolytic deamination of adenosine and deoxyadenosine to inosine and deoxyinosine, respectively, and ammonia. The quarternary structure of its large form consists of two small 45 kD catalytic subunits (SS-ADA) and a large 210 kD membranal complexing protein (ADCP), presumably, a dimer of 110 kD. ADCP=CD26 activates T-lymphocytes and has DPPIV activity, but its binding role to SS-ADA is not clear, yet . In an attempt to explore whether ADCP has a regulatory effect on ADA activity, we examined the activity of SS-ADA bound to ADCP on the cell membrane and in lipid free aqueous solution. Using ^{125}I-SS-ADA, about 50% reduction in the activity of ADA bound to chick embryo fibroblasts (CEF) was observed. In CEF transformed by Rous Sarcoma Virus, the reduction in activity of bound ADA reached up to 80-90%. In aqueous solution the effect of binding to ADCP on SS-ADA enzymatic activity was followed spectrophotometrically. In the presence of 1-100 μM adenosine, the addition of ADCP in molar ratios of 5:1 or 10:1 ADCP to SS-ADA, resulted in 40±5% inhibition in ADA activity. However, in the presence of higher adenosine concentrations (200-1000 μM) and the above molar ratios of ADCP to SS-ADA, 20-30% activation of ADA was found. A kinetic model based on allosteric regulatory mechnism is explored.

Tu-Pos356

PICOSECOND TRANSIENT ABSORPTION STUDIES OF THE PHOTOMODULATING ENZYME NITRILE HYDRATASE. ((Kerry M. Hanson, Bulang Li, John G. Cummings*, Mark J. Nelson* and John D. Simon)). Department of Chemistry and Biochemistry, University of California San Diego, La Jolla, CA 92037-0341, *DuPont, Central Research and Development, Wilmington, DE 1988-0328.

The nitrile hydratases (NHase) compose a class of enzymes that catalyze the hydration of nitriles to their related amides. Ultraviolet photolysis of inactive NHase leads to the photoactivation of the enzyme where and Fe (II) cofactor becomes oxidized to Fe (III) within the protein subunits. We will present picosecond transient absorption data that quantifies the kinetics of the electron transfer process. Related experiments addressing the mechanistic details of this reaction will be discussed.

Tu-Pos357

EFFECT OF TEMPERATURE AND PH ON THE ALLOSTERIC PROPERTIES OF PHOSPHOFRUCTOKINASE FROM *BACILLUS STEAROTHERMOPHILUS* ((V. L. Tlapak-Simmons and G. D. Reinhart)) Dept. of Chem. & Biochem., Univ. of Oklahoma, Norman, OK 73019. (Spon. by D. M. Jameson)

The allosteric properties of phosphofructokinase from *B. stearothermophilus* have been studied in the pH and temperature ranges from 5 to 9 and 6 to 40°C, respectively. The variation of V and V/K with pH suggests that the deprotonation of a single residue is required for full enzymatic activity. The dissociation constants for Fru-6-P, MgADP and PEP all increase, however, when the pH is raised. The coupling constants, which describe the magnitude of the allosteric effect, reveal that as the pH is increased both MgADP and PEP become better activator and inhibitor, respectively. Not only does the activation produced by MgADP weaken as pH decreases, but at low pH and temperature, MgADP actually becomes an inhibitor. PEP also weakens in its effectiveness as an inhibitor at low pH and temperature indicating that MgADP is not simply binding to a predominant "T-form" under these conditions. The inversion of MgADP's effects can instead be easily explained as arising from the largely compensating ΔH and ΔS contributions to the coupling free energy that are perturbed in a systematic manner by pH and temperature. Supported by grant GM33216 from NIH.

Tu-Pos358

ANALYSIS OF THE DYNAMICS OF E. COLI PHOSPHOFRUCTOKINASE TRYPTOPHAN-SHIFTED MUTANTS AS MONITORED BY TRYPTOPHAN FLUORESCENCE. ((F. Janiak-Spens and G. D. Reinhart)) Department of Chemistry and Biochemistry, University of Oklahoma, Norman, OK 73019

Phosphofructokinase from *E. coli* is a homotetramer that contains a single tryptophan per subunit. Using site-directed mutagenesis a series of double mutants have been generated in which the native tryptophan has been replaced with a phenylalanine and a native phenylalanine has been replaced by tryptophan. These "tryptophan-shifted" mutants exhibit catalytic and regulatory properties that are similar to the wild-type enzyme. The mobility of the tryptophans in the mutants in the presence and absence of substrates and allosteric ligands has been determined using time-resolved fluorescence spectroscopy. Local changes in mobility, as monitored by the tryptophan, have been observed throughout the enzyme and these changes have been found to be distinctly different in each mutant. Taken together these local changes provide a more comprehensive picture of the dynamics of the various ligated enzyme forms than that provided solely by the wild-type tryptophan. As such they will present a more thorough test of the hypothesis that changes in the enzyme's dynamics produced by the binding of the various ligands contribute to the coupling entropy that in turn helps to establish the nature and magnitude of an allosteric effect. Supported by grant # GM33216 from the NIH.

Tu-Pos359

TRYPTOPHAN ROTAMERS IN CRYSTALLINE RIBONUCLEASE T1 IN THE PRESENCE AND ABSENCE OF 2'-GMP; A Time-Resolved Fluorescence Study. ((T. E. S. Dahms*, A. J. Bruckman† and A. G. Szabo†)) *Ottawa University, Ottawa, Ont. CA K1H 8M5 †University of Windsor, Windsor, Ont. CA N9B 3P4. (Sponsored by C. Hutnik)

Ribonuclease T1 (RNT1) from *Aspergillus oryzae* has been purified by HPLC and its identity has been verified by electro-spray ionization mass spectrometry. The spectrophotometric assay of RNT1 showed the enzyme to be active. Solution studies were conducted at a pH consistent with those used for crystallization (7.2 for inhibitor free, 5.2 for 2'-GMP bound) to facilitate comparison between the solution and crystal data. The time-resolved fluorescence decay of RNT1 under the aforementioned conditions was consistent with previous studies [Chen et al. (1993) *Biophys. J.* **51**, 865.]. The latter study proposed that for RNT1 in the presence of 2'-GMP or at a pH higher than 5.5, the fluorescence data could be interpreted as two Trp conformational states. Earlier studies from this laboratory have demonstrated the existence of Trp rotamers in single protein crystals. Therefore, the fluorescence of RNT1 single crystals was studied in the presence and absence of 2'-GMP, in order to further investigate the RNT1 model. As expected, three decay times best describe the fluorescence decay of crystalline RNT1 in the presence of 2'-GMP (pH 5.2). The two decay times which are attributed to Trp 59 are shorter in the crystalline state and the decay time assigned to 2'-GMP is longer when compared to solution values. Each decay-time relative proportion varies with crystal orientation providing direct evidence for two Trp side chain conformations both in solution and in the crystalline state. Although Trp 59 has been modelled as one conformation in crystals at pH 7.0 [Martinez-Oyanedel *et al.* (1991) *J. Mol. Biol.* **222**, 335.], minimum perturbation mapping studies suggest that the Trp 59 side chain may exist in two conformations [Haydock *et al.* (1994) *Biophys. J.* **66**, A165.]. The time-resolved fluorescence of RNT1 inhibitor-free crystals (pH 7.2) will be used in comparison with solution values and may provide further insight into the origin of Trp fluorescence deactivation pathways by proteinaceous environments.

Tu-Pos360

ENZYMATIC RESOLUTION OF D AND L ENANTIOMERS OF 7-AZATRYPTOPHAN AND ENZYMATIC SYNTHESIS OF N-ACETYL-L-7AZATRYPTOPHANAMIDE. ((A.G. Szabo[1]*, J.D. Brennan[1], C.W.V. Hogue[2] and B. Rajendran[1])) [1]Department of Chemistry and Biochemistry, University of Windsor, Windsor, Ontario, N9B 3P4, Canada, [2]Department of Biochemistry, University of Ottawa, Ottawa, Ontario, K1H 8M5, Canada.

The separation of D and L enantiomers of 7-azatryptophan is not possible using HPLC conditions that normally are used to separate enantiomers of amino acids. However, reaction of D,L-7AW with chloroacetic acid to produce N-chloroacetyl-D,L-7AW, followed by stereospecific proteolytic digestion of the N-chloroacetyl derivative of D,L-7-azatryptophan produced the free L-7-azatryptophan which could be separated from unreacted N-chloroacetyl-D-7AW by reversed phase HPLC. Preparation of the D enantiomer of 7AW was effected by a different route. D,L-7AW was reacted with the enzyme tryptophanyl-tRNA synthetase of *B. subtilis* (TrpRS) in the presence of adenosine-5'-triphosphate (ATP), Mg^{2+}, and ammonium carbonate. Under these conditions the L-7AW reacts stereospecifically to form L-7-azatryptophanamide (L-7AWA). The L-7AWA was separated from D-7AW by reversed phase HPLC. Reaction of L-7AWA with acetic anyhdride produced N-acetyl-7-azatryptophanamide (NA7AWA), the 7AW equivalent of NATA. Identication of the L and D enantiomers of 7AW was accomplished using a new assay method. TrpRS reacts sterospecifically with L-7AW in the presence of ATP and Mg^{2+} to form a highly fluorescent complex. Detection of this complex is based on its enhanced fluorescence at 315 nm excitation, 360 nm emission after the addition of ATP. This reaction confirmed the presence of pure L-7AW or D-7AW. The results of steady-state and time-resolved fluorescence measurements of D-7AW, L-7AW, L-7AWA and NA-L-7AWA in H_2O at various pH values will be presented and compared to results from the corresponding tryptophan derivatives.

Tu-Pos361

CONSTRUCTION, PROPERTIES, AND SPECIFIC FLUORESCENT LABELING OF A BOVINE PROTHROMBIN MUTANT ENGINEERED WITH A FREE C-TERMINAL CYSTEINE ((Q. Chen & B.R. Lentz)) Dept. of Biochemistry & Biophysics, Univ. of North Carolina, Chapel Hill, NC 27599-7260.

The activation of prothrombin to thrombin is a key membrane-controlled reaction of the blood coagulation cascade. A recombinant bovine prothrombin has been constructed, characterized, and shown to have a roughly native-like conformation. Specific labeling of this molecule was achieved by introducing a cysteine to replace the penultimate residue (Gly580) at the C-terminal end of a previously constructed active site mutant ((Ser528-Ala); Pei et al, 1991, J. Biol. Chem. 266, 9598-9604). The double mutant was expressed in Chinese hamster ovary cells at the level of 0.6-0.8 ug/ml of cell cultural medium. Specific labeling with fluorescein maleimide (FM) was accomplished by limited reduction with DTT to free the engineered cysteine. The stoichiometry of labeling was 0.84 probe/protein. The location of the probe at the C-terminal was confirmed by proteolysis by factor X_a and by carboxypeptidase Y. Both the double mutant and labeled prothrombin could be activated to thrombin by Taipan snake venom and to meizothrombin by ecarin from *E. carinatis* venom, but, as expected, the double mutant meizothrombin did not autolyze as does native prothrombin. The initial rate of activation of double mutant prothrombin by the fully assembled prothrombinase was 55% of that of native prothrombin. As expected, the isolated double mutant activation product showed no amidolytic activity toward a thrombin-specific synthetic chromogenic substrate (S2238). The double mutant thrombin bound to a thrombin active-site inhibitor (dansylarginine-N-(3-ethyl-1,5-pentanediyl)amide), but with lower affinity ($K_d = 3.9 \times 10^{-4}$ M) than observed with native thrombin ($K_d = 1.3 \times 10^{-8}$ M). These results demonstrate for the first time that a native-like but specifically labeled prothrombin has been constructed. This molecule will be an essential tool for elucidating the structural role of membranes during prothrombin activation. In addition, the methods described might be usefully applied to labeling of an odd, engineered cysteine in other disulfide bond-containing proteins. *Supported by USPHS grant HL45916 to BRL.*

Tu-Pos362

FLUORESCENCE STUDIES ON HIV-1 PROTEASE. ((E.D. Matayoshi, K.M. Swift, H.J. Huffaker, T.F. Holzman, R. Edalji, R.L. Simmer, R. Helfrich)) Abbott Laboratories, Pharmaceutical Discovery Research, Dept. of Structural Biology, Abbott Park, IL 60064.

The protease from human immunodeficiency virus 1 (HIV-1 PR) is essential for the maturation of infectious virus and has thus been targeted in the search for selective AIDS therapeutics. It is a homodimeric aspartyl protease consisting of 11 kDa subunits which by themselves are enzymatically inactive. Drug design strategies have been directed at either active site inhibition or at the disruption of dimer assembly. HIV-1 PR activity, inhibitor binding, and dimer stability are sensitive to ionic strength and pH. We have examined the effect of these parameters on the PR by utilizing the fluorescence of native Trp residues 6 and 42, or of a tetramethylrhodamine (TMR) probe attached to Cys 67. Time resolved fluorescence lifetime and anisotropy decay determinations can provide conformational and dynamic information on the PR in a direct way under conditions which are difficult to study by other means. We have observed that the fluorescence anisotropy of TMR-labeled PR is unchanged over PR concentrations down to at least 1 nM at pH 5.5 and 7.5, thus implying a subnanomolar affinity constant between monomers. The time resolved Trp decay at pH 5.5 and low ionic strength is biexponential, consisting of 5.2 ns (90%) and 1.8 ns (10%) components. Both lifetimes and their rotational dynamics change substantially with increasing ionic strength or pH. We have also deduced effects on monomer/dimer conformation from PR fluorescence quenching experiments with I^-.

Tu-Pos363

^{13}C NMR ASSIGNMENTS OF THE HEMIKETAL DERIVATIVE OF [U-^{13}C,^{15}N] PQQ AND METHANOL ((B. Mark Britt and Clifford J. Unkefer)) CST-4 MS C345, Los Alamos National Laboratory, Los Alamos, NM 87545

Pyrroloquinoline quinone (PQQ) has been identified as the prosthetic group of a number of bacterial enzymes involved in the oxidation of methanol and glucose including the methanol dehydrogenase from *Methylobacterium extorquens*. This enzyme employs a reaction cycle that involves the two-electron oxidation of methanol to formaldehyde and two subsequent one-electron oxidations of the two-electron reduced PQQ which *in vivo* are facilitated by cytochrome c_L. Two general mechanisms have been proposed to account for the enzyme's activity: one requires the formation of a hemiketal intermediate between the methanol and the C-5 carbon of the fully oxidized PQQ; the alternate mechanism involves the transfer of electrons from the substrate to the PQQ without the formation of a covalent intermediate. In addition, several mechanisms have been proposed that involve a role for the C-4 quinone function in releasing the formaldehyde product from the hemiketal intermediate and the fully reduced PQQ. However, to date there is little evidence for the formation of the hemiketal intermediate. The purpose of the present study is to test the feasibility of the intermediate mechanism by studying the nature of the interaction of methanol with PQQ as a prerequisite to further studies with the enzyme-bound prosthetic group. [U-^{13}C,^{15}N] PQQ was prepared and ^{13}C-^{13}C COSY spectra were obtained of the acid form in DMSO and of the tri-tetrabutlyammonium salt in DMSO to establish the spectral shifts that accompany deprotonation. The salt was then dissolved in CD_3OH and all spectral shifts identified in the resulting ^{13}C-^{13}C COSY spectrum. All shifts identified are consistent with the proposed hemiketal structure of the intermediate. There is no evidence for hemiketal formation on the C-4 quinone.

Tu-Pos364

EPR AND ENDOR CHARACTERIZATION OF THE TYROSYL RADICALS IN PGH SYNTHASE ((W. Shi, C.W. Hoganson, A.-L. Tsai¶, G.T. Babcock)) Department of Chemistry, Michigan State University, East Lansing, MI 48824; ¶ University of Texas Health Science Center, Houston, TX 77225

Tyrosyl Radicals have been previously observed by electron paramagnetic resonance (EPR) spectroscopy in reactions of either arachidonic acid or various hydroperoxides catalyzed by prostaglandin H (PGH) synthase. The radicals trapped under different conditions can be summarized into three categories based on their EPR signal appearances: the wide-doublet (WD), the narrow-singlet (NS), and the wide-singlet (WS). Line broadening of the hyperfine structures of the EPR spectra imposed difficulty in interpretation and revelation of conformations of the radical species. In this study, we examined the radicals by carrying out low temperature electron nuclear double resonance (ENDOR) experiments equipped with conventional frequency-modulated (FM) as well as novel transient and rapid passage detection methods. An analysis of the ENDOR signals of the strongly coupled β-methylene protons, whose hyperfine couplings are uniquely defined by the configuration of the radicals, allows us to unambiguously characterize and identify these tyrosyl radical species. The results, together with a kinetics study, establish that only the WD and NS tyrosyl signals observed in EPR spectroscopy have distinct side-chain conformations and the WS is, in fact, a mixture of the other two. This conclusion is consistent with a computer simulation work published previously [1]. Together with recent mutagenesis studies, the two distinct tyrosyl radical species are proposed to originate from two individual sites which are both near the heme of the enzyme.

[1] DeGray, J. A., et al, *J. Biol. Chem.*, **267**, 23583 (1992)

Tu-Pos365

CRYSTAL STRUCTURE OF THE Y165F MUTANT OF E. COLI ASPARTATE TRANSCARBAMYLASE. ((Y. Ha and N. M. Allewell)) Department of Biochemistry, University of Minnesota, St. Paul MN 55108. (Spon. by R. A. Nash)

Single site mutations of E. coli aspartate transcarbamylase have very varied effects on ligand affinity, catalytic efficiency and regulation by nucleotides. The structural basis of these effects is as yet poorly understood. We have determined the crystal structure of Y165F which has a mutation at the interface between catalytic subunits and whose functional parameters have a very unusual pH dependence [Yuan et al., Biophys. J. 66, A264 (1994)]. The space group was R3, the resolution 2.6 Å and the R value 0.194. This mutant has a unique tertiary structure, in which the 240s loop, which swings towards the active site in the T->R transition of the wild type enzyme, shifts about 3 Å in the opposite direction. The positions of some sidechains shift by several Å and numerous changes in hydrogen bonding occur. The structural changes propagate to the active site and subunit interfaces, providing a possible explanation for the low catalytic activity and altered allosteric properties of this mutant. Supported by NIH grant DK-17335 to NMA.

Tu-Pos366

THE STRUCTURE OF THE ISOLATED CATALYTIC DOMAIN OF DIPHTHERIA TOXIN. ((M.S. Weiss[1], S.R. Blanke[2], R.J. Collier[2] and D. Eisenberg[1])). [1]Molecular Biology Institute, UCLA, Los Angeles, CA 90024; [2]Department of Microbiology and Molecular Genetics, Harvard University, Boston, MA 02115.

The structure of the isolated catalytic domain of diphtheria toxin (DT) at pH 5.0 was determined at 2.5 Å resolution and refined to an R-factor of 19.7%. The domain is bound to its endogenous inhibitor adenylyl-(3'→5')uridine 3'-monophosphate (ApUp). The structure of this 190 residue domain is essentially identical to the structure of the catalytic domain within whole DT determined at pH 7.5. However, there are two adjacent surface loops that exhibit clear differences when compared to the structure of the catalytic domain in whole DT. Although both loops are at the surface of the protein and are relatively flexible, the chain trace is well defined in the electron density. We ascribe this structural change mainly to the absence of the neighboring transmembrane domain in the isolated catalytic domain as compared to whole DT. The changes are described in detail and their implications for membrane translocation are discussed.

Tu-Pos367

ELECTRON CRYSTALLOGRAPHY REVEALS THE CTD OF RNA POLYMERASE II ((G.D. Meredith, W.H. Chang, S.A. Darst*, Y. Li, D.A. Bushnell, R.D. Kornberg)) Department of Structural Biology, Stanford, CA 94305-5400
*The Rockefeller University, New York, NY 10021.
(Spon. by C.L. Poglitsch)

Negatively-stained two-dimensional co-crystals of S. cerevisiae core RNA polymerase II and an Fab fragment on positively charged lipid layers diffract beyond 20 Å. The Fab fragment binds an epitope at the base of the carboxy-terminal domain (CTD) of the enzyme's largest subunit. There is a single peak, greater than 3 standard deviations, in the difference map between the Fab bound and native enzyme. This site is independently corroborated by a similar analysis on RNA polymerase II lacking the CTD. This is the first localization of a functionally important domain of RNA polymerase II.

Tu-Pos368

AN ACTIVE SITE GLUTAMIC ACID OF *BACILLUS CIRCULANS* XYLANASE HAS A pK_a OF 6.8; FTIR EVIDENCE. ((J. Davoodi[1], W. W. Wakarchuk[2], R. L. Campbell[2], P. R. Carey[1], and W. K. Surewicz[2])) 1. Department of Biochemistry, Univ. of Ottawa, Ottawa, Ontario K1H 8M5 Canada. 2. Institute for Biological Sciences, National Research Council of Canada, Ottawa, Ontario K1A 0R6 Canada.

We have previously reported that glutamic acids 78 and 172 are crucial for catalytic activity of the *Bacillus circulans* xylanase (1,4-β-D-xylanohydrolase, EC 3.2.1.8) with molecular weight of 20 kDa [Wakarchuk, W. W., Campbell R. L., Sung, W. L., Davoodi, J., and Yaguchi, M. (1994) Protein Science 3, 467-475.]. Here we show that for the wild type enzyme an acid side chain titration occurs at pH 6.8 in the FTIR spectrum. This titration is absent in both of the forms E78Q or E172Q and this evidence, taken with X-ray crystallographic data, indicates that glutamic acid 172 has a pK_a of 6.8. This high pK_a value is ascribed to the proximal glutamic acid 78 side chain. The presence of two nearby negatively charged side chains leads to some destabilization of the protein as evidenced by calorimetric measurements. Decreasing pH or removing either Glu 172 or Glu 78 enhances protein stability by decreasing or removing this electrostatic repulsion.

Tu-Pos369

Simulation studies of the phospholipase A2--membrane interactions: desolvation effect of the membrane surface and the role of charge--charge interactions ((F. Zhou and K. Schulten)) Beckman Inst., 405 N. Mathews, Urbana, IL61801

The interaction between the human synovial phospholipase A2 and the membrane bilayer has been studied by molecular dynamics simulation. The model of PLA2--DLPE and DLPE--POPC membrane complexes were constructed by placing the interfacial recognition site of PLA2 on membrane surface, with different penetration depth into the bilayer. Binding of the PLA2 caused slight reorganization of the lipid head groups, but had little effect on the protein structure and the lipid hydrocarbon structure. 2--3 lipid molecules were found to be desolvated when PLA2 was tightly bound to the membrane surface, due to the hydrophobic residues in the interfacial recognition site, and the dielectric constant of the microinterface was found to be decreased . No such effects were found when PLA2 was loosely bound. Both free energy calculations and continuum electrostatics calculation suggested that PLA2 favors binding on negatively charged membrane surface, but the preference for such lipids only occur on part of the interfacial recognition site, ie., the membrane binding surface of the protein is electrostatically inhomogenious. Calculations suggest that negatively charges on membrane surface induces a tight association of PLA2 with the lipid head groups, and causes a subsequent desolvation of a few lipids, and therefore, the well--known surface activation of PLA2.

Tu-Pos370

THE AFFINITY FOR CA^{2+} OF *A. P. PISCIVORUS* PHOSPHOLIPASE A_2 INCREASES OVER THREE ORDERS OF MAGNITUDE DURING RAPID HYDROLYSIS OF LARGE UNILAMELLAR VESICLES. ((B.K. Lathrop, G.S. Rule, and R.L. Biltonen)) University of Virginia, Department of Pharmacology, Charlottesville, VA 22908.

Phospholipase A_2 from *A. p. piscivorus* (PLA_2), when catalyzing the hydrolysis of large unilamellar vesicles of dipalmitoylphosphatidlycholine (LUVs), demonstrates a lag time prior to a rapid acceleration in velocity referred to as a "burst". A 120 percent increase in intrinsic fluorescence occurs simultaneously with this burst. We have sought to understand the nature of this fluorescence change by genetically modifying the three tryptophan residues in this enzyme.

Recombinant PLA_2 ($rPLA_2$) has been expressed and shows identical enzymatic properties and one-dimensional NMR spectra as venom ($vPLA_2$). Site-directed mutagenesis was used to construct the following enzymes: W20F, W31F, W119Y and W20F:W119Y (W31+). All enzymes showed kinetic parameters equivalent to $vPLA_2$ within a factor of three. All enzymes bound small unilamellar vesicles (SUVs) equivalently and showed a lipid-dependent increase in fluorescence. All enzymes except W31F showed a calcium-dependent increase in intrinsic fluorescence.

The fluorescence of W31+ was sensitive to changes in the occupancy of the Ca^{2+} binding site when catalyzing the hydrolysis of LUVs. The lag time was dependent on Ca^{2+} concentrations in the millimolar range, but the magnitude of the Ca^{2+}-dependent fluorescence change was independent of Ca^{2+} concentration above 3 μM. This result demonstrates that the affinity of Ca^{2+} for PLA_2 or the enzyme-substrate complex increases at least three orders of magnitude at the burst. (Supported by NSF and NIH.)

Tu-Pos371

AN EXPRESSION SYSTEM FOR SELENOMETHIONINE-LABELED BOVINE PANCREATIC PHOSPHOLIPASE A_2

((J. Ahn and M. Caffrey)) Chemistry Dept., The Ohio State University, Columbus, OH 43210.

Phospholipase A_2 (PLA2, E.C. 3.1.1.4) catalyses the hydrolysis of the ester linkage at the *sn*-2 position of membrane forming phospholipids to release a fatty acid and a lysophospholipid. PLA2 has peripheral membrane protein-like characteristics. The long-term objective of this project is to establish the assorted membrane topologies of PLA2 with x-ray standing waves (XSW) as the primary tool. The XSW approach is optimally suited for use with a test protein that contains intrinsic and/or extrinsic heavy atoms which act as structural benchmarks. Thus, an expression system for selenomethionine-labeled PLA2 using bacteriophage T7 RNA polymerase was constructed. With it, highly purified native (Met^8-) and Se-Met^8-PLA2 were obtained based on SDS-PAGE analysis combined with Coomassie Blue staining. The activity of the two proteins are comparable as judged by enzyme kinetic assay on dioctanoyl phosphatidylcholine (DC_8PC) micelles using a home-built pH-stat (native PLA2: k_{cat} = 675 s^{-1}, K_m = 1.4 mM; Se-Met^8-PLA2: k_{cat} 325 s^{-1}, K_m = 0.7 mM). Accordingly, this minimally perturbed and labeled protein is a suitable model for use in XSW membrane topology studies of PLA2.

Supported by NIH DK 45295

Acknowledgements: We thank Dr. M-D. Tsai (The Ohio State University, Columbus, OH) for providing the PLA2 synthetic gene used in this project.

Tu-Pos372

MEMBRANE POTENTIAL REGULATES SEA URCHIN SPERM ADENYLYL CYCLASE.

((Beltrán C. Zapata O. and Darszon A.)) Departamento de Genética y Fisiología Molecular, Instituto de Biotecnología-UNAM, Cuernavaca Mor. México.

Sea urchin sperm, as many species, must undergo the acrosome reaction (AR) to fertilize the homologous egg. Induction of AR by FSG from egg jelly or by artificial treatments is temporally correlated with the activation of adenylyl cyclase (AC). Both AR and AC activation are dependent on extracellular Ca^{2+}. FSG also induces a K^+-dependent hyperpolarization followed by a depolarization and AR in *Lytechinus pictus* sea urchin sperm. High-K^+ (30-40 mM) ASW inhibits the hyperpolarization, the subsequent depolarization and AR (González-Martínez & Darszon, 1987, *FEBS lett.* **218**:247). *Paramecium* AC which is not regulated by G proteins can be activated by hyperpolarization of its plasma membrane (Schultz *et al*, 1992, *Science* **255**:600). Sea urchin sperm AC shares several properties with the *Paramecium* enzyme. In this work we explored the effect of membrane potential on AC regulation.

We found that artificial hyperpolarization of *L. pictus* sea urchin sperm diluted in K^+-free seawater (valinomycin/0KASW) or in Na^+-free ASW (0NaASW), increased [cAMP]. The rise in [cAMP] persisted even in the absence of $[Ca^{2+}]_e$, although to a lesser extent. Similar results were obtained when *S. purpuratus* sperm were hyperpolarized in 0NaASW (this species does not undergo a steady valinomycin-induced hyperpolarization in 0KASW). AC stimulation in 0Na0CaASW required addition of the phosphodiesterase inhibitor IBMX. In *S. purpuratus* high K^+ (50KASW) blocked cAMP stimulation induced by FSG and the AR. In both species artificial alkalinization of pH_i with 10 mM NH_4Cl rose cAMP levels as described for *S. purpuratus* (Cook & Babcock, 1992, *J. Biol. Chem.* **268**:22402). The egg peptide *speract* had a synergistic effect on the hyperpolarization-induced AC stimulation which was enhanced by IBMX. These results indicate that as in *Paramecium*, sea urchin sperm AC can be regulated by the membrane potential and that this regulation is pH_i-independent, they also confirm the participation of Ca^{2+} in the regulation of this enzyme.

This work was supported by grants from Howard Hughes Medical Institute, DGAPA and CONACyT.

Tu-Pos373

β-SUBUNITS of VOLTAGE-DEPENDENT *SHAKER* K^+ CHANNELS ARE MEMBERS of an ALDO-KETO REDUCTASE SUPERFAMILY.

((Tom McCormack and Ken McCormack*))Department of Biochemistry, New York University, *Max-Planck-Institut für Experimetelle Medizin, Abteilung 11.

Amino acid sequence alignments of bovine and rat *Shaker* K+ channels β-subunits (Rettig, et al. *Nature* **369**, 289 (1994)) with members of the aldo-keto reductase family of proteins, in conjuction with high-resolution strutcural information obtained for two of the reductases, indicate that the β-subunits are NADP(H) or NAD(H) dependent oxidoreductive enzymes (manuscript submitted). This suggests a novel association and potential interaction between voltage-dependent ion channel proteins, which determine membrane excitability properties, and enzymatic proteins likely to be involved in regulating as of yet unknown oxidoreductive biochemical pathways. Rettig et al., have reported a striking modulation of *Shaker* α-subunit excitability properties via β1 N-terminal inactivation and intracellular glutathione redox state. The homologies described here, other studies (Rudy, et al. *Neuron* **1**, 649 (1988)) and the fact that β2 does not contain a similar N-terminus suggest two other interesting possibilities. 1) Through intermolecular association, an oxidoreductive-enzymatic role of the β-subunits is regulated by or colocalized to the α-subunits. 2) β-subunit modulation of α-subunit activity may not be limited to the N-terminus of β1; the role of the likely β-subunit cofactors NADP(H) or NAD(H) in α-subunit modulation will be described.

Tu-Pos374

S100A AND S100B PROTEINS ACTIVATE CYCLIC NUCLEOTIDE PHOSPHODIESTERASE IN A CALCIUM DEPENDENT MANNER.

((Ying Yuan, Himanshu Parikh, Vidya Krishnan and Hiroshi Mizukami)) DRBB, Department of Biological Sciences. Wayne State University, Detroit, Michigan 48202.

S100a and S100b are calcium binding proteins consisting of two subunits. They are rich in neuronal cells, but found in lesser quantities in other cell types. At present, their function remains speculative. We tested to find if S100 proteins stimulate the function of beef heart phosphodiesterase (PDE) or not, using fluorescent 2'-(N-methyl)anthraniloyl guanosine-3'-5'cyclic monophosphate (Mant-cGMP) as the substrate. Mant-cGMP was excited at 280 nm and the change in fluorescence was monitored at 444 nm in a buffer consisting of 10 mM MOPS, 90 mM KCl, 5 mM $MgCl_2$, and 1 mM EGTA at PH 7.0 using a Hitachi F-2000 fluorescence spectrophotometer. The results indicate that the activation of PDE requires the presence of both S100a or S100b protein and calcium. The estimated K_m values for PDE stimulated with S100a and S100b in the presence of Ca^{2+} are 3.5 uM and 2.4 uM, respectively. Their V_{max} values are 0.013 uM sec^{-1} and 0.015 uM sec^{-1}, respectively. These values are similar to what have been reported for calmodulin.

Tu-Pos375

B. PERTUSSIS ADENYLATE CYCLASE TOXIN ENTERS CELLS THROUGH A VOLTAGE DEPENDENT PROCESS.

((X. Yi, M. C. Gray, G. Szabo, E.L. Hewlett and A.S. Otero)). Departments of Molecular Physiology and Biological Physics, Medicine and Pharmacology. University of Virginia School of Medicine. Charlottesville, VA 22908.

Adenylate cyclase toxin (AC toxin) from *B. pertussis* is a 177 kDa calmodulin-activated enzyme which has the ability to enter eukaryotic cells and convert endogenous ATP into cAMP. Little is known, however, about the mechanism of cell entry. We now report that this process has a very steep and obligatory dependence on the electrical potential across the plasma membrane. Intoxication of atrial cells, as reflected by increases in cAMP-stimulated calcium currents, is readily observed within minutes of exposure to AC toxin when myocytes are held at negative potentials, but hindered at membrane potentials positive to -45 mV, and is altogether prevented when the membrane is kept at potentials positive to 0 mV. The voltage dependence is a property of the intoxication process, and not of events that occur downstream from toxin entry, such as activation of protein kinase A and phosphorylation of calcium channels. In addition, our results indicate that the voltage dependent step takes place after toxin binding, and appears to correspond to the translocation of the catalytic domain across the cell membrane. *Supported by NIH grants to E.L.H., G.S. and A.S.O.*

Tu-Pos376

INDUCED TRANSITIONS, CONFORMATIONAL RELAXATION, AND USE OF LIGAND BINDING ENERGY.

((C. J. Ritz-Gold)) Biomolecular Sciences, Fremont, CA 94536.

Induced transitions are thought to play a key role in many cellular processes, including regulation of enzyme activity, receptor activation, and energy transduction. These transitions are typically represented as processes in which intrinsic ligand binding energy is used to "pay for" an energetically-unfavorable conformational change. Likewise, the transition pathway is commonly viewed as a 2-step process in which rapid ligand attachment to the low-affinity conformation precedes slower isomerization to the high-affinity conformation.

Here we seek a better understanding of induced transitions by looking at how ligand binding energy is used during the transition. In particular, we regard the protein globule as the system and focus on changes in structure and energy. This approach is based on a double-minimum energy surface representation similar to that used to describe coupling between electron & atom group transfer processes and conformational transitions (Kuznetsov & Ulstrup, in: Protein Structure: Molecular and Electronic Reactivity, Austin et al, 1987). We find that induced transitions may be regarded as processes of energy transformation in which: presence of steric misfit between ligand and binding site results in input of potential energy to the system and destabilization of the low-affinity conformation, presence of energy barriers for conformational rearrangement leads to energy storage, fulfillment of latent bonding interactions and conformational distortion (partial relaxation) results in energy conversion, and relaxation to the high-affinity conformation leads to transduction and/or dissipation of the stored energy.

Tu-Pos377

TEMPORAL RESOLUTION OF RAPID KINETIC EVENTS FOR CELLULAR STUDIES IN CYTOMETRY

((L.D. Scampavia; J. Ruzicka; G.D. Christian)) Department of Chemistry BG-10 University of Washington, Seattle WA 98195 USA.

Flow cytometry is a spectroscopic technique for the rapid measurement of important biological properties of cells or organelles, and for the physical separation of desired subpopulations based on these measured properties. The introduction of Flow Injection [FI] analysis into cytometry can provide a basis for accurate solution handling and improved temporal resolution in cytometric experiments [1,2]. A FI cytometric system designed for kinetic analyses allows cytometric interrogation of kinetic events in a working range of 100 milliseconds to several minutes with ≤30 millisecond resolution. Consequently, the elucidation of intracellular events is determined through the response of many cells for fixed and variable time frames. This device is demonstrated by monitoring intracellular enzymatic activities of glucose dehydrogenase and glutathione S-transferase in erythrocytes.

[1] W. Lindberg, L Scampavia, J Ruzicka, G.D. Christian: Fast Kinetic Measurements and On-line Dilution by Flow Injection Cytometry. *Cytometry* 1994 16: 324-330
[2] L Scampavia, G. Blankenstein, J Ruzicka, G.D. Christian: Laminar Jet Mixing for Rapid Kinetic Analysis in Flow Injection Cytometry. *Cytometry* [submitted 1994]

TOXIN AND VIRAL CHANNELS

Tu-Pos378

CRYSTALLIZATION OF THE α POLYPEPTIDE OF THE KP6 KILLER TOXIN.

((W.L. Duax, D. Ghosh, D. Langs, M. Erman, W. Pangborn P. Vuchot, C.-M. Park, J. Bruenn and R. Straubinger)) Hauptman-Woodward Medical Research Institute, 73 High St., Buffalo, NY 14203 and SUNY Buffalo, Amherst, NY 14260-1200,

The killer toxin KP6 from *Ustilago maydis* is a virally encoded secreted protein toxin that kills sensitive *Ustilago* cells. It is composed of two monomeric polypeptides (α and β) that interact at the cell membrane to create ion channels, resulting in an efflux of potassium and death of the target cells. Among channel-forming toxins, KP6 is unique in requiring two non-complexed polypeptides, and among channel-forming toxins from eucaryotes it is unique in having a specific putative membrane protein receptor. The protein sequences of all the *Ustilago* toxins have been determined and a 40 mg sample of the α and β peptide has been prepared from a single culture. Single crystals of the α subunit (space group P6322, a=b=48.35Å, c=123.92Å, α=β=90°, γ-120°) have been prepared and a native data set to 2.3Å resolution (93.4% complete) has been collected. Preliminary CD results show that both KP6α and KP6β are composed primarily of beta sheet structure and become entirely beta sheet in the presence of phospholipids. Techniques used to pursue structure determination will include multiple isomorphous replacement, molecular replacement, and *ab initio* direct methods with and without anomalous dispersion data. Heavy atom compounds are being screened in soaking experiments on single crystals of KP6α and crystallization experiments are in progress on samples of KP6β. The molecular weight, potential presence of three and four disulfide bridges and spatial evidence that the structure of KP6α and KP6β are primarily made up of β strands suggest that these three-dimensional structures may share common features with several toxins for which X-ray crystal structure determinations have been reported. Intensity data from native crystals will also be used to test new methods of macromolecular phase determination being developed in the molecular biophysics department of the Hauptman-Woodward Medical Research Institute. Research supported in part by NIH Grant GM32812.

Tu-Pos379

SINGLE SITE MUTATIONS IN THE CONSERVED ALTERNATING ARGININE REGION AFFECT IONIC CHANNELS FORMED BY CryIA(a), A *BACILLUS THURINGIENSIS* (*Bt*) TOXIN.

((J.L. Schwartz*,+, L. Potvin*, D. Dean#, R. Laprade+)) *BRI, National Research Council, Montreal, Que, H4P 2R2, +GRTM, University of Montreal, Montreal, Que, Canada, H3C 3J7 and #Dept of Biochemistry, Ohio State University, Columbus, OH43210, USA

CryIA(a), a *Bt* lepidopteran-specific toxin, is a 3-domain protein (Grochulski et al., 1994). Domain I contains 7 α-helices and may be responsible for channel formation in cell membranes. Domain II, involved in recognition of, and binding to susceptible cells, consists of 3 antiparallel β-sheets. The role of Domain III, a sandwich of 2 antiparallel β-sheets, is unknown. It contains 3 of the 5 highly conserved blocks found in CryI toxins. Of particular interest is block 4 (four alternating arginines) which is adjacent to block 2 (which includes the last two helices of Domain I). Mutants were constructed by replacing in block 4 $^{R}521$ (positive charge) by D, E, H, K or Q (-, -, +, + and neutral, respectively) and $^{R}527$ by K. They were examined electrophysiologically in planar lipid bilayers. The mutants formed channels at similar dosage (approx. 10 μg/ml). The channels were cation-selective (V_r around -25 mV). There was no apparent difference in kinetic behaviour or voltage-dependence of the channels. However, the conductances of $^{R}521^{E}$, $^{R}521^{K}$, $^{R}521^{Q}$ and $^{R}527^{K}$ were significantly smaller than that of the wild-type protein. These results may explain the reduction of toxicity observed in silkworm bioassays.

Tu-Pos380

ASSOCIATION OF BOTH SUBUNITS OF USTILAGO MAYDIS TOXIN, KP6, FORMS LARGE VOLTAGE-INDEPENDENT CHANNELS

((M. Zizi*, A. Finkler#, Y. Koltin#, *Dept. Physiology, K. U. Leuven, 3000 Leuven, Belgium, Molecular Biotechnology, Tel Aviv University, 69978 Ramat Aviv, Israel))

Double-stranded RNA viruses leading to the expression of a killer (toxin-secreting) phenotype exist in the corn smut pathogen, Ustilago maydis. Three toxin specificities are known: KP1, KP4 and KP6, each toxin being made of two polypeptides. KP6 lethality on plated sensitive cells depends on K^+ concentration in the plating medium, therefore an eventual membrane permeabilization by the toxin was investigated. Purified α and β subunits of KP6 were reconstituted into planar phospholipid membranes. Addition of KP6 to membranes bathed in 150 mM KCl (10 mM Hepes, pH 7.2) led to stepwise current fluctuations compatible with channel openings and closings. Only the combination of both subunits -never α or β alone- yielded the channels. Single channel conductance was 31 pS (and multiples thereof). Reversal potential experiments showed a non-strict cation selectivity (3.5-fold preference for K^+ vs Cl^-). With time, increasingly larger events could always be recorded (up to 1-2 nS). These had a decreasing ion selectivity (1.6-fold K^+ preference for 2 nS events) consistent with an increasing pore size. The channels were voltage-independent between -70 and +70 mV. This channel-forming activity (small and large events) could be immunoprecipitated by polyclonal antibodies against the subunits, ruling out an eventual contaminant as responsible for the channel activity. This ability of KP6 subunits to form large channels may be part of the toxin lethal effect.

Tu-Pos381

THE STRUCTURES AND CHANNEL ACTIVITIES OF TUMOR NECROSIS FACTORS-α AND ß AT NEUTRAL AND LOW pH.

((B.J. Wisnieski, R.L. Baldwin, S. Sinha, T. Mirzabekov, and B.L. Kagan)) UCLA, Los Angeles, CA 90024.

TNF-α (cachectin) and TNF-ß (lymphotoxin) are secreted primarily by macrophages and T-cells, respectively. Low pH enhances TNF-α-induced cytolysis of cancer cells and TNF-α-membrane interactions including binding, insertion, and ion channel formation. Interestingly, TNF-α also increases Na^+ influx in target cells. Recently, TNF-ß was found to exhibit many similar properties. Crosslinking and intramembranous photolabeling show that the trimeric forms of TNF-α and ß are maintained upon insertion into the bilayer. Insertion is greatly enhanced with frozen bilayers as compared to fluid bilayers even though the binding efficiency is much lower; hence, binding and insertion are distinct processes. Proof that surface-exposed TNF-α is intramembranous is that sequenced proteolytic cleavage products bear the membrane-restricted photoactivable probe 12APS-GlcN. Intrinsic fluorescence and ANS binding assays show that low pH-enhanced membrane interactions stem from reversible acid-induced conformational changes. Use of vesicle-embedded proteins to make planar bilayers revealed that acid-facilitated protein insertion precedes expression of voltage-gated conductance. At high *trans*-negative voltages, channels close more frequently and re-opening fails. *Trans*-addition of anti-TNF antibodies also causes loss of channel activity. We propose that channel formation occurs when cracked or splayed trimers bind and penetrate the bilayer. Reannealing is such that the membrane-embedded form of TNF exhibits a slightly relaxed trimeric structure. The trimer's structural plasticity appears to be a major determinant of its channel-forming ability. The directionality of bilayer penetration conforms with X-ray data, which shows that receptor binding to the monomeric interfaces of TNF poises the tip of the trimeric cone directly above the target cell membrane. [NIH GM22240 & ACS IM-716 (BJW), NIMH MH43433 & MH01174 (BLK), and USPHS/NRSA HL07386 (RLB).]

Tu-Pos382

SELECTIVE PROTON PERMEABILITY AND PROTON ACTIVATION OF INFLUENZA A VIRUS M2 PROTEIN CHANNELS EXPRESSED IN MEL CELLS. (I. Chizhmakov, F. Geraghty, A. Hayhurst, M. Antoniou, D. Ogden, A.J.Hay) N.I.M.R., Mill Hill, London, NW7 1AA, UK.

The 'flu virus coat protein M2 is responsible for dissipation of pH gradients across endosomal membranes during viral exocytosis and for pH induced viral uncoating. Direct evidence that M2 forms a proton permeable channel activated by external protons in mammalian membranes is obtained from whole cell patch clamp of MEL cells stably transfected with Weybridge or Rostock strains of M2. Cells were perfused internally with N-methyl glucamine-HEPES (pH 7.3) or NMG-MES (pH 6.0) and externally with NMG-HEPES/MES pH 4.0 - 8.0. Currents evoked by solutions of low pH reversed close to the equilibrium potential for H^+ (or OH^-) gradients and were not influenced by Na^+, K^+ and Cl^- ions. Inward currents showed saturation at high external $[H^+]$, with voltage-dependent apparent K's of 4 μM (-80 mV) to 10 μM (0 mV). The saturation of current at high $[H^+]$ suggests permeation by H^+ rather than OH^- ions. H^+ permeability was activated by low pH externally (but not internally) in Weybridge M2 and had an apparent K of 50 nM $[H^+]$. Permeability in Rostock M2 was constant at $[H^+] > 1$ nM. No increase of current variance was seen during activation, suggesting a small unitary conductance or high open probability. Currents were blocked irreversibly by anti-flu drug rimantadine (5-50 μM).

Tu-Pos383

Viral and Cellular Proteins Induce Cl^- Currents in Xenopus Oocytes. ((K. Shimbo[1,2], D. Brassard[2], R. A. Lamb[2,3], L. H. Pinto[1].)) (1) Dept of Neurobiol., (2) Dept of Biochem., Mol. Biol. and Cell Biol. and (3) Howard Hughes Med. Institute Northwestern Univ. Evanston IL 60208

When oocytes were injected with large quantities of mRNA encoding a cellular protein, Isk, or either of two viral proteins, M_2-A30T+V of influenza A virus or NB of influenza B virus, we observed ionic currents induced upon hyperpolarization to ca. -130 mV that resembled the currents induced in water-injected oocytes which were more strongly hyperpolarized (to -180 mV). For all four currents (1) the selectivity sequence was $F^->Cl^->Br^->I^-$, (2) the Vrev changed 10-40 mV per ten-fold decrease in $[Cl^-]$, (3) the equivalent gating charge was 2.0-3.3 e^-, (4) DIDS (1 mM), SITS (2 mM), 9-AC (3 mM) blocked by ca. 70%, and (5) amplitude was increased by lowered pH. The time course of this current was dependent upon the batch of oocytes and not the mRNA injected. Only oocytes that expressed a quantity of total protein above a certain "threshold" produced these voltage-activated currents. For oocytes injected with small quantities of Isk mRNA, depolarization induced a slowly activated outward current, and for oocytes injected with small quantities of M_2-A30T+V mRNA, a current activated by low pH also flowed. These results are consistent with the M_2-A30T+V and Isk proteins expressing a current intrinsic to themselves for low expression levels. However, all three proteins also facilitate the induction of an endogenous Cl^- current for high expression levels.

CONNEXINS

Tu-Pos384

VOLTAGE DEPENDENT CURRENTS IN XENOPUS BLASTOMERES. ((N. Mulrine, A. Miller & A. E. Warner)) Dept. of Anatomy & Developmental Biology, University College London, Gower St., London WC1E 6BT, United Kingdom

Cells isolated from blastula stage Xenopus embryos show wide variation in their membrane properties (Slack & Warner, 1975, J.Physiol., 248, 97). To investigate whether this is associated with specification of the embryonic axis, we labelled specific dorsal & ventral cells in tier 2 of the 32-cell embryo with a fluorescent lineage marker and examined the membrane properties of their progeny. Late blastulae were dissociated into single cells by exposure to Ca-free solution and currents recorded from labelled progeny using whole-cell switch clamp. Cells were held at the zero-current potential (mean +/-sem, -20mV+/-1.3, n=25.). In 30% (n=20) of ventral and 80% (n=5) of dorsal cells, there was no voltage-activated time-dependent current between -100 to 50 mV; at more positive potentials there was slight delayed outward rectification (ratio of slopes 2.2). The mean resting conductance was 1.3nS. In 70% of ventral cells and 1 dorsal cell, we recorded a novel outward current that activated within a few ms at potentials positive to about 40mV and decayed slowly (mean tau at 100mV = 220ms). In these cells, the initial slope conductance between 40 and 100mV was 117nS (range 35 to 257nS), about 20 times greater than the slope conductance at negative potentials. Tail currents reversed near 0mV, suggesting that this current may be carried through a non-selective cation channel. The mean resting conductance was 7.9nS. Blastomere pairs have a large gap junctional conductance (Spray et al., 1981 JGP, 77,77) We used double whole cell switch clamp to record gap-junctional currents in pairs of dorsal or ventral cells. The junctional conductance was about 40nS, 5 to 40 times larger than the resting single cell conductance, with pronounced trans-junctional voltage dependence.

Tu-Pos385

RECONSTITUTED CONNEXIN CHANNELS: SELECTIVE PERMEATION BY NEUTRAL MOLECULES & ACTIVITY IN HORIZONTAL BILAYERS ((C.G. Bevans, R.A. Brutyan, C. DeMaria & A.L. Harris)) Dept. Biophys., Johns Hopkins Univ., Baltimore MD 21218 (Spons. by D. Fambrough)

The relative permeability of connexin (Cx) channels to four neutral molecules was determined. Cx from rodent liver was affinity-purified using a monoclonal antibody against Cx32 (Rhee & Harris, *FASEB J.* 3:A602) and incorporated into unilamellar liposomes. Permeability was assayed by the change in liposome density due to outward movement of a small entrapped permeant and inward movement of a larger external molecule (Harris *et al.*, *J. Membr. Biol.* 109:243). When the membrane is permeable only to the smaller molecule, liposome density increases to an extent consistent with osmotically-driven loss of aqueous volume constrained by limiting membrane curvature. The assay is unaffected by large variation in channel open probability since permeability to the larger molecule is assessed only for those liposomes freely permeable to the smaller molecule. Cx purified from rat liver was permeable to sucrose (342Da) and raffinose (596Da), and essentially impermeable to metrizamide (789Da) and nycodenz (821Da). Mouse liver Cx was permeable to sucrose only. In addition, Lucifer Yellow flux through mouse Cx channels was much lower than that through rat Cx channels, consistent with a narrower pore. Both preps contain Cx32 and Cx26 (Kordel *et al.*, *Biophys. J. 54*:A192), but the proportion of Cx26 is greater in the mouse prep. The observed differences in permeability may be due to the influence of Cx26 on dimensions of the pore, with important consequences for intercellular communication and its modulation.

Cx was also reconstituted in horizontal "solvent-free" bilayers (see Brutyan & Harris abstract). Both preps showed similar properties (mouse channels required higher voltages to close) that compared favorably with properties in vertical "solvent-containing" bilayers (Harris *et al.*, *Mol. Br. Res.* 15:269). The horizontal bilayer system greatly facilitates reconstitution of Cx channels as compared with other methods. The relation between the observed single channels and their differential regulation and permeability is being examined. Support: NIH GM36044 & ONR N00014-90-J-1960.

Tu-Pos386

VASCULAR ENDOTHELIAL CELLS: CHANNEL CONDUCTANCE AND CHANGE IN EXPRESSION WITH TIME. ((D.C. Spray, M. E. El-Sabban, G.J. Christ, and L.K Moore)) Albert Einstein College of Medicine Bronx, NY USA 10461

Gap junctions in the vasculature provide a conduit for communication between cells and provide for syncytial behavior resulting in coordinated vasomotor responses. We have characterized gap junction expression between bovine aortic endothelial cells in terms of channel unitary conductance, and expression of the gap junction proteins and mRNA's for Cx43, Cx40 and Cx37. Our studies support those previous reports of changes in connexin expression in the vessel wall associated with wounding of the endothelium or isolation into culture. Within 24 hours post isolation for primary culture changes in unitary conductance occurs, from those resembling what has been reported for Cx 37 and Cx40, suggesting a change in channel expression. At one week in culture the population resembles that of Cx43 type channels. Application of a variety of techniques, including dual whole cell voltage clamp, dye injection, and calcium imaging, has enabled us to begin to model the mechanism of gap junction-mediated changes in vessel tone during responses to both normal and abnormal physiology.

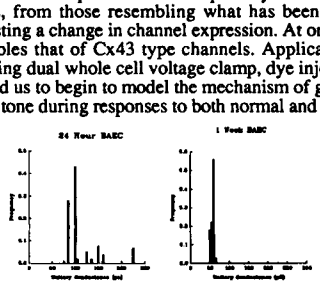

Tu-Pos387

GAP JUNCTIONS IN TELEOST HORIZONTAL CELLS: SINGLE CHANNEL ANALYSIS AND VOLTAGE DEPENDENCE SUGGEST MULTIPLE TYPES ((L.K. Moore and D.C. Spray)). Albert Einstein College of Medicine, Bronx, NY 10461.

Modulation of intercellular communication in the retina causes changes in receptor field size and modifies spatial gain of the visual system. These changes can be mediated by neurotransmitters such as dopamine. To date, the specific connexins expressed in teleost retina are unknown and their channel properties have not been thoroughly characterized. In this study we have determined the unitary conductances of channels formed between homologous and heterologous horizontal cell pairs. H1, H2 and H3 cell pairs and heterologous pairs (distinguished by cell shape and size) were studied using the dual whole cell voltage clamp technique. Unitary conductances recorded in these gap junction channels depended on the cell type. In all cell types a population of 65 and 100 pS channels predominated, however 120 and 200 pS channels were observed in H2 and H3 homologous pairs, and their occurrence was enhanced at transjunctional voltages below 40 mV. Pattern of individual channel activity (in absence of uncoupling agents) also differed. Examination of voltage dependence in mixed pairs suggests asymmetry in response of these junctions to depolarizing and hyperpolarizing voltage pulses, possibly indicating contribution of different connexin proteins by each cell of the pair.

Tu-Pos388

IN SITU MEASUREMENTS OF PANCREATIC β-CELL GAP JUNCTION CONDUCTANCE. ((D. Mears, N.F. Sheppard, Jr., A. Sherman[†], I. Atwater[‡] and E. Rojas[‡])) Department of Biomedical Engineering, Johns Hopkins University, Baltimore, MD 21205 and [‡]NIDDK, NIH, Bethesda, MD 20892.

Studies of the electrical and secretory behavior of single pancreatic β-cells and those within intact islets of Langerhans indicate that cell-to-cell communication may play an important role in shaping islet glucose responsiveness. Nevertheless, the biophysical properties of β-cell gap junctions have not been well characterized. We have measured the parallel gap junction electrical conductance between a β-cell and its nearest neighbors under physiological conditions by voltage-clamping single β-cells within the microdissected mouse islet of Langerhans. The holding current records in 11.1 mM glucose consisted of bursts of inward current due to the oscillating membrane potential of surrounding β-cells. The potential record of the impaled cell, obtained in current clamp mode, was used to estimate the electrical behavior of the surrounding β-cells, and the parallel coupling conductance was calculated by dividing the magnitude of the current bursts by that of the voltage bursts. Coupling current bursts were observed in each β-cell studied (n=25). The histogram of coupling conductance from these cells was bimodal with peaks at 2.4 and 3.4 nS, indicating possible heterogeneity in intercellular communication from islet to islet or at different locations within the islet. Electrical coupling was reversibly decreased when the temperature was lowered from 37 to 29°C and when the extracellular calcium concentration was increased from 2.6 to 7.6 mM. Forskolin (10 μM) reversibly increased the coupling conductance. We conclude that the *in situ* voltage-clamp technique provides a means of measuring gap junction electrical conductance under physiological conditions, and that electrical coupling among β-cells is extensive and dynamic within the islet of Langerhans. (Supported in part by N.S.F. ECS-9058419 and NIH 5 T32 GM7057)

Tu-Pos389

DIFFERENTIAL REGULATION BY PHOSPHORYLATION OF SEVERAL GAP JUNCTION CHANNEL CONDUCTANCES. ((B.R. Takens-Kwak, M.M.P. Hermans, H.R. de Jonge*, H.J. Jongsma and M. Chanson)) Dept. of Medical Physiology, Utrecht University, Utrecht and * Dept. of Biochemistry, Erasmus University, Rotterdam, the Netherlands.

The regulation of gap junctional conductance (g_j) by the interplay of protein kinases and phosphatases has been proposed more than a decade ago. Similar phosphorylating treatments applied to various tissues and cell lines have been shown to alter dye- and electrical coupling in different or even opposite ways. One possibility to explain this variability can be differential expression of connexin and kinase isoforms in these preparations. To determine whether several gap junction channels are differently modulated, we studied single-channel conductances (γ_j) of Cx45, Cx43, Cx32 and Cx26 channels under very similar conditions of phosphorylation. For this purpose, dual whole-cell voltage-clamp was performed on SKHep1 cells, an adenocarcinoma endogenously expressing Cx45. These cells were stably transfected with cDNAs encoding for Cx43, Cx32 or Cx26. To activate protein kinase C (PKC) the control bath solution was supplemented with 100 nM of the phorbol ester TPA, whereas PKA and PKG were activated by adding respectively the non-hydrolysable agonists 5p-5,6DCl-cBiMPS (20 μM) and PET-cGMP (20 μM) to the electrode solution (with CsCl as the current-carrying ion). To reach the single-channel level, g_j was reduced with 1.5 mM heptanol or halothane. Under control conditions, Cx45 gap junction channels exhibited a unitary conductance of 35 pS, Cx43 channels exhibited multiple conductance states of ~30, 60 and 90 pS. In contrast to previous reports, Cx32 channels displayed small conductances around 50 pS; Cx26 exhibited a main conductance of 145 pS, smaller sizes of 65-100 pS were also detected. In the presence of TPA, the 30 pS Cx43 unitary conductance was predominantly observed. A novel γ_j of ~20 pS was also detected. The inactive phorbol ester αPDD did not alter the control distribution of Cx43 channels. Addition of TPA did not affect the γ_j's of Cx45 and Cx26 channels. In the presence of 5p-5,6DCl-cBiMPS, the main γ_j of Cx26 channels increased to ~160 pS whereas Cx43 and Cx45 unitary conductances did not change. In the presence of PET-cGMP, the endogenous Cx45 channels exhibited, in addition to 35 pS, a novel γ_j of ~20 pS. This 20 pS γ_j could also be detected in Cx43 and Cx26 transfected cells. Whereas the main γ_j of Cx26 channels was not affected under these conditions, the 60 and 90 pS conductances were less frequently observed in Cx43 transfected cells. This latter effect appeared to be specifically attributable to PKG activation since addition of the non-hydrolysable PKG antagonist Rp-cGMP (100 μM) to the electrode solution restored the control Cx43 distribution. The effects of various phosphorylating treatments on Cx32 channels are currently under investigation. Taken together, these results point to differential sensitivity of connexin isoforms exposed to identical phosphorylating conditions.

CHANNELS IN THE NUCLEUS

Tu-Pos390

MODULATION OF NUCLEAR ION CONDUCTANCE BY CA AND ATP. ((R. Assandri, F. Bertaso and M. Mazzanti)) Dept. Physiology and Biochemistry, State University of Milano, I-20133, Milano Italy.

An affacinating problem faced by cell biologists since several years concerns the possibility that nuclear envelope discriminates cellular components traffic in and out of the nucleus. It is not clear yet, for example, if in the cytoplasm and in the nucleus the calcium rises at the same time and in the same quantity. There are no doubts that in physiological conditions nuclear envelope do not represent a barrier for ions and small solutes. Some authors suggest that in certain conditions it is possible that nucleo-cytoplasmic pathways modify their size way below 9-10 nm functional diameter creating, two electrically separate environments. In addition, if there is the possibility to interact with the nuclear resting potential from outside, the presence of nucleo-cytoplasmic pathways that can be regulated could represent more than just a suggestion. In the present paper we investigate on the kinetics of the nuclear ionic channels and in particular on the multiple current levels that are possible to observe during *on-nucleus* patch-clamp experiments. We also tested the effect of external (cytoplasmic) calcium on the nuclear ionic conductances to clarify if there are interactions or modulations of the current flow. Finally we studied the effect of ATP to test its modality of action on isolated nuclei.

Tu-Pos391

MEASURING CALCIUM GRADIENTS ACROSS THE NUCLEAR ENVELOPE. ((L. Stehno-Bittel, C. Perez, and D. Clapham)) Dept. of Pharmacology, Mayo Foundation, Rochester, MN 55905

Isolated, intact nuclei from *Xenopus laevis* oocytes take up and release Ca^{2+} in response to intracellular messengers resulting in the formation and dissipation of Ca^{2+} gradients across the nuclear envelope as measured by confocal microscopy (Stehno-Bittel et al., Neuron, *in press*). A comparison of the fluorescence values of Ca^{2+}-sensitive dyes (salt form) in quiescent nuclei versus cytoplasm showed consistently higher fluorescence in nuclei, especially with the dye fluo-3. Nuclear fluorescence was associated with the nucleoplasm because removal of the nucleoplasm from isolated nuclei abolished fluorescence emission. *In vitro* calibration studies measured the Fluo-3 fluorescence emission in water, buffer, permeabilized nuclei, and cytoplasm with free Ca^{2+} clamped at concentrations of 10 to 2000 nM. In these experiments both dye and Ca^{2+} concentrations were controlled. The fluorescence/Ca^{2+} concentration relation was similar for Fluo-3 diluted in water, buffer or cytoplasm. However, emission from nuclear Fluo-3 rose steeply at low Ca^{2+} concentrations, so that at 100 nM free Ca^{2+} the nuclear fluorescence was twice as high as measurements from water, buffer or cytoplasm. Similar experiments with other dyes (Ca^{2+} Green and Indo-1) did not exhibit as large a discrepancy between nuclear and cytoplasmic *in vitro* fluorescence. Ratio values from Indo-1 were not statistically different when diluted in nuclear versus buffer environments. The results suggest that Fluo-3, one of the most frequently utilized single wavelength Ca^{2+} dyes, has a higher fluorescence emission in a nuclear environment, which is independent of dye and Ca^{2+} concentrations. Ca^{2+} gradients across the nuclear envelope may exist, but Fluo-3 artifacts limit its usefulness in measuring possible gradients.

Tu-Pos392

NUCLEAR CHANNEL ACTIVITY IS REGULATED BY THE ACTIN CYTOSKELETON. ((A. G. Prat, and H. F. Cantiello)) Renal Unit, Massachusetts General Hospital East, and Department of Medicine, Harvard Medical School, Massachusetts.

We recently demonstrated that actin filaments are novel second messengers involved in the regulation of ion channels. Since intracellular signals may target the nucleus, we investigated the possibility that the actin cytoskeleton also controls nuclear membrane function. In this report we used patch-clamp techniques to assess the role of actin on nuclear channel activity. Isolated nuclei were obtained from A6 epithelial cells and allowed to sediment onto glass coverslips. This procedure yielded an almost pure nuclei preparation, >95%. The nucleus-attached patch-clamp technique was performed using a 115 mM KCl (Ca^{2+}-free) buffer in both pipette and bath. Spontaneous ion channel activity was observed in 65 % of the patches (n=40). The most prevalent ion channel showed a conductance of 400-600 pS, and was slightly more permeable to sodium over potassium. The cation-selective channels also showed various subconductance states. Addition of actin (monomeric, 5 μM) to the bathing solution induced ion channel activity in 57 % of the experiments (n=14). Channels were also activated by the toxin cytochalasin D (5 μg/ml, n=3/5) or the actin-binding protein DNAse I (20 μM, n=5/9), thus indicating that both the "cytosolic" actin cytoskeleton as well as intranuclear cytoskeletal components may be involved in the transduction of intracellular signals reaching the nucleus. Thus, the possibility exists that ionic signals generated at the plasma membrane level may be linked to the nucleus via the actin cytoskeleton.

Tu-Pos393

A SIGNAL TRANSDUCTION PATHWAY FOR INHIBITION OF VOLTAGE DEPENDENT CALCIUM CHANNEL ACTIVITY IN SMOOTH MUSCLE CELLS. ((M. Tomasic and M.I. Kotlikoff)) Depts. Clinical Studies/NBC and Animal Biology, University of Pennsylvania, Philadelphia, PA 19104. (Spon. by R.E. Forster)

Conflicting data exist with respect to the action of β-adrenergic agonists on voltage dependent calcium channels (VDCC) in smooth muscle. Bath addition of isoproterenol or forskolin resulted in 66 ± 28 % (n = 7) and 53 ± 22 % (n = 5) decrease, respectively, in channel activity. To determine if cAMP dependent protein kinase is involved in this inhibition pathway, cultured human and equine airway smooth muscle cells were microinjected with the catalytic subunit of A-kinase while simultaneously recording single channel events in the on-cell patch clamp configuration. The concentration of the catalytic subunit in the injectate was 50 unit/ml. The estimated dilution of injectate is 100 to 1000 fold based on a 20 pl cell volume when injecting for 100 ms at 35 kpa. Open-state probability (nPo) was reduced to 0.72 ± 0.19 (n = 11) compared to control following microinjection. These reductions occurred without significant change in cell transmembrane potential. No decrease ocurred following microinjection of boiled catalytic subunit (n = 7), or of intact catalytic subunit (50 unit/ml) plus 2 mM AMP-PNP (n = 5). These data suggest that β-adrenergic modulation of ASM VDCC activity may be mediated, in part, by cAMP dependent protein kinase through phosphorylation of either the calcium channel or a nearby regulatory protein. (Supported by NIH HL-45239)

Tu-Pos394

THE INHIBITORY EFFECT OF NIFEDIPINE ON Ca^{2+} CURRENT AND LEFT VENTRICULAR PRESSURE DEPENDS ON THE LEVEL OF β-ADRENERGIC STIMULATION IN RAT HEART. ((A. Legssyer, L. Hove-Madsen, J. Hoerter and R. Fischmeister)) INSERM CJF 92-11, Université de Paris-Sud, Faculté de Pharmacie, F-92296 Châtenay-Malabry, France.

We have compared the effect of nifedipine (NIF) on L-type Ca current (I_{Ca}) in isolated myocytes, and on left ventricular pressure (LVP) in isovolumic Langendorff perfused hearts under basal and phosphorylating conditions. I_{Ca} was measured under whole-cell patch-clamp conditions by depolarizing the cell every 4s to 0mV from a -80mV holding potential. Under basal conditions, NIF inhibited I_{Ca} with an IC_{50} of 398 nM (n=5). In the presence of 0.1μM ISO, which stimulated I_{Ca} by 95±23% (n=5), the inhibitory effect of NIF required higher concentrations to develop (IC_{50}=1087 nM, n=5). The maximal effect of NIF was not changed by ISO, since 100μM NIF reduced I_{Ca} by more than 95% in both conditions. In the absence of ISO, 0.1μM NIF reduced LVP in the whole heart by 36±2% (mean±s.e.m., n=8). However, perfusion of the heart with 0.1μM ISO, which at steady-state enhanced LVP by 46±13% (n=4), totally eliminated the inhibitory effect of 0.1μM NIF on LVP (-5±3%, n=4). The stimulatory effect of ISO on LVP was reversed by 1μM atenolol, a β1-adrenergic antagonist. While at this concentration atenolol did not modify LVP nor the inhibitory effect of NIF on LVP in the absence of ISO, it restored the inhibitory effect of 0.1μM NIF on LVP in the presence of 0.1μM ISO (-34±10%, n=4). These results demonstrate that β-adrenergic stimulation reduces the inhibitory effect of NIF on cardiac I_{Ca} and contraction. These effects are likely due to a reduced affinity of phosphorylated Ca channels for NIF.
Supported by a grant from Zeneca-Pharma.

Tu-Pos395

CYCLIC GMP-DEPENDENT PROTEIN KINASE REGULATION OF THE L-TYPE CALCIUM CURRENT IN NEONATAL RAT VENTRICULAR MYOCYTES. ((K. Sumii and N. Sperelakis)) Dept. of Molecular and Cellular Physiology, Univ. of Cincinnati, Cincinnati, OH 45267. (Spon. by S. H. Bryant)

Regulation of L-type Ca^{2+} channel current ($I_{Ca(L)}$) by cGMP-dependent protein kinase (PK-G) was investigated in neonatal rat ventricular myocytes using whole-cell voltage clamp with internal perfusion. $I_{Ca(L)}$ was elicited by a depolarizing pulse to +10 mV from a holding potential (HP) of -40 mV. Stimulated $I_{Ca(L)}$ (by 2 μM ISO) was inhibited to the basal level by internal perfusion with 50 nM PK-G (accompanied by a potent and unhydrolyzable PK-G activator, 8Br-cGMP, 100 nM). When $I_{Ca(L)}$ was enhanced by the Ca^{2+} channel agonist, Bay-K-8644 (1 μM), the enhanced basal $I_{Ca(L)}$ was also reduced by internal perfusion with PK-G (50 nM). Basal $I_{Ca(L)}$ (non-stimulated through the cAMP/PK-A pathway) was also inhibited to various degrees (large, medium, or small) by internal application of PK-G (25 nM). The average inhibition was 40.2 % (n = 34). This inhibition by PK-G was blocked by the PK-G substrate peptide (cG-PKI, 300 μM), and was smaller (8.8 %) when the HP used was -80 mV. Heat-inactivated PK-G (with 8Br-cGMP) had very little effect on basal $I_{Ca(L)}$. Relatively specific PK-G inhibitors, such as cG-PKI, H-8, or Rp-8-pCPT-cGMPS, were sometimes able to partially reverse the inhibition (5 out of 25 cells). The variable degrees of inhibition of basal $I_{Ca(L)}$ may be explained by a balance between endogenous PK-A and PK-G activities: (1) If the endogenous PK-G activity (basal) is already high, exogenous PK-G has little inhibitory effect. (2) If the endogenous PK-G activity is low (or relatively low when the PK-A pathway is activated by isoproterenol), application of exogenous PK-G strongly inhibits $I_{Ca(L)}$. In summary, the activation of the PK-G pathway antagonizes the stimulatory effect of the PK-A pathway.
Supported by NIH grant HL-31942.

Tu-Pos396

PROTEIN KINASE C STIMULATES CA^{2+} CURRENT IN PREGNANT RAT MYOMETRIAL CELLS. ((M. Kusaka, K. Shimamura and N Sperelakis)) Department of Molecular and Cellular Physiology, University of Cincinnati, Cincinnati, OH 45267-0576.

To investigate the possible regulation of the voltage-dependent Ca^{2+} channels by protein kinase C (PKC) in uterine smooth muscle, whole-cell voltage clamp was performed in myometrial cells isolated from late pregnant (18-19 day) rat uterus. A phorbol ester (PKC activator), phorbol 12-myristate 13-acetate (PMA, 300 nM), increased the L-type Ca^{2+} current ($I_{Ca(L)}$) by 19.0 ± 4.6 % (n =10, $p < 0.01$) at pCa 7. At pCa 6, $I_{Ca(L)}$ was augmented to about the same degree. The effect of PMA was dependent on the Ca^{2+} concentration in the pipette solution: PMA did not affect the current in low Ca^{2+} (pCa 10 or 8). PMA did not change the holding current or shift the current/voltage relationship for $I_{Ca(L)}$. Staurosporine, a protein kinase C inhibitor, partially reversed the effect of PMA. Another phorbol ester, phorbol 12, 13-dibutyrate (PDB), also increased $I_{Ca(L)}$, but an inactive phorbol ester, 4α-phorbol 12, 13-didecanoate, did not affect the current. These results indicate that the Ca^{2+}-dependent isoform of PKC may play a role in regulating Ca^{2+} channel function in pregnant rat myometrial cells, and therefore may be involved in control of uterine contraction.

Supported by NIH grant HL-26170.

Tu-Pos397

SINGLE CATION CHANNELS, CALCIUM INFLUX AND EFFECTS OF ANGIOTENSIN-II AND NITRIC OXIDE IN SMOOTH MUSCLE CELLS FROM RABBIT AORTA.
((V.M. Bolotina, R.M. Weisbrod and R.A. Cohen))
Boston University Medical Center, Boston, MA 02118, U.S.A.

This study is aimed at understanding the role of ion channels in contraction and relaxation of vascular smooth muscle cells (SMC). Using the Fura-2 fluorescence technique, we studied Ca^{2+} influx into the cells induced by a contractile agent, angiotensin-II (AII), and using patch clamp technique we studied single ion channels which could mediate this influx. Here we present evidence that AII applied to the cell activates small (3 pS) Ca^{2+}, Ba^{2+}, Na^{+} -conducting cation channels in cell-attached configuration in cultured SMC from rabbit thoracic aorta. These channels are active at both high negative and high positive membrane potentials and show no inactivation with time at any membrane potential. These cation channels may be responsible for AII-induced Ca^{2+} influx into cultured aortic SMC cells from rabbit, as these SMC lack typical voltage-gated calcium channels. Here we also show that nitric oxide (NO), the well known relaxing factor, inhibits Ca^{2+} influx into SMC in dose-dependent manner. Regulation of small cation channels described in this study could be involved in NO-induced inhibition of Ca^{2+} influx and SMC relaxation.

Tu-Pos398

FACILITATION OF T-TYPE Ca CURRENT IN FROG CARDIOMYOCYTES. ((Julio L. Alvarez, Lourdes S. Rubio and Guy Vassort)) INSERM U.390, CHU Arnaud de Villeneuve, 34295 Montpellier cédex 5, France.

In a recent work (Alvarez and Vassort (1992) J.Gen.Physiol. 100:519-545) we described in bullfrog atrial cardiomyocytes a T-type Ca current that was sensitive to various compounds including several neurohormones. Moreover, the β-adrenergic induced increase in current was not cyclic AMP-dependent. We now report that this current, like other Ca currents, can exhibit "facilitation" i.e. an increase over its peak control amplitude under specific experimental conditions. Like the L-type Ca current, the T-type one did not show full inactivation by high prepulse depolarizations, a phenomenon not related to Ca-dependent inactivation in this case. Moreover, high prepulses could facilitate the current elicited by a depolarizing test pulse when this protocol was applied in the presence of isoproterenol. Facilitation was further enhanced in the presence of the poorly-hydrolysable analogs GTPγS or ATPγS but, in no case, was sustained; that excluded the involvement of Ca channel phosphorylation. Besides, facilitation was prevented by GDPβS and by pre-incubation with pertussis toxin; two experimental conditions that reduced and increased the basal T-type Ca current respectively. Our results suggest that high prepulse depolarizations relieve a G-protein dependent inhibitory tone which controls the T-type Ca current.

Tu-Pos399

DEPLETION OF INTRACELLULAR Ca^{2+} STORES ACTIVATES A Ca^{2+} CURRENT IN RAT BASOPHILIC LEUKEMIA CELLS (RBL-1). ((G. Schofield and M.J. Mason)) Dept. of Physiol., Tulane Univ., New Orleans, LA 70112.

Fluorescence measurements of $[Ca^{2+}]_i$ have confirmed the existence of electrogenic Ca^{2+} uptake stimulated by thapsigargin-mediated release of intracellular Ca^{2+} stores in RBL-1 cells. Experiments were undertaken using the whole cell, tight seal patch clamp configuration to isolate and characterise the Ca^{2+} current activated following depletion of Ca^{2+}_i stores. Passive pool depletion was achieved by dialysis with pipette solutions containing high concentrations of Ca^{2+} chelator (in mM; 85 CsGluconate, 20 CsBAPTA, 2 $MgCl_2$, 5 NMGCl, 0.1 Na_2GTP, 10 HEPES, pH 7.4). Immediately following break-in, 250 ms ramps from -125 to +60 from a holding potential of -40 mV were delivered at 3 second intervals. In the presence of external solutions designed to minimize other conductances (in mM; 140 NMGGluconate, 1 $MgCl_2$, 10 glucose, 20 sucrose, 8 $CaCl_2$, 20 HEPES, pH 7.4, free $[Ca^{2+}]$≈1.5) an inwardly rectifying current of approximately 10 pA at -120 mV consistently developed following dialysis of the cell interior (Fig.; record a and b were recorded 3 and 84 seconds after break-in respectively). Changes in $[Ca^{2+}]_o$ altered the magnitude of the current and the reversal potential in a fashion consistent with a Ca^{2+} current. This current was markedly inhibited by extracellular Ni^{2+} and La^{3+}. Measureable inward currents were observed when Ca^{2+} (8 mM) was substituted with Ba^{2+} or Mn^{2+}. A second current with similar inwardly rectifying properties and displaying inhibitory sensitivity to extracellular Ni^{2+} and Ba^{2+} was observed when extracellular solutions contained K^+. As a result of the presence of this inwardly rectifying K^+ current, we caution against the use of K^+ containing solutions in investigations of Ca^{2+} currents in RBL cells.

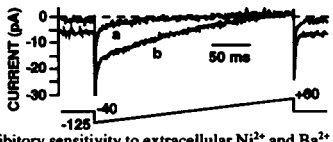

Tu-Pos400

INHIBITION OF CAPACITATIVE Ca^{2+} ENTRY BY ATP DEPLETION IN RAT THYMIC LYMPHOCYTES. ((I. Marriott and M.J. Mason)) Dept. of Physiology, Tulane University School of Medicine, New Orleans, LA 70112.

This study was performed to investigate the requirement for cellular ATP in the increase in plasma membrane Ca^{2+} permeability activated by the release of Ca^{2+} from intracellular stores in rat thymic lymphocytes (Capacitative Ca^{2+} Entry). The permeability state of this pathway following activation by a combination of Ca^{2+} depletion and thapsigargin addition was probed in control and ATP-depleted cells using fluorimetric measurements of $[Ca^{2+}]_i$ and membrane potential, and unidirectional measurements of Ca^{2+} uptake using $^{45}Ca^{2+}$. Cells depleted of ATP by incubation in solution devoid of glucose and containing oligomycin, antimycin A and 2-deoxy-D-glucose displayed markedly inhibited Ca^{2+} uptake via the capacitative Ca^{2+} entry pathway. This is based upon the following observations; 1) ATP depletion inhibits the increases in $[Ca^{2+}]_i$ associated with Ca^{2+} uptake via the capacitative Ca^{2+} entry pathway, 2) ATP depletion inhibits Mn^{2+} uptake following emptying of intracellular Ca^{2+} stores, 3) ATP depletion inhibits unidirectional $^{45}Ca^{2+}$ uptake following release of Ca^{2+} from intracellular stores and, 4) ATP depletion markedly inhibits the membrane potential depolarization attributed to electrogenic Ca^{2+} uptake via capacitative Ca^{2+} entry. These data cannot be explained on the basis of a loss of the transmembrane electrochemical gradient for Ca^{2+}, a direct inhibitory effect of the ATP-depletion procedure on the capacitative Ca^{2+} entry pathway, or an inhibitory effect of the inhibitors of ATP production on the ability of thapsigargin to release Ca^{2+} from intracellular stores. Rather, these data provide evidence for a requirement of high energy phosphate donors for the activation of the plasma membrane Ca^{2+} permeable pathway activated by release of Ca^{2+} from intracellular stores.

Tu-Pos401

ECONAZOLE BLOCKS DEPLETION-ACTIVATED CA^{2+} CURRENT IN JURKAT CELLS FROM AN EXTRACELLULAR SITE. ((E.P. Christian, J.A. Togo, K.T. Spence, and P.G. Dargis)) Department of Pharmacology, Zeneca Pharmaceuticals, Wilmington, DE 19897.

Calcium depletion from intracellular stores activates a plasmalemmal calcium current (calcium-release activated current; I_{CRAC}) in non-excitable cells (Hoth and Penner, *Nature* **355**:353-356,1992). Microfluorometry has demonstrated that imidazole antimycotics (e.g., econazole) block I_{CRAC} in the micromolar range (Alvarez et al., *Biochem. J.* **274**:193-197, 1990), but the blocking site and mechanism remain unsettled. We studied details of econazole block of I_{CRAC} in Jurkat cells with the whole cell patch clamp technique. The recording pipette contained 0 mM Ca^{2+} and 10 mM EGTA to passively deplete internal stores and activate I_{CRAC}. Econazole blocked I_{CRAC} in a concentration-dependent manner (IC_{50}≈10 μM; maximal block at 30 μM ≈75% of total I_{CRAC}). The block developed with relatively slow exponential kinetics (τ=23.4 sec at 10 μM; n=4), suggesting an indirect site of action. However, dialyzing the cytosol with econazole via the pipette solution (concentrations ranging from 0.1-30 μM; n=35) did not significantly (P=0.44) alter I_{CRAC} current density, when compared to control cells (n=21). In experiments where econazole was dialyzed intracellularly, subsequent application of econazole (1-30 μM) to the cell exterior blocked I_{CRAC} in a concentration-dependent manner. These data indicate that econazole blocks I_{CRAC} by interacting at an extracellular site.

Tu-Pos402

ACUTE AND CHRONIC EFFECTS OF PHENYLEPHRINE ON HYPERTROPHY AND L- AND T-TYPE CALCIUM CURRENTS IN NEONATAL RAT VENTRICULAR MYOCYTES. ((John P. Gaughan, Colleen A. Hefner and Steven R. Houser)) Temple Univ. Sch. of Med., Phila. PA 19140.

The density of I_{CaL} and I_{CaT} are altered during development and in severe cardiac hypertrophy and heart failure. To study the cell signaling producing these changes in calcium channel expression, we induced hypertrophy in neonatal rat ventricular myocytes with the α-1 adrenergic agonist, phenylephrine (P). We measured I_{CaL} and I_{CaT} after acute (<1 hr) and chronic (48 hrs) exposure to 20μM P. Peak I_{CaL} density was increased 247% (-3.97±.74 C vs -9.83±1.24 P pA/pF, n=19, p<0.05) and I_{CaT} density was unchanged (-2.04±.51 C vs -1.85±.46 P pA/pF, n=15) following acute exposure. This increase in I_{CaL} was blocked by propranolol (10^{-5}M) but not by the PKC inhibitor, staurosporine (.2μM in pipette). After 48 hrs in culture there was a significant increase in I_{CaL} in C. P caused significant myocyte hypertrophy but I_{CaL} density was significantly less than in C (-10.7±1.2 C vs -4.7±.8 P pA/pF, p<.05, n=22). I_{CaT} density increased in proportion to cell size and was not different in C and P (-3.38±.59 C vs -2.23±.49 P pA/pF, n=14). Staurosporine (2nM in culture) blocked the hypertrophy induced by P. We conclude that the acute effect of P on I_{CaL} is primarily a β-adrenergic effect while the chronic effect results from α-adrenergic activation of PKC which reduces I_{CaL} and increases I_{CaT} channel expression.

Tu-Pos403

L-TYPE CALCIUM CHANNEL AVAILABILITY IN A7R5 CELLS. ((J. Serrano, C. Obejero-Paz, R. Matteo and A. Scarpa)). Dept. Physiol. & Biophys., Case Western Reserve University. Cleveland OH 44106. (Spon. Jose Whittembury)

Membrane depolarization does not always result in L-type calcium channel opening. We studied the kinetic mechanisms that underlie this gating behavior using A7r5, the cell attached configuration of the patch clamp technique, and 110 mM Ba^{2+} as the current carrier. Channel availability depends on both, holding potential and stimulation rate. At holding potentials of -80, -40 and -20 mV, and 0.14 Hz stimulation rate, channel availability equals (mean ± SD) 54 ± 16 % (n=5), 53 ± 16 % (n=5), and 18 ± 1 % (n=2) respectively. At 0.71 Hz, channel availability decreases to 34 ± 1 % (-80 mV) and 2 ± 1 % (-40 mV, n=2). Null and active sweeps tend to occur in clusters (runs). The distribution of active runs as resulted from three experiments carried out at holding potentials between -80 and -100 mV, and frequencies of stimulation between 0.5 and 1 Hz was fitted to a single exponential function (τ 2.6 ± 1.3 s). By contrast two exponential functions with time constants of 0.6 ± 1.3 s and 11.0 ± 4.5 s are required to fit the null run histograms. The faster time constant represents an upper estimation since is shorter than the sampling period. Interestingly, short null runs and active runs tend to be grouped in clusters. Our results indicate that at least two mechanisms control channel availability in A7r5 cells.
Supported by NIH grant HL41618.

Tu-Pos404

COMPARISON OF Ca CURRENT IN RABBIT AND RAT VENTRICULAR MYOCYTES ((W. Yuan, K.S. Ginsburg and D. M. Bers)) Loyola University Chicago, Maywood, IL 60153.

Ca regulation differs greatly in rabbit and rat ventricular myocytes. The rabbit appears to depend more on sarcolemmal Ca fluxes. L-type Ca current (I_{Ca}) was measured as the Cd-sensitive current with 2 mM Ca_o using whole cell voltage clamp with 10 mM EGTA in the pipette and other ionic currents blocked. Peak I_{Ca} did not differ greatly (~10 pA/pF), but the E_m for peak I_{Ca} and half-maximal activation were both more negative in rat (by ~8 mV), while steady state inactivation was more positive in rat. This results in a larger "window" current in rat (Fig). In rat I_{Ca} decline during a step to -5 mV was also significantly slower and recovery from inactivation at E_m=-90 mV was faster. Voltage clamp pulses resembling action potentials (AP) from the two species were used to measure the Ca influx via I_{Ca} in the absence of Ca_i transients. In rat myocytes E_m steps to -5 mV and Rat-AP clamp (both 100 ms) allowed comparable Ca influx (9.3±1.9 & 8.5±1.3 μmol/l cell) where Rabbit-AP clamp produced much more Ca influx than the step (both 200 ms, 26.9±6.8 *vs* 13.6±2.6 μmol/l cell). The smaller window I_{Ca} in rabbit cells mitigated this difference, such that the Ca entry in rabbit with a Rabbit-AP was 13±2 μmol/l cell, but still higher than rat with Rat-AP. We conclude that a) there are fundamental differences in I_{Ca} in rat and rabbit myocytes b) the Ca influx during an AP can differ greatly from a square pulse and c) much more Ca entry is expected in rabbit myocytes.

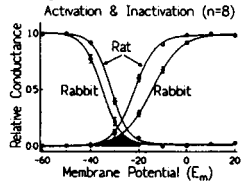

Tu-Pos405

CALCIUM CURRENTS IN STOMATOGASTRIC NEURONS OF *CANCER PRODUCTUS*. ((L.M. Hurley and K. Graubard)) Department of Zoology, University of Washington, Seattle, WA 98195.

The stomatogastric ganglion of decapod crustaceans is a major model system for studies of motor pattern generation. However, little is known about the properties of the calcium currents that are thought to underlie essential neuron behaviors. We are pharmacologically classifying calcium currents in 2 different stomatogastric motor neuron preparations: 1) in cultured somata and 2) at the GM neuron termination onto the gm1b muscle. Unidentified neuronal somata (50-100 μm) were pulled from the ganglion by suction so that they had few or no neurites and were cultured (after Panchin et.al. 1993) for 4-5 days. In order to reduce outward current and maximize inward current, TEACl (100 mM final concentration) and CaCl2 (26 mM final concentration) were substituted for equimolar amounts of NaCl and MgCl2, respectively. Up to 100mM CsCl was also sometimes added to the bath. The intracellular electrodes were filled with 1M TEACl and 5mM BAPTA.

In two-electrode voltage clamp of cultured neurons, inward current (seen in 20/27 cells) showed rapid activation at steps positive to -30 mV and slow calcium-dependent inactivation. The current was not blocked by TTX (2μM, n = 4), and was blocked by the divalent cations Cd2+ (500 μM, n = 4) and Mn2+ (10 mM, n = 2). It was also reversibly blocked by the dihydropyridine nifedipine at concentations of 50-100 μM (n = 9). In the absence of TEA, nifedipine and divalent cations reversibly blocked a component of outward current. At the GM-gm1b neuromuscular junction, nifedipine did not block evoked post synaptic potentials (50-100 μM, n = 2). These results suggest that there are at least 2 calcium current subtypes in stomatogastric neurons.

Supported in part by NSF predoctoral fellowship and NIH training grant.

Tu-Pos406

ELECTROPHYSIOLOGICAL CHARACTERISTICS OF SKELETAL AND CARDIAC MUSCLE SODIUM CHANNELS EXPRESSED IN THE TSA201 CELL LINE. ((M. Chahine, E. Plante, L.-Q. Chen and R. G. Kallen)) Québec Heart Institute, Laval Hospital Research Center, Laval University, St.-Foy, Québec, G1V 4G5 and Dept. of Biochem. & Bioph. Univ. of Pennsylvania, Sch. of Med. Philadelphia, PA 19104-6059.

The α subunit encoding for voltage-gated sodium channels, rSkM1 (rat skeletal muscle subtype1) and hH1 (human heart subtype1) have been cloned and expressed in *Xenopus* oocytes or in mammalian cell lines. In this study hH1 and rSkM1 were expressed in tsA201 (HEK293) cells, a human kidney cell line, and their electrophysiological behavior was compared using patch-clamp methods. Our results show that: **1)** The current-voltage relationships show different patterns, hH1 currents activate at -70mV but rSkM1 currents activate at -60mV. The peak current is at -30 mV for hH1 and -20mV for rSKM1, respectively. **2)** The kinetics of inactivation of hH1 are slower than of rSkM1, for exemple at -20mV τ_h=0.93±0.04ms for hH1 and τ_h=0.62±0.03ms for rSkM1(mean±sem). **3)** The steady-state inactivation-voltage relationship shows a shift of about 27mV ($V_{1/2}$= -102mV, k_v=5.6 and $V_{1/2}$= -74.9mV, k_v=4.8 of hH1 and rSkM1, respectively). **4)** The recovery from inactivation is significantly slower for hH1 (79.6ms) than for rSkM1 (4.2 ms) at -30mV (HP= -100mV).

We are using rSkM1-hH1 chimeric sodium channels to identify structural variations responsible for their biophysical behavior.

Tu-Pos407

PHYSIOLOGICAL LEVELS OF MAGNESIUM PRODUCE PERSISTENT CALCIUM CURRENT BLOCK IN CRUSTACEAN NEURONS. ((J.E.Richmond, B.Yuen, E.Sher and I.M. Cooke)) University of Hawaii, Honolulu, HI 96822. (Spon. by I.M. Cooke)

The X-organ-sinus gland, a major peptide neurosecretory system of Crustacea, has been used to study excitation-secretion coupling. We have recently characterized the high-voltage activated (HVA) calcium channels in the crab *Cardisoma carnifex* X-organ somata, which show similar electrophysiological properties to those of the sinus-gland terminals. We observed that the relative amplitudes of currents carried by Ca^{2+} and Ba^{2+} approached unity under normal physiological conditions. Since Ba^{2+} is usually more permeable than Ca^{2+} through HVAs we investigated the possibility that the high level of Mg^{2+} (24mM) found in crab saline was affecting the relative ion fluxes through the channel pore. In initial experiments using 52mM Ca^{2+} and Ba^{2+}, when Mg^{2+} was removed from the external solution the peak Ca^{2+} current amplitude increased by only 13 ±2.5 % (n=15) whereas the Ba^{2+} current increased by 74±12% (n=11). A dose-response curve for the blocking action of Mg^{2+} on Ca^{2+} and Ba^{2+} current amplitudes confirmed that the blocking efficacy of Mg^{2+} is greater for 52mM Ba^{2+} than 52mM Ca^{2+}. However, when the permeant divalent ion concentration was lowered to physiological levels (13mM), removal of Mg^{2+} caused a similar increase in both the Ca^{2+} and Ba^{2+} currents, (58±5% (n=12) and 72±5% (n=12) , respectively). These results can be explained on the basis of competition of the impermeant ion Mg^{2+} and permeant ions (Ca^{2+} and Ba^{2+}) for the same binding site within the calcium channel pore.

The resultant inhibition of calcium channels by Mg^{2+} at physiological levels of both ions predicts that secretion from the X-organ-sinus gland would be enhanced under Mg^{2+} free conditions. Preliminary results suggest that removal of Mg^{2+} does enhance peptide secretion.

Supported by NIH grant R01 NS-15453 and the University of Hawaii Foundation.

Tu-Pos408

PUTATIVE N-TYPE CALCIUM CHANNELS RECORDED FROM FROG SYMPATHETIC NEURONS. ((Keith S. Elmslie)) Department of Physiology, Tulane University Medical School, New Orleans, LA, 70112.

Our recent recordings of macroscopic calcium current in the presence of 90-100 mM Ba^{2+} have demonstrated that the N-type calcium current activates at voltages > 0 mV, while a novel calcium current activates at voltages ≥ -40 mV (Elmslie et al., 1994, Neuron **13**: 217). The novel current was selectively inactivated by holding the potential at -40 mV. Since previous recordings of single calcium channels from frog sympathetic neurons have focused on voltages ≤ 0 mV (Lipscombe et. al., 1989, Nature **340**: 639; Delcour et al., 1993, J. Neurosci. **13**:181), I was interested in examining the single calcium channels in the voltage range where N- current is active.

Using a holding potential of -40 mV to inactivate novel channels, I have observed 2 channel types with conductances of 20 and 26 pS. In BayK 8644, the 26 pS channel shows long open times during the step and long tail openings upon repolarizing to -40 mV. This channel has been observed in 3 of 10 patches and appears to be an L-type calcium channel. The 20 pS channel has been observed in 7 of 10 patches. It has a mean current amplitude at +30 mV of -0.66 pA (range -0.52 to -0.87 pA) and is active at voltage steps ≥ 0 mV. These characteristics are similar to the N-channel recorded from rat sympathetic neurons (Plummer et al., 1989, Neuron **2**: 1453; Rittenhouse and Hess, 1994, J. Physiol. **474**: 87). Thus, I have tentatively classified this as an N-channel. The 20 pS N-channel differs from channels previously recorded from frog sympathetic neurons in the voltage range of activation and inactivation and in having a larger single channel current (-1.3 pA vs. -0.5 to -0.8 pA at 0 mV).

Tu-Pos409

TERFENADINE BLOCKS TIME-DEPENDENT CA, NA AND K CHANNELS IN GUINEA PIG VENTRICULAR MYOCYTES. ((Z. Ming, C. Nordin)) Albert Einstein College of Medicine, Bronx NY 10461.

Terfenadine has been shown to block delayed rectifier K^+ channels (i_K), but it is structurally related to diphenylalkamine L-type Ca^{2+} channel (i_{Ca}) blockers and has been reported to cause inexcitability of Purkinje fibers. To test the hypothesis that terfenadine binds specifically to highly time-dependent channels independent of cation selectivity, we investigated the effect of terfenadine on i_K, i_{Ca} , time-dependent Na^+ channels (i_{Na}) and inward rectifier K^+ current (i_{K1}) using standard whole cell patch clamp techniques in isolated guinea pig ventricular myocytes. Values were determined as follows: i_{Ca}: peak inward current on step from -40 to 0 mV; i_{Na}: peak inward current on step from -90 to -40 mV following 300 msec clamp from -40 to -90 mV; i_K: peak outward tail current at -40 mV following 300 msec step from -40 to +10 mV; i_{K1}: steady state outward current at -50 mV. Experiments were controlled for time of internal dialysis: all measurements (37°, mean±SD, pA/pF) in the table below were made 10 minutes following dialysis in cells in control Tyrode solution (Na^+ 137mM, Ca^{2+} 1.8mM, K^+ 5.4 mM) (C) or control solution plus terfenadine 3 x 10^{-6} M (T). Significance (*): $p < 0.05$.

	n	i_{Ca}	i_{Na}	i_K	i_{K1}
T	5	-4.2±2.3*	-2.9±3.4*	0.25±0.38*	2.5±1.4
C	5	-13.0±4.3	-65.4±15.2	0.89±0.13	2.3±2.0

Near total suppression of i_{Ca} and i_{Na} developed following 20 minutes exposure to terfenadine. Rates of inactivation were not affected. Doses less than 1 mM had almost no effect on any current. These results suggest that terfenadine specifically blocks highly time- and voltage-dependent channels, possibly by binding to a common protein structure, not related to pore selectivity, which is associated with activation of ion conductance.

Tu-Pos410

BIOPHYSICAL CHARACTERISTICS AND MODULATION OF BI(Q-TYPE) Ca^{2+} CHANNELS. ((M. Wakamori, *T. Niidome, *K. Katayama and Y. Mori)) Inst. Molec. Pharmacol. & Biophys., Univ. of Cincinnati, Cinti., OH 45267, *Eisai Co., Ltd., Tsukuba, Ibaraki 300-26, Japan

The existence of Q- and R-type Ca^{2+} channels in neurons, in addition to T-, N-, L- and P-types, has been recently demonstrated. The Q-type channel is the high-voltage activated, sensitive to ω-conotoxin(ω-CgTx)-MVIIC and partially sensitive to ω-agatoxin-IVA. The modes of modulation for the Q-type are not known, because it is difficult to record from native cells which express multiple types of Ca^{2+} channels. We have, therefore, examined biophysical properties of the Q-type channel and its modulation using a BI clone expressed with α_2 and β_1 subunits into baby hamster kidney (BHK) cells which have no endogenous Ca^{2+} channels.

The expressed channels showed voltage-dependent activation and inactivation, unitary conductance(15pS) and high sensitivity to ω-CgTx-MVIIC that are characteristic of the Q-type. Dibutyl(db)-cAMP increased Ba^{2+} current (I_{Ba}) in a concentration-dependent manner. Augmentation of I_{Ba} by 100μM db-cAMP was 3x in amplitude. When BHK cells were dialyzed with GTPγS, the BI channels did not show the slow activation phase of I_{Ba}; however the BIII (N-type) channels showed it. This well-known suppression of N-type channels was relieved by short strong conditioning pulses. These data show that the modulation of Q-type (BI) channels in BHK is different from N-type channels.

Tu-Pos411

CALCIUM CHANNELS IN GLOMUS CELLS AND THEIR REGULATION BY OXYGEN TENSION. ((R. J. Montoro and J. López-Barneo)) Dept. Fisiol. Méd. Biofís. Universidad de Sevilla. 41009 Sevilla. Spain. (Spon. by G. Alvarez de Toledo).

Glomus cells are the primary sensory receptors of the carotid body responsible for the hyperventilatory response to lowered blood PO_2. The chemoreceptive property of these cells is primarily conferred by O_2-sensitive K^+ channels, whose inhibition at low PO_2 leads to Ca^{2+} entry and subsequent transmitter release. We have now tested whether PO_2 can alter the various high-threshold, voltage-activated, Ca^{2+} channel types present in these cells. Exposure to hypoxia (switching from PO_2 of 145 to 20 mmHg) leads to a reversible reduction of the Ca^{2+} current which, in many cells, is strongly voltage-dependent. At -10 mV the inhibition is 20 to 30% of control, but it is almost negligible at +20 mV. Approximately 50% of the channels are of the L-type (blocked by 5 μM nifedipine). N and P-type Ca^{2+} channels (blocked by 1 μM ω-conotoxin GVIA and 0.1 μM ω-agatoxin IVA, respectively) are also present, as well as some channels resistant to the three drugs used. Low PO_2 appears to exert a similar regulatory action on the various classes of high-threshold Ca^{2+} channels, although this aspect has not yet been studied in detail. On the other hand, Na^+ currents studied over a full range of membrane potentials were unaffected by low PO_2. Our data demonstrate the presence of O_2-sensitive Ca^{2+} channels in glomus cells which, in conjunction with O_2-sensitive K^+ channels, may contribute to the complex relationship existing between PO_2 and the secretory activity of these cells.

Tu-Pos412

MODULATION OF Ca^{2+} CURRENTS AND CYTOSOLIC Ca^{2+} IN SMOOTH MUSCLE CELLS OF THE PULMONARY ARTERIAL TREE BY CHANGES IN O_2 TENSION. ((J.Ureña, A.Franco and J.López-Barneo)) Dept. Fisiol. Méd. Biofís. Universidad de Sevilla. 41009 Sevilla. Spain. (Spon. by V. Ceña)

In the pulmonary circulation arterial tone is under the influence of local O_2 tension (PO_2). Since we have shown the existence of O_2-sensitive Ca^{2+} channels in systemic arterial myocytes, we tested the possibility that similar channels could be present in pulmonary vascular smooth muscle. Exposure of voltage-clamped cells to physiologically relevant levels of low PO_2 (between 145 and 20 mmHg) reversibly inhibits the L-type component of the Ca^{2+} current. The effect of low PO_2 is strongly voltage-dependent as the current is predominantly inhibited during depolarizations to membrane potentials below 0 mV. This reponse, similar to what occurs in systemic myocytes, is seen in cells dispersed from the main trunk of the pulmonary artery. An opposite effect (lack of inhibition or even potentiation of current amplitude at negative membrane potentials) was occasionally observed in cells from peripheral arterial branches. Fura-2 loaded myocytes exhibited oscillations of cytosolic Ca^{2+} whose frequency was regulated by Ca^{2+} entry through voltage-gated channels. These cells displayed a broad variety of changes in cytosolic [Ca^{2+}] during hypoxic treatment. However, the most frequent response was, as in systemic arteries, attenuation of the Ca^{2+} oscillations. These data suggest the existence of regional variations along the pulmonary arterial tree in the response to changes in PO_2 .

Tu-Pos413

ALTERED CA CURRENTS IN HUMAN MYOTUBES WITH MUTANT SKELETAL MUSCLE DHP RECEPTORS. ((I. Sipos, Cs. Harasztosi, K. Jurkat-Rott, R. Heine, L. Kovacs, F. Lehmann-Horn and W. Melzer)) Dept. Applied Physiology, University of Ulm, D-89069 Ulm, Germany; Dept. Physiology, University Medical School of Debrecen, H-4012 Debrecen, Hungary

We have studied Ca currents in myotubes from patients with hypokalemic periodic paralysis which show an arginine to histidine exchange in the S4 segment of either repeat II or IV of the α1 subunit of the skeletal muscle DHP receptor (Jurkat-Rott et al., Hum. Mol. Gen. 3, 1415-1419, 1994). For both mutations an elevated average density of a rapid Ca current component ("third type", Rivet et al., Neurosic. Letters 138, 97-102, 1992) was found. Myotubes with mutation R528H (IIS4) showed normal activation of the slow L-type current at the hõlding potential of -90 mV but exhibited a shift of the voltage dependence of steady state inactivation by about 40 mV to more negative potentials. For mutation R1239H (IVS4), the average density of the DHP-sensitive Ca current was reduced to about one third while the inactivation curve was biphasic and could be fitted by a dual Boltzmann function with average midpoint voltages of +3.4 mV and -45.2 mV. These results suggest that both DHP receptor mutations affect the skeletal muscle L-type Ca channel by favouring its voltage-dependent inactive state.

Tu-Pos414

HIGH VOLTAGE-ACTIVATED CALCIUM CURRENTS OF NEURONS FROM THE RAT VENTROBASAL THALAMUS. ((Paul J. Kammermeier and Stephen W. Jones)) Departments of Neuroscience and Physiology & Biophysics, Case Western Reserve University, Cleveland, OH 44106.

We have studied the effects of dihydropyridines (DHPs) and ω-conotoxin GVIA (CgTx) on high voltage-activated (HVA) calcium currents of acutely isolated thalamic relay neurons, using whole-cell patch clamp recording. The charge carrier was 25 mM Ba^{2+}, and Na^+ and K^+ were replaced with TEA. 1 μM CgTx blocked 20 ± 5% of the current (n = 5, ± SD). The DHP agonist (+)202-791 (0.3 μM) increased the peak current to 198 ± 63% of control (n = 5). (+)202-791 induced slowly deactivating tails upon repolarization to -50 mV; activation kinetics were also slowed. The DHP antagonist nimodipine (5 μM) inhibited 37 ± 11% (n=4) of the steady-state current at 0 mV (near peak current) from a holding potential of -80 mV, and inhibited 88 ± 3% (n = 4) of the (+)202-791-enhanced tails. 1 μM nimodipine was less effective (52 ± 16% block of slow tails, n = 3). We conclude that thalamic neurons have L-current, N-current, and HVA current(s) resistant to both DHPs and CgTx.

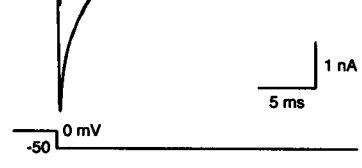

Tu-Pos415

INHIBITION BY LOCAL ANESTHETICS OF CALCIUM CHANNELS IN ANTERIOR PITUITARY CELLS. (Z.-L. Xiong and G.R. Strichartz) Department of Anesthesia Research Laboratories, BWH, Harvard Medical School, Boston, MA02115. Local anesthetic (LA) inhibition of Ca^{2+} channels was investigated and compared with that of nicardipine (NICAR) in GH_3 cells by whole-cell voltage clamp. In 10 mM Ba^{2+}, depolarization above -40 mV evoked a slowly-inactivating I_{Ba}. Extracellular lidocaine (LID) inhibited I_{Ba} without changing the activation threshold, the voltage of peak current, or the reversal potential. Inhibition was greater at a holding potential (HP) of -60 mV (IC_{50}=1.2 mM) than at -80 mV (IC_{50}=2.6 mM). This depolarization-induced potentiation developed over 0.1-10 sec after membrane depolarization began. NICAR also dose-dependently inhibited I_{Ba} with a IC_{50} of 90 nM (at a HP of -80 mV). Both LID and NICAR shifted the I_{Ba} steady-state inactivation curves to left. Double-pulse protocols revealed that LID (1 mM) accelerated the depolarization-induced inhibition (inactivation) of I_{Ba}, but had no effect on the hyperpolarization-induced channel re-activation. NICAR also accelerated the depolarization-induced inactivation of I_{Ba} but also slowed the hyperpolarization-induced re-activation. In addition, the relative inhibitory action of LID on I_{Ba} was unaffected in the presence of NICAR. LID appears to have a direct action on membrane Ca^{2+} channels, similarly to the voltage-dependent action of dihydropyridine (e. g., NICAR). However, this action and, by implication, binding site, is separate and independent from that of dihydropyridine. Another local anesthetic, bupivacaine, also depressed I_{Ba}, but the potency was 14 times greater than that of LID. In addition, both LAs strongly inhibited the fast Na^+ current in the same cells at 10 - 20 times their potency on Ca^{2+} channels. Thus, inhibition of Ca^{2+} currents probably does not account for the analgesic actions of intravenously administered LID (ca. 10 μM), but may contribute to spinal anesthesia by LA (present in CSF at ca. 1mM). (GM 15904 to GRS).

Tu-Pos416

NERVE GROWTH FACTOR-INDUCED REDUCTION IN Ba^{2+} CURRENT INACTIVATION IN ADULT SYMPATHETIC NEURONES IS INDEPENDENT OF NEURITE ELONGATION. ((S. Lei, W.F. Dryden and P.A. Smith)). Dept. Pharmacol., Univ. Alberta, Edmonton, Canada, T6G 2H7.

In order to understand the mechanisms that are available for the long-term control of I_{Ca} in adult neurones and the possible relationship between I_{Ca} and neurite extension, bullfrog sympathetic ganglia (BFSG) were enzymatically-dissociated and the neurones placed at low density in a defined (serum-free) culture medium. B-cells were identified on the basis of input capacitance (C_{in} > 70pF) and the properties of I_{Ca} examined using whole-cell recording with 2mM Ba^{2+} as a charge carrier. After 12d in culture, peak I_{Ba} (maximum peak current normalized for cell size) was reduced to 47% of control when the holding potential (V_h) was -60mV but to only 68% of control when V_h was -90mV (P<0.05; n>20 for all measurements). Since the currents evoked from -60mV were decreased more than those from -90mV, increase in inactivation (at -60mV) likely contributed to this decrease in I_{Ba}. Inclusion of 200ng/ml 2.5s NGF in the culture for 12d restored I_{Ba} to the control values attained from both -90 and -60mV (P<0.01; n>20) as might be expected if part of NGF's action is attributable to a decrease in inactivation. Also, I_{Ba} recorded at -10mV in the absence of NGF decreased (inactivated) by 45% in 500ms whereas that recorded in the presence of NGF inactivated by only 35%. Alterations in I_{Ca} are unlikely to be associated with growth of neurites because increases in C_{in} occurred after 3d in culture with and without NGF whereas I_{Ba} decreased in the absence of NGF and the NGF-induced increase in I_{Ba} took about 6d to develop. Supported by MRC (Canada)

Tu-Pos417

ANOMALOUS GATING OF DIHYDROPYRIDINE-SENSITIVE CALCIUM CHANNELS IN RAT SKELETAL MYOBALLS

((Andrea Fleig & Reinhold Penner))*Department of Membrane Biophysics, Max-Planck-Institute for Biophysical Chemistry, 37077 Göttingen, Germany*

Skeletal muscle cells are thought to possess more dihydropyridine binding sites than functional calcium channels, suggesting the presence of non-conducting ("silent") DHPRs. We report in rat skeletal myoballs the presence of a Ca channel with anomalous gating behavior that is "activated" or "primed" at positive potentials without conducting significant Ca current during depolarization. However, upon repolarization of the membrane to negative potentials it generates large tail currents. The anomalous Ca channels in myoballs are sensitive to dihydropyridines but activate about seven times slower (τ = 270 ± 22 ms, n = 5) than the known L-type channels of skeletal muscle (τ = 42 ± 9 ms, n = 5). Tail currents exhibit at least two deactivation time constants. The relative amplitudes of the two deactivation components are strongly voltage-dependent with the slow component ($\tau_{slow} \approx 20$ ms) increasing in parallel with the pulse currents, whereas the fast component ($\tau_{fast} \approx 2$ ms) requires stronger depolarizations and keeps augmenting with the pulse potential. The slow component is likely due to tail currents associated with the pulse currents, whereas the fast deactivating tail currents might correspond to the anomalous tail currents. We propose that these anomalous-gated Ca channels represent the postulated silent dihydropyridine receptors and that they may play a role in the voltage control of excitation-contraction coupling.

Tu-Pos418

Pharmacological Effects of Ca^{2+} Chelators on Calcium Currents in Bovine Chromaffin Cells

(Matthias Bödding & Reinhold Penner), Max-Planck-Institute for Biophysical Chemistry, 37077 Göttingen, Germany

The Ca^{2+} chelators EGTA and BAPTA are widely used in electrophysiological measurements of Ca currents in order to decrease Ca^{2+} induced inactivation of Ca currents. Recent studies have shown that Ca^{2+} chelators can directly interfere with proteins, e.g. IP-3 receptors or protein kinases. Here we present evidence that these commonly used Ca^{2+} chelators have complex effects on Ca currents in chromaffin cells, unrelated to chelating internal free Ca^{2+}. Both EGTA and BAPTA affect the peak amplitude in a concentration dependent manner: Concentrations ranging from 100µM to 30mM increase, but higher doses suppress current amplitudes. Concomitantly, high BAPTA concentrations shift the IV curve by about 20 mV to more positive potentials, while the slope factor remains constant (≈ 6 mV). The voltage dependence of the activation time constant τ_a shifts to positive potentials in parallel with the IV curve. Thus BAPTA seems to act mainly on the voltage dependence of the calcium cannels, but does not seem to affect their kinetics. EGTA has minor effects on the halfmaximal activation $V_{1/2}$, the slope factor (≈ 8 mV) or activation kinetics. From our data, it seems hat BAPTA has more adverse effects on Ca channel characteristics than EGTA. However, peak current amplitudes are significantly influenced by both BAPTA and EGTA concentrations. Thus, when using either of these Ca^{2+} chelators, one should consider their pharmacological effects on Ca channels.

Tu-Pos419

MECHANISM OF ALPHA-2 ADRENERGIC MODULATION OF CANINE PURKINJE ACTION POTENTIAL.

((J.J. Cai and H. Lee)) University of Iowa, Iowa City, IA 52242.

We have demonstrated that α_2-adrenergic stimulation prolongs action potential duration in isolated canine Purkinje fibers via a pertussis toxin-sensitive G protein. This study attempts to identify the ionic mechanism through which α_2-adrenergic stimulation produces such APD effects. Using standard microelectrode techniques, isolated canine Purkinje fibers were superfused with Tyrode's buffer at 37 °C and paced at 1 Hz. The effect of the α_2-specific agonist UK 14,304 (UK, 0.1 µM) and yohimbine (Y, 0.1 µM) on APD50 and APD90 were measured at baseline (BL), in the presence of 4-amino-pyridine (4AP, 1 mM), mefenamic acid (MA, 10 nM), and *d*-sotalol (S, 10 µM). The results are summarized below (mean ± SEM):

APD50 (ms)			APD90 (ms)			
BL	UK	UK+Y	BL	UK	UK+Y	n
240±20	256±20*	244±19**	325±18	342±18*	332±18**	8
4AP	4AP+UK	4AP+UK+Y	4AP	4AP+UK	4AP+UK+Y	
343±29*	333±31	316±32	468±38*	464±39	441±41	7
MA	MA+UK	MA+UK+Y	MA	MA+UK	MA+UK+Y	
336±20*	348±21**	332±20**	418±19*	433±19**	421±17**	6
S	S+UK	S+UK+Y	S	S+UK	S+UK+Y	
401±28*	416±29**	400±28**	493±30*	515±31**	494±30**	6

* p<0.05 compared with BL; **p<0.05 compared with preceding intervention.

Also, whole cell recordings in isolated canine Purkinje cells showed the transient outward potassium current (I_{to}) was inhibited by UK 14,304. These results suggest that α_2-adrenergic stimulation prolongs the Purkinje APD by inhibition of I_{to}.

Tu-Pos420

ARE ALTERATIONS IN ACTION POTENTIALS AND MYOPLASMIC CA TRANSIENTS IN HEART FAILURE CAUSED SIMPLY BY REDUCTION IN CHANNEL DENSITY?: A COMPUTER MODEL ANALYSIS.

((C. Nordin)) Albert Einstein College of Medicine, Bronx NY 10461.

Cells from hearts of guinea pigs with congestive heart failure (CHF) secondary to gradual onset ascending aortic constriction (F. Siri et al, Am J Physiol 257:H1016,1989) are characterized by a wide variety of alterations in physiologic function, including lengthening of action potential duration, reduced magnitude of current density of L-type Ca^{2+} channel (i_{Ca}) and delayed rectifier K^+ (i_K) currents, and weaker contractile force secondary to reduced peak magnitude and lengthening of free myoplasmic Ca^{2+} transients. Several groups have also reported reduced number of sarcoplasmic reticulum (SR) Ca^{2+} ATPase, SR Ca^{2+} release channel, and sarcolemmal Na-K ATPase molecules per unit membrane. To test the hypothesis that hypertrophy and failure cause changes in physiologic function simply as the result of quantitative reduction in density of ion transport molecules, we examined the response of a computer model of transmembrane current and intracellular Ca^{2+} flux in the isolated guinea pig myocyte (C. Nordin, Am J Physiol 265:H1117,1993) to changes in sarcolemmal and SR channel densities. Simple redundancy of capacitance did not cause appropriate change in intracellular concentration. The set of physiologic data was best fit with the following modifications of density (normalized to capacitance, % of control): i_{Ca} and inward rectifier K^+ channels, 80%; SR Ca^{2+} and Na-K ATPase pumps, 70%; SR Ca^{2+} release and i_K channels, 50%; time-independent plateau K^+ channels, 30%. No alteration was required in Na-Ca exchange. Selective reduction in the density of specific channels accounted for all major physiologic alterations in CHF myocytes except reduced difference in action potential duration between CHF and control with increased stimulation rate. These findings suggest that the process of hypertrophy and failure affects physiologic function, including contractility itself, primarily through altered genetic regulation of membrane density of ion transport proteins, and that reduction in density is not a function of a single control mechanism, but of different feedback for each specific protein.

Tu-Pos421

ATP-ACTIVATED GTP-DEPENDENT CALCIUM-PERMEABLE CHANNELS IN MACROPHAGES. EFFECT OF INTRACELLULAR CALCIUM ON CURRENT SUBLEVELS.

((A.G. MAMIN, K.I. KISELYOV, G.N. MOZHAYEVA)) Institute of Cytology, Russian Academy of Sciences, St. Petersburg, Russia

Cell-attached and whole-cell experiments on rat macrophages demonstrated that an ATP receptor and calcium channel are coupled by a G protein. Inward currents were observed when the extracellular solution contained micromolar concentrations of ATP and Ba^{2+}, Ca^{2+}, or Na^+ were the only permeant cations. The ATP receptor was defined to be of the P_{2Z} class. Channel activity decreased rapidly after patch excision and could be restored by the application of 100 µM GTP or GTPγS to the internal surface of the membrane. The channel exhibited four conductance levels. With Ba as a permeant cation, subconductance levels were: 3.5, 7, 10, and 15 pS. Channels were selective for Ca^{2+} - PCa:PBa:PNa:PK = 68:30:3.5:1. Elevation of the intracellular free calcium concentration ($[Ca^{2+}]_i$) in the nano/micromolar range resulted in a gradual decrease of the mean current with a dissociation constant for the calcium-binding site(s) of about 10^{-7} M. The mean current depended on changes in the distribution of conductance sublevel occupation such that with $[Ca^{2+}]_i$ elevation the first sublevel increased and the third and fourth sublevels decreased in their relative weights. The weighted sublevel current, equal to the average current passing through the channel at each opening, was 0.54 pA at pCa 8, 0.35 pA at pCa 7 and 0.29 pA at pCa 6 (-30 mV). Po, calculated as a ratio between the mean current and the weighted sublevel current, showed only a slight decrease with the $[Ca^{2+}]_i$ rise.

Tu-Pos422

CARDIAC NON-SELECTIVE CATION CURRENT ACTIVATED BY OXY-RADICAL STRESS AND LYSOPHOSPHATIDYLCHOLINE: VOLTAGE-DEPENDENCE AND BLOCK BY Ni^{2+}.

((W.C. Cole, R.I. Jabr, E.A. Aeillo and E. Morales)) Department of Pharmacology and Therapeutics, University of Calgary, Calgary, Alberta, Canada, T2N 4N1.

Extracellular oxy-radical stress (OR) and lysophosphatidylcholine (LPC) activate non-selective cation conductance (NSCC) despite high intracellular Ca^{2+} chelation with EGTA or BAPTA (5-10 mM; Biophys J 66:A434; J Clin Invest 88:1819). We employed isolated guinea pig ventricular myocytes and whole-cell voltage clamp to describe two novel properties of NSCC activated by LPC (20 µM) or OR from a combination of dihydroxyfumaric acid (3 mM) and ADP:$FeCl_3$ (0.5:0.05 mM). Bath and pipette in mM; LiCl 120, CsCl 5.4, $MgSO_4$ 3, TEA^+ 10, $BaCl_2$ 0.2, nicardipine 0.01, TTX 0.01, HEPES 5, pH 7.4 and CsCl 140, $MgCl_2$ 1, Na$_2$ATP 5, TEA^+ 20, EGTA or BAPTA 5, pH 7.2, respectively. Voltage ramps from -130 to +30 mV (8 s) during LPC or OR elicited a quasi steady-state current reversing at ~-20 mV which had an N-shaped I-V relation with reduced current negative to -50 mV. The basis for this voltage-dependence was explored with 250 ms test pulses to between -30 and -120 mV after 1.5 s depolarizations to +30 mV. Peak current during the test pulse (i.e. immediately after the transient) had a linear I-V relation. However, the current decayed with time to a sustained level with an N-shaped I-V relation identical to that obtained with ramps. The time constant for decay was voltage-dependent, rising from 20 to 250 ms between -120 and -70 mV. Both the ohmic, quasi-instantaneous as well as the voltage-dependent, sustained components of NSCC activated by LPC or OR were blocked by external Ni^{2+} (5 mM). The voltage-dependence and block by divalent cation are novel properties for cardiac NSCC, but were reported for receptor-operated NSCC in smooth muscle (J Physiol 424:57; J Physiol 442:447). Supported by MRC (MT-10569 to WCC). RIJ was a CHSF trainee.

Tu-Pos423

A DOUBLE-BARRELLED PERFUSION OF SINGLE CELLS FOR THE STUDY OF SUBCELLULAR COMPARTMENTATION INVOLVED IN ION CHANNEL REGULATION. ((J. Jurevicius and R. Fischmeister)) INSERM CJF 92-11, Univ. Paris-Sud, Fac. Pharmacie, 92296 Châtenay-Malabry, France. (Spon. by R. Ventura-Clapier)

Hormonal regulation of ion channel activity often involves a sequence of biochemical events, such as the production or degradation of a 2nd messenger and the activation of a protein kinase. However, little is known on the subcellular localization of these events. It is reasonable to assume that a hormone should be more potent if its action is mainly "local", i.e. if all the sequential events take place in a restricted region near the channel, than if one (or several) intermediate reactant is allowed to diffuse away and affect remote channels in a "distant" manner as well as other processes within the cell. In an attempt to quantify "local" vs. "distant" effects of a hormone, we developed a method based on the use of two patch-clamp pipettes and a double-barrel extracellular perfusion. The method was tested on frog ventricular cells. A rod-shaped cell (150-500μm long) was sealed at both ends to two patch-pipettes. One or both of the pipettes were in the whole-cell or perforated patch recording configuration. Moving the two pipettes independently allowed to expose the cell transversally to two different solutions ejected at high speed (2-3 cm/s) from two capillaries (i.d. =400μm) separated by an intermediate wall ≈5μm thick. Elimination of Ca^{2+} ions from one solution (0Ca) induced a reduction in the amplitude of the whole-cell calcium current (I_{Ca}) that was used to estimate the portion of the cell surface exposed to each solution. Adding a drug either to the 0Ca- or the Ca-containing solution, allows to evaluate respectively the "distant" or "local" effect of the drug on I_{Ca}.

Tu-Pos424

EFFECT OF SURAMIN ON THE FACILITATION OF SODIUM CURRENTS IN FROG NEUROGLIA BY NERVE IMPULSES. ((Hector Marrero, Jannette Acevedo and Richard K. Orkand)) Institute of Neurobiology and Departments of Physiology and Pharmacology, University of Puerto Rico-Medical Sciences Campus, San Juan, P.R. 00901 (Spon. by Walmor C. De Mello)

Using both loose-patch clamp and whole cell patch-clamp recording from glial cells on the surface of the intact frog optic nerve, we have demonstrated that the voltage-dependent inward sodium currents in the glial cells are increased about 3 fold for 1 sec. following a train of impulses (10 Hz for 1 sec.) in the underlying axons (H. Marrero and R.K. Orkand, Proc. R. Soc. Lond. B, 1993, 253:219-224). This facilitation is prolonged in low Ca^{2+} (0.3 mM) and inhibited in high Ca^{2+} (8 mM). We now report that the ATP antagonist suramin (0.2-1 mM) dramatically increases this facilitation 3 fold and slows its decay. ATP (1-5 mM) increases the amplitude of the glial sodium currents but has no clear effect on the facilitation. Furthermore, the effect of suramin to increase the facilitation persists in the presence of ATP. The effect of suramin is decreased by the addition of 5 mM Mg^{2+} or 7-10 mM Ca^{2+}, and increased by the addition of 5 mM Co^{2+}. The results suggest that the increase in facilitation produced by suramin is related to its properties as a chelator rather than as an ATP antagonist.

Tu-Pos425

ELECTRICAL ACTIVITY AND CALCIUM INFLUX REGULATE ION CHANNEL DEVELOPMENT IN EMBRYONIC *XENOPUS* SKELETAL MUSCLE. ((Paul Linsdell and William J. Moody)) Dept. of Zoology, University of Washington, Seattle WA98195. (Sponsored by Mark S. Cooper)

Embryonic skeletal muscle cells from the frog *Xenopus laevis* can be identified before they express voltage-gated ionic currents, and will develop potassium, sodium and calcium currents in a temporally stereotyped manner if isolated at this stage and grown in culture. We find that the development of both potassium and sodium currents under these conditions are dependent on electrical activity, as both are reduced by culturing in the presence of tetrodotoxin. The mechanism linking electrical activity and current development appears to involve calcium entry through voltage-gated calcium channels. These results indicate that the expression of different channel types by these cells is influenced by the activity of channels already present, suggesting a degree of coordination between the expression of different channel types.

Tu-Pos426

EFFECTS OF CELL SWELLING ON ACTION POTENTIAL DURATION IN GUINEA-PIG VENTRICULAR MYOCYTES. ((J.I. Vandenberg, S.A Rees, A.R. Wright, V.W. Twist, and T. Powell)) University Laboratory of Physiology, Parks Road, Oxford, UK

Osmotic swelling of guinea-pig ventricular myocytes causes activation of a chloride conductance, an increase in the delayed rectifier K^+ conductance (I_K) and inhibition of Na^+-Ca^{2+} exchange; all of which would be expected to shorten action potential duration (APD). However, cell swelling also causes inhibition of the inward rectifier K^+ conductance (I_{K1}) which would be expected to lengthen APD. In this study we have used the Amphotericin B permeabilised patch recording technique to characterize the effects of cell swelling on APD measured at 90% repolarization (APD-90) in freshly isolated adult guinea-pig ventricular myocytes. Cells were swollen by decreasing the osmotic strength of the external solution (mM: NaCl, 100; sucrose, 80; KCl, 5.4; $MgCl_2$, 1; $CaCl_2$, 1.8; NaH_2PO_4, 0.33; glucose, 11; HEPES, 5; pH adjusted to 7.4 with NaOH at ~35°C) by removal of sucrose. The patch pipette contained (mM: K_2SO_4 65; NaCl, 10; $MgCl_2$, 1.8; EGTA, 1; HEPES, 5; pH adjusted to 7.2 with KOH, osmolality adjusted to 290 mosM with sucrose). Amphotericin B was dissolved in DMSO and added to pipette solutions to a final concentration of 240 μg/mL. Cell-swelling caused a small but significant lengthening of APD-90 after 1 minute (108.5 ± 1.7 %, n=23, $p<0.05$) but after 3 minutes APD-90 was no longer significantly diffferent from control (107.4 ± 6.9 %, n=9). Cell swelling was also associated with depolarization of the resting membrane potential (E_m, 1.46 ± 0.29 mV after 1 minute and 1.95 ± 0.57 mV after 3 minutes). In high pipette Cl^- experiments (K_2SO_4 and NaCl replaced with KCl) there was no significant change in APD-90 (101.9 ± 2.0 %, after 1 minute and 94.7 ± 7.1% after 3 minutes exposure to hypotonic solution, n=6) but there was a larger depolarization of E_m (2.31 ± 0.71 mV after 1 minute and 4.92 ± 1.29 mV after 3 minutes). The initial increase in APD-90 suggests a reduction in I_{K1} is the predominate early effect of cell swelling but that after 3 minutes this effect is balanced by changes in other ionic conductances. Depolarization of E_m is most easily explained by changes in E_K (secondary to dilution of $[K^+]_i$) but the greater effect seen with high $[Cl^-]_{pip}$ suggests $[Cl^-]_i$ could also be important.

Tu-Pos427

BLOCKING EFFECT OF KETAMINE STEREOISOMERS AT DIFFERENT CA^{2+} CHANNEL TYPES OF RAT DORSAL ROOT GANGLION NEURONS

((A. Scholz, N. Kuboyama, G. Hempelmann[1] and W. Vogel))
Physiologisches Institut, Aulweg 129, and [1]Anaesthesiologie und Operative Intensivmedizin, Klinikstr. 29, Justus-Liebig-Universität, 35392 Giessen, Germany

The effects of two stereoisomers of ketamine on different Ca^{2+} channels were tested in acutely dissociated rat DRG neurons by the patch-clamp technique in whole-cell mode. The ketamine was externally applied by inserting the pipette with the cell into a multi barrel system.

N-type Ca^{2+} currents, measured as a difference between peak and sustained current during a 200 ms impulse at a test potential of 0 mV, were relatively insensitive to ketamine in external high TEA solution containing 2.2 mmol/l Ba^{2+}. L-type Ca^{2+} currents, discriminated as sustained current at the end of a 200 ms impulse at a test potential of +10 mV, displayed a higher sensitivity. The Hill coefficients were 1.1 and 0.96 respectively. T-type Ca^{2+} currents, obtained from peak current evoked by impulses to a test potential of -40 mV, demonstrated the highest affinity to racemic ketamine.

Ca^{2+} channel	R-(+)	S-(-)
N-type	3	6
L-type	0.4	0.8
T-type	0.002	

half maximal inhibiting concentration (IC_{50}) values in mmol/l.

The blocking effects of ketamins on Ca^{2+} channels of all types tested were reversible. Similar to that block of local anesthetics the block of ketamine showed use dependence and was potential independent for L and N-type Ca^{2+} channels and did not change the activation kinetics of the currents.

The results suggest that a block of Ca^{2+} channels of DRG neurons could contribute to peridural or spinal cord anesthesia. This blockade is compared with the one known for Na^+ channels and could explain the differences observed in clinical use for stereoisomers of ketamine.

Tu-Pos428

ABNORMAL VOLTAGE-ACTIVATED CALCIUM CURRENTS IN CULTURED MOUSE TRISOMY 16 HIPPOCAMPAL NEURONS, A MODEL OF DOWN SYNDROME. ((Z.Galdzicki, A.Balbo, R.Pearce, S.I.Rapoport, J.Stoll)) LNS, NIA, NIH, Bethesda, MD 20892.

The trisomy 16 (Ts16) mouse is considered to be an animal model of Down syndrome (human trisomy 21). Primary cultures of hippocampal neurons were prepared from normal and Ts16 mouse fetuses of 15-16 days gestational age. Electrophysiological recordings were made of calcium currents obtained from neurons, cultured for 2-4 weeks, using the whole-cell configuration. From a holding potential of -90 mV, 12 depolarizing steps of 10 mV were applied. The currents were blocked by external application of 2 mM $CdCl_2$, and partially blocked by 5 μM nifedipine. Data were taken from 23 control and 19 Ts16 neurons and currents were normalized by capacitance. Mean peak calcium inward current was -17.3 pA/pS at a membrane potential 6.2 mV for control and -26.5 pA/pS at 2.2 mV for Ts16 neurons. This result was quantitatively corroborated by binding studies of dihydropyridine PN200-110 to calcium L-channel, which showed almost a 70% increase in the number of dihydropyridine binding sites for Ts16 neurons as compared to controls. We conclude that the density of L-type high-voltage activated calcium channels is significantly greater in Ts16 than control hippocampal neurons, which may increase free intracellular calcium concentration during activation. This, in conjunction with the possible overexpression of the metabotropic receptor, GluR5, the gene for which is localized on mouse chromosome 16, may cause abnormal synaptic networking and changes in long-term potentiation.

Tu-Pos429

MECHANISM OF INTRACELLULAR ACIDIFICATION CAUSED BY HIGH-K^+ DEPOLARIZATION OF NERVE FIBERS. ROLE OF NONINACTIVATING Na^+ CHANNELS.
((O.Valkina, O.Vergun, V.Turovetsky* and B.Khodorov*)) Uljanovsky Pedagogic University; Moscow State University; *Inst. of General Pathology and Pathophysiology, Moscow.

Frog sciatic nerve and its thin bundles were loaded with fluorescein diacetate to monitor changes in cytoplasmic pH (pH_i) caused by high-K^+ depolarization. Isoosmotic substitution of external K^+ for Na^+ at pH_o 7.4 led to a steady concentration-dependent (10-120mM K^+) decrease in pH_i. Elevation of pH_o to pH 8.5 prevented or even reversed these changes in pHi indicating they strong dependence on transmembrane H^+-fluxes. Removal of Ca^{2+} from the external solution or addition to it Co^{2+}or Ni^{2+}; or K^+ channels blocker TEA (10mM); or the blocker of putative H^+-channels Zn^{2+} (100μM), did not attenuate K^+-induced decrease in pH_i. In contrast blockade of Na^+ channels by 1-5 μM TTX prevented effectively the effect of high K^+ on pH_i. The conclusion is drawn that in frog nerve fibers lowering of pH_i induced by a prolonged membrane depolarization is mainly due to an enhanced H^+-influx through noninactivating Na^+ channels. (Supported by ISF, MBA 000)

Tu-Pos430

USE OF MANGANESE TO MONITOR CHANGES IN CALCIUM PERMEABILITY OF NEURONAL MEMBRANE CAUSED BY A TOXIC GLUTAMATE TREATMENT OF CULTURED NERVE CELLS.
((B.Khodorov*, V.Pinelis*, D.Fajuk*, T.Storozhevych*, N.Vinskaya*, S.Koshelev*, O.Vergun*, L.Khaspekov+, A.Lyzhin+, N.Isaev+, I.Victorov+)) *Institute of General Pathology and Pathophysiology, *Institute of Pediatrics, +Brain Res. Institute, Moscow, Russia.

The rate of Mn^{2+}-induced fluorescence quenching (RFQ) was used as a relative measure of plasma membrane Ca^{2+} permeability (P_{Ca}) during and after a toxic glutamte (GLU) treatment of cultured hippocampal neurons and cerebellar granule cells loaded with Fura-2. Some limitations of the method were estimated using the mathematical model of a competitive binding of Mn^{2+} and Ca^{2+} to Fura-2. Judging by changes in FFQ, P_{Ca} is greatly increased only in the beginning of GLU application but then it gradually declines due to a Ca^{2+}-dependent slow desensitization of NMDA channels. Closure of NMDA channels after the termination of GLU treatment leads to a further fast decrease in P_{Ca}. In spite of this cytolasmic Ca^{2+} may remain at a high plateau level. This supports the hypothesis that an impairment of Ca^{2+} extrusion systems rather than a persistent increase P_{Ca} underlies Ca^{2+} overload of the cell in the post-glutamte period. (Supported by ISF, MBA 000)

Tu-Pos431

SIZE-DEPENDENT INTERACTION OF BLOCKING DRUGS WITH THE GATING MACHINERY OF NMDA CHANNELS.
(S.Koshelev and B.Khodorov) Institute of General Pathology and Pathophysiology, Moscow, Russia.

Aspartate-induced ionic currents in NMDA channels in mechanically isolated hippocampal neurons have been recorded by using patch-clamp method in whole-cell configuration. It was revealed that blockade of open channels by some drugs (including tetrabutylammonium /TBA/, tetrapenthylammonium /TPeA/, 9-aminoacridine, tacrine) impedes the subsequent channels desensitization or deactivation (closing). This manifests itself by an appearence of a transient OFF-response after the termination of a combined (aspartate plus blocker) application ("hooked tail current"). The size of the blocker molecule seems to be a major factor determining its capability of exerting such a gate-immobilizing action on NMDA channels. This in particular follows from the fact that in contrast to TBA and TPeA, the other tetraalkylammonium ions with shorter alkyl chains do not hinder channel gating. The data obtained strongly suggest that NMDA channels are provided with the inactivation gate and that closing of the latter underlies so-called NMDA receptor channels desensitization. (Supported by ISF, MBA 000)

LIPIDS: PHYSICAL PROPERTIES

Tu-Pos432

LAMELLAR PHASE POLYMORPHISM IN INTERDIGITATED BILAYER ASSEMBLIES.
((J.T. Mason, R.E. Cunningham, T.J. O'Leary, and M. Batenjany)) Department of Cellular Pathology, Armed Forces Institute of Pathology, Washington, DC 20306-6000.

Saturated mixed-chain-length phospholipids (PLs) that adopt a mixed-interdigitated gel phase packing display an unusual thermotropic behavior, in which the phase behavior seen in calorimetric cooling scans is dependent upon the thermal history of the sample in the gel phase. Freshly prepared bilayer suspensions of these PLs exhibit a single exotherm upon cooling that is 4-6°C lower than the single endotherm seen in heating scans of the same samples. After incubation at low temperatures, two exotherms are seen in cooling scans of these bilayer suspensions, the original exotherm and a new exotherm that is 1-2°C lower than the single endotherm seen in heating scans of the same samples. We have examined the morphology of these bilayer suspensions by electron microscopy to determine the origin of this thermotropic behavior. Our results indicate that low temperature incubation of these PL bilayer suspensions leads to fusion of vesicles in the suspension, whose size is below about 0.2μm in diameter, into aggregates that form extended lamellar sheets. These bilayer sheets are shown to be the source of the higher temperature exotherm seen upon cooling of the incubated samples, whereas the remaining closed vesicles are the source of the lower temperature exotherm. The implication of these findings for the reversibility of interdigitated gel to liquid-crystalline phase transitions and the role of molecular geometry in the formation of interdigitated bilayers will be discussed.

Tu-Pos433

PERMEABILITY OF ETHANOL-INDUCED INTERDIGITATED MEMBRANES.
((H. Komatsu and S. Okada)) National Institute of Health Sciences, 540 Osaka, JAPAN

It has been suggested by many workers using model membranes that the interdigitated structure formation plays an important role in regulating many functions of biomembranes. In our previous study (H. Komatsu *et al.*, B.B.A., submitted), we demonstrated the participation of interdigitated structure formation in ethanol-induced membrane fusion. In the present study the control of membrane permeability was investigated as one of the biomembrane functions, and the effects of ethanol on the permeability of large unilamellar vesicle (LUV) (average diameter: 250 nm), comprised of dipalmitoyl phosphatidylcholine, were studied by monitoring the leakage of bulky fluorescent dye, calcein, entrapped in the inner aqueous phase of LUV. The permeability was estimated from the apparent rate constant of calcein leakage at 25 °C. The permeability depended on ethanol concentration and the largest permeabillities were observed in the region of 0.6 M to 1.2 M ethanol. In these concentrations the normal bilayer (L_β') and interdigitated (L_βI) phases coexist and the membrane is in the phase-separated state. This agreed with the phenomenon observed from proton permeability (Zeng *et al.*, Biophys. J. 65:1404[1993]). These are similar to the well-known phenomena that the permeability is induced in the phase-separated state at the gel/liquid-crystalline transition temperature. The permeability in the L_βI phase above 1.2 M ethanol was slightly larger than that in the L_β' phase below 0.6 M. The calcein permeability coefficient (evaluated by taking into consideration the changes in the size and the thickness of liposomal membranes) will be estimated and the possibility of biomembrane permeability control by the interdigitated membrane formation will be discussed.

Tu-Pos434

INTERDIGITATION DOES NOT AFFECT TRANSLATIONAL DIFFUSION OF LIPIDS IN LIQUID CRYSTALLINE BILAYERS. ((Vincent Schram and T. E. Thompson)) Dept. of Biochemistry, University of Virginia, Charlottesville, VA 22908.

Asymmetric phosphatidylcholine molecules with one acyl chain twice as long as the other, below their phase transition temperature, form a mixed interdigitated bilayer in which the longer acyl chain spans the entire bilayer. This results in a three acyl chain cross-sectional area per headgroup. There is experimental evidence to suggest that, above their phase transition temperature, these molecules still exhibit partial interdigitation, with the longer acyl chain extending partially into the opposite leaflet. Moreover, the molecular packing density in these fluid interdigitated phases seems higher than in the fluid phase formed by symmetric phosphatidylcholines. Using the fluorescence recovery after photobleaching technique (FRAP), we have investigated the translational diffusion in multilayers of a fluid phase interdigitated phosphatidylcholine, C18C10PC. We used as a fluorescent probe either a phospholipid analogue of the same acyl chain composition, NBD-C18C10PE or the symmetric equivalent of the same molecular weight, NBD-DMPE. Translational diffusion coefficients were determined using both probes in multilayers of dimyristoylphosphatidylcholine (DMPC) and in a mixture of C18C10PC/DMPC (60/40 mol.). We found that in a given lipid matrix, both NBD-C18C10PE and NBD-DMPE diffuse at the same rate. Moreover, the diffusion coefficients show no significant differences in either the C18C10PC or the DMPC lipid matrix. These results suggest that in bilayers of fluid C18C10PC, the reduction in free area subsequent to an increase in molecular packing is compensated by an increase in acyl chain dynamics. This result is in agreement with the data obtained by relaxation NMR (Halladay et al., 1990, Biophys. J. 58: 1449-1461.), which suggests that the interdigitation in a fluid-phase asymmetric phosphatidylcholine is highly dynamic. (This work is funded by NIH Grants GM-14628 and GM-23573)

Tu-Pos435

DETECTION, STRUCTURE AND ORIENTATION OF AMPHIPATHIC PEPTIDES AND PHOSPHOLIPIDS ON MONOLAYERS : AN "IN SITU" APPROACH BY PMIRRAS ((I. Cornut, B. Desbat, and J. Dufourcq)) C.R.P. Pascal, CNRS, 33600 Pessac and LSMC, Univ. Bordeaux I, 33405 Talence, France.

Cytotoxic amphipathic peptides kill cells by direct interaction with membranes. Melittin is one of the best known and more potent member of this familly. We designed peptides, from 12 to 22 residue long, only constituted by Leu & Lys residues properly located in sequence to generate ideally amphipathic α helices. They proved to be up to 8 times more active than melittin (I. Cornut et al., FEBS Lett. 349, 29-33, 1994)

In the μM range, pure peptides form films at the air-water interface. At lateral pressure π = 0.05 - 3 mN/m "in situ" good quality PMIRRAS spectra are characteristic of peptides in α-helix at the interface with a specific orientation. The Leu, Lys peptides gave amide bands of helices with their axis parallel to the interface, the orientation of melittin is different and varies according to the physico-chemical conditions.

Dimyristoylphosphatidylcholine when spread at interface at $9 < \pi < 30$ mN/m gives PMIRRAS spectra where the phosphate , ester and methylene bands are characteristic of oriented molecules, the higher the pressure the more ordered are the chains.

Addition of peptide either to preformed lipidic film or by co-spreading of lipid peptide mixtures allows to detect by PMIRRAS both ester and amide I bands attributed to both components which allow to define lipid to peptide molar ratio R_I in the film (R_I ~ 50). In mixed films the lipid bands indicate structural changes induced by the presence of the peptide. Conversely the analysis of the amide-band allows to conclude Leu, Lys peptides and melittin remain in α-helix. The helix of Leu, Lys peptides remains parallel to the interface, i.e. almost perpendicular to the lipid chains. The orientation of melittin differs.

Tu-Pos436

FORMATION OF HORIZONTAL BIMOLECULAR MEMBRANES FROM LIPID MONOLAYERS ((R.A. Brutyan[1,2] and A.L. Harris[1])) [1]Dept. Biophysics, Johns Hopkins Univ., Baltimore, MD 21218 & [2]Inst. of Biotechnol., Yerevan 375056, Armenia

To facilitate study of reconstituted ion channels, a device for formation of horizontal "solvent-free" lipid bilayers (Montal & Mueller, *PNAS 69*:3561) was developed and methods of incorporating channel protein into them were characterized.

The upper chamber is a hemisphere (or hemicylinder) with a bilayer aperture through thin Teflon at its pole. It is attached at the equator to a rod (like a spoon handle) that can be axially rotated by a rotation stage, and positioned over a lower chamber (Petri dish) with convex surface down. Initially, the hemisphere is rotated so that after buffer is added to both chambers, the bilayer aperture remains above the buffer level for pretreatment with hexadecane. Once monolayers are formed and volatile solvent has evaporated, the upper chamber is smoothly rotated back to form a bilayer across the aperture and bring it to a final horizontal position. Rotational symmetry of the upper chamber insures equal changes in hydrostatic pressure across the bilayer, and permits the upper electrode to remain mounted on the upper chamber or suspended from above during bilayer formation.

To explore the advantages of this technique, *S. aureus* α-toxin channels were reconstituted by addition of protein to the bath and by liposome fusion. In both cases, application of submicroliter aliquots of toxin in a dense, hypertonic buffer directly to the bilayer's upper surface increased efficiency of reconstitution more than 1000-fold as compared with addition distant from the bilayer followed by stirring (as for a vertical bilayer). The application of a local, transient osmotic gradient to the bilayer apparently provides the transbilayer osmotic force for liposome fusion (Cohen *et al., JGP 75*:251), affords control over number of fusion events, and after stirring leaves the bilayer in essentially symmetric buffers. This highly efficient technique is promising for reconstitution of proteins of limited availability in purified form, such as connexin (see Bevans *et al.* abstract). Support: ONR N00014-90-J-1960 & NIH GM36044.

Tu-Pos437

DETERMINATION OF EQUILIBRIUM LIPID MONOLAYER SURFACE TENSION BY DETACHMENT OF AN FEP TEFLON PIN ((J.T.Buboltz and G.W.Feigenson)) Section of BMCB, Cornell University, Ithaca, NY 14853

We are interested in studying bilayer lipid interactions by making precise measurements on an air-water (surface) phase in equilibrium with the bilayer (bulk) phase. Toward that end, we prepare air-water interfacial lipid films by deposition from a subphase suspension, and make surface tension measurents by detachment of an FEP teflon pin. We have found the low-surface-energy FEP pin to be much less perturbational than the conventional high-surface-energy platinum pin. Therefore, for phospholipid interfacial films, use of FEP teflon yields data that are significantly more precise. Of course, an FEP pin implies finite (and variable) contact angles; this would seem the central problem with such a low-energy wetting surface. But we have found that analysis of the sample detachment force curve can uniquely determine the surface tension, independent of contact angle.

Here, we explicate the measurement itself and describe the theoretical analysis that relates the experimental force curve to interfacial tension. We will also discuss some considerations in preparing equilibrium films from subphase deposition, and present evidence that the overall strategy is sensitive to bilayer interactions.

Tu-Pos438

INTERACTION OF DIPYRIDAMOLE WITH PHOSPHOLIPID LANGMUIR MONOLAYERS. ((Galina P. Borissevitch, Marcel Tabak and Osvaldo N. Oliveira Jr.)) Instituto de Química de São Carlos, USP; Instituto de Física de São Carlos, USP; Cx.Postal 369,13560-970, São Carlos, SP, Brasil.

The effect of a coronary vasodilator dipyridamole (DIP) on phospholipids was studied in Langmuir monolayers formed at the water-air interface. At pH5.9 (Milli-Q water), close to DIP protonation pK5.8, DIP included in monolayers induces changes of both liquid expanded (LE) and liquid condensed (LC) regions of π-A isotherms and of surface potential (SP), as well. The changes are not monotonous for a zwitterionic lipid DPPC: for DIP:DPPC ratios below 0.02 the LE state shifts from 80 to 95Å^2 and the pressure of LE to LC transition increases from 7 up to 14 mN/m.. At higher DIP concentrations the LE shifts back to 80Å^2 and the pressure of LE to LC transition decreases to 10 mN/m. SP changes are maximum at the same DIP content. Monolayers of DPPC mixed with a negatively charged DPPS from brain (DPPC:DPPS = 5:1) have isotherms with a very expanded LE region, LC practically absent. DIP induces a gradual shift of the LE to smaller A values and appearance of the LC one. At highest DIP concentration used (DIP:lipid=0.2), when all DPPS charges are neutralized by DIP, the isotherm is similar to that for DPPC+DIP. SP dependence is as in previous case. For a negatively charged DPPG a gradual expansion of the LE up to 110Å^2 and decrease of the LC one with simultaneous SP increase are observed. At pH7.15 (DIP deprotonated) the effect upon isotherms is close to that for pH5.9 while SP changes are reduced. DIP interacts with lipids in monolayers, forming complexes, the nature of which depends on the charge states of both the polar lipid head and of DIP.

Support: CNPq, FINEP, FAPESP.

Tu-Pos439

SURFACE PRESSURE MODULATION OF THE CONFORMATION OF POLY(L-LYSINE) BOUND TO PHOSPHOLIPID MONOLAYERS. ((M. Pézolet and J. Labrecque)) CERSIM, Dép. de chimie, Université Laval, Québec, Canada and ((B. Desbat)) LSMC, Université de Bordeaux I, Talence, France

The conformation and orientation of the basic polypeptide poly(L-lysine) (PLL) bound to dimyristoylphosphatidic acid (DMPA) monolayers have been studied by polarized infrared spectroscopy. The measurements were carried out on monolayer films either transferred on solid substrates by the Langmuir-Blodgett technique or *in situ* at the air-water interface. The latter experiments were performed by reflection-absorption measurements using a specially designed miniature trough and the polarization modulation technique. The results show that the conformation of the DMPA-bound polypeptide depends strongly on the phospholipid molecular area and the surface pressure of the film. At a surface pressure of 31 mN/m, the conformation of bound PLL is mostly α-helical, while at 45 mN/m it contains a significant amount of β-sheet. Polarization measurements on the amide I and amide A bands show that both types of secondary structure are parallel to the plane of the interface. The results also indicate that the polypeptide affects the lipid acyl chain packing symmetry as well as the degree of hydration of the ester carbonyl groups. The phosphate group of DMPA also undergoes a reorientation upon binding of PLL.

Tu-Pos440

ROLES OF PHOSPHATIDYLGLYCEROLS AND CALCIUM ON INTERACTION OF PULMONARY SURFACTANT PROTEIN SP-A WITH PHOSPHOLIPIDS IN SPREAD MONOLAYERS AT THE AIR-WATER INTERFACE. ((S. Taneva and K.M.W. Keough)) Department of Biochemistry, Memorial University of Newfoundland, St. John's, Newfoundland, Canada A1B 3X9

SP-A is necessary for generation of tubular myelin (TM), a phospholipid-protein subfraction of surfactant involved in the formation of the surface film in alveoli. The structure of TM is dependent on interactions of lipids with specific surfactant proteins and calcium ions. We studied the interaction of SP-A with dipalmitoylphosphatidylcholine (DPPC) and dipalmitoylphosphatidylglycerol (DPPG) in spread monolayers at the air-water interface, in the presence or absence of calcium in the subphase. The mean areas in binary SP-A/DPPC films showed non-ideal behavior, which was Ca^{2+}-independent. In the absence of calcium, the addition of 30 mol% of DPPG removed the interactions between SP-A and DPPC, as suggested by the additivity of the mean areas in ternary SP-A/(DPPC:DPPG) monolayers. Electrostatic repulsion between SP-A and DPPG, both negatively charged at physiologic pH, possibly accounted for the immiscibility between SP-A and DPPC:DPPG mixture. Ca^{2+} restored interactions between SP-A and DPPC:DPPG in the monolayers, suggesting a role for Ca^{2+}-dependent electrostatic effects between SP-A and PG in governing the overall interactions of SP-A with mixtures of phospholipids. (Supported by MRC Canada.)

Tu-Pos441

THE ROLE OF CHOLESTEROL IN SURFACTANT FUNCTION IN LUNG INJURY. ((V. Skita, S. Kavel, R.S. Thrall)) Biomolecular Structure Analysis Center and the Departments of Biochemistry, Medicine and Surgery, Univ. of Connecticut Health Center, Farmington, CT 06032.

An increase in surfactant neutral lipids, predominantly cholesterol (CH) has been observed in our lung injury animal models. The greatest increase appears to correlate with improved lung function. We hypothesized that this increase in CH is beneficial due to its ability to stabilize the functional activity of the surfactant in the presence of increased plasma proteins. To test this hypothesis, a Langmuir trough was used to measure surface pressure isotherms as a function of mean molecular area (mma) for a variety of model surfactant preparations. To mimic protein leakage into the alveolar hypophase (ie. lung injury) differing amounts of rat serum albumin (RSA) was added to the subphase prior to spreading of the surfactant monolayer. The surfactant protein C (SP-C) and CH composition of the surfactant was also varied. The phospholipid components, dipalmitoylphosphatidylcholine and dioleoylphosphatidylglycerol, have been previously optimized to 8:2 (mol:mol). In all cases, the model surfactants were able to achieve a maximal surface pressure of ~ 70 mN/m at a mma < 40 $Å^2$. RSA caused the surfactant films to expand at low surface pressures (e.g. 20 mN/m) in all cases; the effect was substantially minimized by CH in surfactant preparations containing SP-C. [Supported by NIH HL45284, and by grants from the Council for Tobacco Research, CT Research Foundation, and Boehringer-Ingelheim.]

Tu-Pos442

ORDERED DOMAINS IN FILMS OF PULMONARY SURFACTANT ((S.B. Hall, K. Maloney, B. Korcakova, D.W. Grainger, W. Schief, and V. Vogel)) Oregon Health Sciences University and Oregon Graduate Institute of Science and Technology, Portland, Oregon; University of Washington, Seattle, Washington

Pulmonary surfactant is the mix of mostly phospholipid with small amounts of protein and neutral lipid which lowers surface tension in the alveolar air spaces of the lung. When interfacial films of this material are compressed by changes in alveolar surface area during normal respiration, surface tension falls to extraordinarily low levels. Prior studies suggest that the ability of surfactant films to reach high surface pressures during compression requires refinement of the composition of the surface film, with collapse of the more fluid components from the interface resulting in a more stable film. This hypothesis requires that regions of the film differ in their structural stability and in their composition. In these studies, we have used epifluorescence and Brewster angle microscopy to demonstrate the presence of discrete structural domains within interfacial monolayers of surfactant obtained from calf lungs on a Wilhelmy balance during compression at 23°C. We also studied preparations of calf surfactant which lacked specific constituents to determine if individual components alter the extent of these domains. For the surfactant phospholipids alone, the ordered domains reached 20% of the interfacial area. The addition of proteins or neutral lipids both altered the shape of domains, but had opposite effects on the extent of ordered area. The fraction of the surface film occupied by the ordered domains decreased with the addition of proteins, but initially increased for neutral lipids. In complete preparations of calf surfactant, neutral lipids appeared dominant, and total area of domains exceeded that for the phospholipids alone. These results show that pulmonary surface does develop regions of ordered structure during compression, and that the proteins and neutral lipids in this mixture alter the extent and shape of the domains.

Tu-Pos443

INTERACTION OF A LUNG PHOSPHOLIPID-BINDING PROTEIN WITH PHOSPHOLIPID MONOLAYERS. ((S. Koppenol, G. Zografi, F.H.C. Tsao*)) School of Pharmacy and the Department of Pediatrics and Perinatal Center*, University of Wisconsin-Madison, Madison, WI 53706.

A calcium-dependent phospholipid binding protein (PLBP), believed to be a member of the annexin family of proteins, has been isolated from the cytosolic fraction of rabbit lung. Evidence has been obtained implicating PLBP in lung development and surfactant biogenesis possibly through its ability to mediate bilayer fusion, a critical process involved in both the storage of lung surfactant and its subsequent delivery to the alveolus. In this study, we have used phospholipid monolayers as model interfaces to study PLBP-phospholipid interactions that are important to this process. Single component monolayers of dipalmitoyl-phosphatidylcholine (DPPC), dipalmitoyl- (DPPG), 1-palmitoyl-2-oleoyl- (POPG), and dioleoyl- (DOPG) phosphatidylglycerol; and mixed monolayers of DPPC with each of the phosphatidylglycerols (PG) spread to various initial surface pressures were used with and without Ca^{2+} ions present in the subphase (pH 7.4, 25°C). Surface pressure changes ($\Delta\pi$) upon addition of various concentrations of PLBP into the underlying solution were measured as an indication of the tendency of the protein to penetrate into the monolayer and to interact. The results of these experiments indicate that PLBP interacts specifically with the anionic PG lipids as opposed to zwitterionic DPPC in a Ca^{2+}-dependent manner, and in the order POPG>DPPG>DOPG. Decreasing the amount of anionic lipid (at constant π) in the mixed monolayers resulted in decreased PLBP-phospholipid penetration. In all cases, $\Delta\pi$ decreased to zero at initial π>25mN/m, indicating that penetration of the protein into the monolayer only occurred at degrees of molecular packing associated with π<25mN/m.

Tu-Pos444

MEMBRANE HYDRATION AND STRUCTURE ON AN ATOMIC LEVEL AS SEEN BY TWO- DIMENSIONAL NMR IN COMBINATION WTH HIGH-SPEED SAMPLE SPINNING.((F. Volke & A. Pampel)) University of Leipzig, Faculty of Physics and Geosciences, Biomembranes, Linnestr. 5, D-04103 Leipzig, Germany.

The position and the dynamics of structural important water in lamellar lipid-model membranes was determined on an atomic level using a combination of proton-magic-angle spinning NMR and NOESY. Here, we report studies on POPC (1-palmitoyl-2-oleoyl-sn-3-phosphocholine) where a nonionic surfactant $C_{12}EO_4$ (dodecyl-tetra-ethylene-oxid-ether) was intercalated into the lipid matrix. In the Lα phase of the pure lipid, water was found to be positioned to within <0.4 nm for all segments of the POPC headgroup, the glycerol backbone and even within the hydrocarbon region, as to be seen from *negative* cross peaks in the NOESY-MAS experiment. The surfactant dehydrates the lipids and is found to be positioned mainly in the hydrophobic part of lipid matrix. This is supported by ^{13}C-NMR MAS measurement of the isotropic chemical shift and the spin-lattice-relaxation time.These studies have high potential to investigate membrane protein hydration and structural organization in a lipid bilayer surounding.

Tu-Pos445

MECHANISM OF STABILIZATION OF LIPOSOMES BY SUGARS DURING AIR DRYING. ((J. H. Crowe, F. A. Hoekstra, and L. M. Crowe)) Molecular and Cellular Biology, University of California, Davis, and Plant Physiology, Wageningen University.

We have shown previously that liposomes can be freeze-dried in the presence of disaccharides. We now show that they can also be preserved when they are air-dried. When vesicles of egg PC-PS (9:1) were air dried in the presence of ≥ 50 mg/ml sucrose, they retained as much as 100% of their original contents. Final preparations contain <0.05 g H_2O/g lipid. The factors that destabilize are fusion, which occurs at water contents ≤ 1.0 g H_2O/g lipid, and the increase in phase transition that accompanies extreme dehydration (<0.3 g H_2O/g lipid). Depression of T_m in the dry lipids is required for stabilization. Vitrification of the sugars during drying is essential but not sufficient for preservation in the driest liposomes. Dextran, which has a T_g much higher than that of the sugars, is ineffective, and acts as a non-competitive inhibitor for preservation by disaccharides. Glucose is a competitive inhibitor for preservation by disaccharides, but is in itself ineffective. It depresses T_m but fails to prevent fusion. Inspection of state diagram showed that at room temperature glucose is not vitrified until H_2O content < 0.05 g H_2O/g glucose. When the samples were air-dried at lower temperatures, they are below T_g at the critical H_2O contents, and glucose preserves them. The dry liposomes must be stored at temperatures < T_g. (Supported by IBN93-08581 from NSF and N00014-94-1 from ONR).

Tu-Pos446

PHASE AND HYDRATION BEHAVIOR OF LIPID MEMBRANE-WATER INTERFACES USING DANSYL DERIVATIVE FLUORESCENT PROBES: STATIC AND DYNAMIC STUDIES.

((Delia L. Bernik*, R. Martín Negri# and E. Aníbal Disalvo*))
*FFyB; # INQUIMAE ,FCEyN, Univ. de Buenos Aires, Argentina.

Comparative studies of dansylphosphatidylethanolamine (DPE) and dansyldihexadecylamine (DA) fluorescent properties indicate that the chromophoric group of those probes is located at different levels at the membrane-water interface. Both probes are sensitive to subtle changes in polarity of their microenvironment produced either by changes in composition or temperature (phase state of the lipids). The behavior of these probes in bilayers composed by saturated phosphatidylcholine, phosphatidylglicerol and their mixtures were studied at different temperatures in the gel and fluid state.
The analysis of the Stokes shifts allows to estimate values of the local dielectric constant at the interfaces. Its physical significance is limited by the hypothetical values of the polarizability of the interfaces used in the calculations.
Phase and hydration behavior of the bilayers for different curvature radii were studied by means of the solvent relaxation mechanism exhibited by dansyl probes using simultaneous analysis of Stokes shifts, fluorescence intensity and fluorescence decay time measurements.
With funds from Fundación Antorchas and UBACyT.

Tu-Pos447

DEPENDENCE OF INTER-LIPID HYDROGEN BONDING ON LIPID HEAD GROUP DYNAMICS AND HYDRATION. ((S.J. Slater, C. Ho, C.D. Stubbs)) Dept. of Pathology and Cell Biology Thomas Jefferson University, Philadelphia PA 19107.

The relationship between head group motional dynamics and the strength of lipid-lipid hydrogen bonding that occurs via the extended network of water molecules termed the "hydration layer" was investigated. To achieve this the effects of increasing the level of PC unsaturation, PE or cholesterol, and perturbation by alcohols on the desorption rates of NBD-labeled phospholipids from donor vesicles, a measure of hydrogen bond strength, were measured. These rates were compared with rotational correlation times (ϕ) and with dansyl-PE fluorescence lifetimes (τ), as a measure of head group hydration. The effect of n-alkanols and increasing the donor vesicle PC unsaturation, either in the *sn*-2-acyl, or symmetrically in the *sn*-1- and *sn*-2-acyl chains, was to decrease τ, potentiate NBD-PC desorption rate (k_{off}) and increase ϕ. However, the inclusion of PE or cholesterol in PC donor vesicles, which also decreased τ, had a *negligible* effect on k_{off} and ϕ. Further, values of τ for vesicles of *sn*-1,2-diunsaturated PC were *less* than those of *sn*-2-unsaturated PC, containing the same number of double bonds/PC, while k_{off} and ϕ values remained unchanged. These observations indicate that k_{off}, and therefore lipid-lipid hydrogen bond strength, correlate with head group motional dynamics as measured by ϕ, rather than with "static" quantities such as head group hydration, measured by τ. The lack of effect of cholesterol on ϕ, k_{off}, and therefore on lipid-lipid hydrogen bond strength may due to the conformational inflexibility of the 3-β-OH group. Consistent with this, while a series of n-alkanols which are conformationally flexible, increased k_{off} and ϕ with a potency directly proportional to the hydrophobicity (Meyer-Overton), the effects on k_{off} of a series of cycloalkanols, in which the -OH is also, as with cholesterol, conformationally restricted, were less than predicted from the partition coefficients. Accordingly, inserting a methylene between the cycloalkane ring and -OH, and thus relieving conformational rigidity, restored the potency of the effect on desorption rate.

Tu-Pos448

EFFECT OF N-ALKANOLS ON LIPID BILAYER HYDRATION.
((C. Ho, S.J. Slater and C. D. Stubbs)) Department of Pathology and Cell Biology, Thomas Jefferson University, Philadelphia, PA 19107

The potencies of anesthetics and alcohols are a linear function of the oil/water partition coefficient, the so called Meyer-Overton relationship. This has led to "*lipid theories*" of anesthesia and alcohol effects. which are based on the finding of a linear relationship of the magnitude of lipid perturbance with membrane-buffer partition coefficient. However, the low magnitude of lipid perturbance induced by pharmacologically relevant concentrations of anesthetics and ethanol is considered a weakness in this theory. Further, the finding that some soluble proteins contain hydrophobic pockets that bind anesthetics, and the demonstration of effects with a potencies that follow the Meyer-Overton relationship has led to alternate "*protein theories*" of anesthesia. Recently, studies have shown cases where potencies of the effects of n-alkanols on membrane protein function do not follow Meyer-Overton, suggesting a specific sites of interaction with a protein, rather that a non-specific perturbation of the lipid bilayer. In this study, using a simple model lipid bilayer system we demonstrate that the potency of the effect of n-alkanols on lipid interchain hydration is also a non-linear function of chain length (non-Meyer-Overton). The measurements were made using the fluorescence lifetime of DPH tethered to the *sn*-2 position of phosphatidylcholine as a probe of hydration. It was found that fluorescence lifetime *decreased* upon addition of ethanol, *opposite* to the effect of longer chain alkanols (C4-C6) which *increased* DPH-PC fluorescence lifetime. By contrast, the potency of the effects on the level of head group hydration, probed by measuring the fluorescence lifetime of dansyl-PE, was a linear function of alkanol chain length (C2-C6). These results indicated that non-Meyer-Overton behavior, such as a lack of effects of longer chain alcohols on a membrane protein function, does not preclude a role of lipid bilayer perturbance. Altered levels of interchain hydration, especially at the protein-lipid interface, could have significant effect on protein conformation and hence on function.

LIPOSOMES

Tu-Pos449

SPONTANEOUS TRANSFER OF PEG-PHOSPHATIDYL ETHANOLAMINE BETWEEN PHOSPHOLIPID BILAYERS.
((Anthony W. Scotto, Helen Seow and Adam Wos)) Dept. of Medicine, Cornell University Medical College, New York, NY 10021.

The formation and characterization of LUVs prepared by the inclusion of poly-(ethylene glycol)$_{5000}$-phosphatidylethanolamine (PEG-PE) to generate sterically stabilized liposomes for in vivo therapies have been examined. Modification of preformed LUVs with micellar PEG-PE to form LUVs with PEG-PE limited to the outer bilayer leaflet results in the formation of PEG-LUVs with varying ratios of PEG-PE to bilayer phospholipid and a loss of bilayer phospholipid to the micelles. The formation of PEG-LUVs by co-hydration of PEG-PE with the vesicle lipids and extrusion through 0.1 μm membranes results in a uniform population of PEG-LUVs as demonstrated by equilibrium density centrifugation analysis. Molecular sizing chromatography indicates the presence of large mixed micelles and occasionally small mixed micelles in the liposome preparations. Therefore, these purified PEG-LUVs were used to examining the potential transfer of the PEG-PE to other non-PEG containing LUVs. Results indicate that the PEG-calyx is not a stable modification to the liposome since significant transfer of the PEG-PE occurs within 2 hrs at 37°C. The transfer is dependent on the concentration of the acceptor LUVs and collisional transfer is presumably the major transfer mechanism. This loss of the surface pegylation presumably will allow for interaction of the liposome surface with opsins in the blood. Alterations of the lipid composition of the bilayer may retard this transfer process but a more secure anchoring of PEG to the bilayer structure is necessary if surfaced modified liposomes are to be used as long lived in vivo delivery vehicles. (Supported by NIH grants RR-06854 & GM-44749).

Tu-Pos450

STEROL REGULAR DISTRIBUTION IN PHOSPHATIDYLCHOLINE BILAYERS. ((Parkson Lee-Gau Chong)) Dept. of Biochemistry, Temple Univ. School of Medicine, Philadelphia, PA 19140 & Dept. of Biochemistry, Meharry Medical College, Nashville, TN 37208. (Spon. by J. H. Collins)

The lateral organization of cholesterol is an important, but not well understood, membrane phenomenon. In the present study, we employ a new concept to the study of sterol lateral distribution in membranes. We examined the fractional concentration dependence of dehydroergosterol ($\Delta^{5,7,9,(11),22}$-ergostatetraene-3β-ol) fluorescence in the liquid crystalline state of dimyristoylphosphatidylcholine multilamellar vesicles. Dehydroergosterol is a naturally occuring fluorescent sterol found in several biological membranes and resembles both cholesterol and ergosterol in its physiological properties. A number of intensity drops were observed at specific mole fractions, as predicted from a hexagonal super-lattice model. The fluorescence dips provide compelling evidence that a naturally occurring sterol can be regularly distributed at fixed compositional fractions, consistent with the presence of hexagonal super-lattices in the fluid membranes. A new model is proposed for sterol lateral organization in liquid crystalline phosphatidylcholine bilayers. According to this model, regularly distributed regions coexist with irregularly distributed regions. The extent of regular distribution varies periodically with sterol mole fraction and consequently similar variations take place in the membrane volume and lipid packing. This level of modulation in local membrane structure by minute changes in sterol concentration should have profound implications in the functional role of cholesterol content in cell membranes (supported in part by the Naval Research Laboratory and the ARO).

Tu-Pos451

SUPPORTING EVIDENCE FOR STEROL REGULAR DISTRIBUTION IN LIQUID CRYSTALLINE PHOSPHATIDYLCHOLINE BILAYERS. ((Parkson Lee-Gau Chong, Frederick L. Chun, Anthony Golsorkhi, Khanh Truong and Istvan P. Sugar#)) Dept. of Biochem, Temple Univ. School of Medicine, Philadelphia, PA 19140 and #Dept. of Biomath. Science, Mt. Sinai Medical Center, NY, NY 10029

We have measured the steady-state fluorescence anisotropy and the fluorescence lifetime of 6-propionyl-2-dimethylamino-naphthalene (Prodan) in dimyristoylphosphatidylcholine (DMPC) multilamellar vesicles containing varying amounts of cholesterol (22.5-27.5 mol%) at 25 °C. The data were measured using three sets of optical filters: Schott KV389, KV389+BG12 and KV520. Using the two-site model (a less-polar disposition and a more-polar disposition for Prodan in membranes as described in Chong (1988) *Biochemistry* 27, 399), we have calculated that the percentage of Prodan at the more-polar site reaches a local minimum at around 25 mol% cholesterol. In a separate study, we have measured the steady-state polarization of diphenylhexatriene (DPH) fluorescence in cholesterol/DMPC mixtures. We found that the DPH polarization does not vary with cholesterol content monotonically; instead, the polarization reaches a local maximum at 20 and 25 mol% cholesterol in DMPC. These two concentrations are critical mole fractions for sterol regular distribution in membranes (Chong (1994) *Proc. Natl. Acad. Sci.*, in press). Also, the variations of the DPH and Prodan fluorescence parameters with cholesterol content are consistent with our previous finding that membrane defect (an area more likely to be filled with an aqueous medium) is more abundant at the noncritical mole fractions than at the critical mole fractions (Chong et al. (1994) *Biophys. J.* 66, 2029) (supported by the Naval Research Lab.).

Tu-Pos452

SURFACE CHARACTERIZATION OF STERICALLY STABILIZED LIPOSOMES. ((Joel A. Cohen[1], Valentina Khorosheva[1] and Martin C. Woodle[2])) [1]University of the Pacific, San Francisco, CA 94115 and [2]Liposome Technology, Inc., Menlo Park, CA 94025.

Sterically stabilized liposomes are of pharmaceutical interest because of their ability to evade blood macrophages and hence to circulate in the bloodstream for extended times. Such liposomes have considerable potential as intravenous carriers of drugs. Steric stability is conferred by the end-grafting of polymers, typically polyethylene glycol (PEG), to the liposome surface. We hypothesize a strong dependence of the plasma lifetimes of these liposomes on the thickness of their polymer coat, perhaps via a coat-mediated suppression of protein and macrophage binding. Hydrodynamic thicknesses of the polymer coats were measured by particle electrophoresis of liposomes having constant surface-charge density and PEG-grafted lipids at various mole fractions and various PEG molecular weights. The polymer coat slows the liposomes by hydrodynamic drag, thus affecting the zeta potential. The shear-surface distances (hydrodynamic coat thicknesses) were calculated from the zeta potentials by use of the Gouy-Chapman-Stern theory. The PEG-lipid mole content ranged from 0.5% (mushroom regime) to 10% (brush regime), and the PEG molecular weights ranged from 350 (7 monomers) to 5000 (115 monomers). The coat thicknesses ranged from 5 Å to 60 Å. These thicknesses are shown to correlate with the biological halflives of PEG-grafted liposomes in rats.

Tu-Pos453

pH-SENSITIVE LIPOSOMES WITH SERUM STABILITY. ((V. A. Slepushkin and N. Düzgünes)) Department of Microbiology, University of the Pacific, 2155 Webster Street, San Francisco, CA 94115.

We are developing pH-sensitive liposomes with prolonged circulation in the bloodstream as a potential delivery system for anti-sense oligonucleotides and ribozymes. We have determined the stability and pH sensitivity of liposomes in 50% human serum as a first step for selection of liposomes with extended half-lives *in vivo*, utilizing a calcein release assay. Cholesteryl hemisuccinate (CHEMS)/phosphatidylethanolamine (PE) liposomes were quite stable in serum ($T_{1/2}$=24 h), and additon of polyethylene glycol (PEG)-PE (which sterically stabilizes phosphatidylcholine (PC)/cholesterol (Chol) liposomes and prolongs their circulation), did not significantly enhance their stability. Incorporation of PEG-PE in pH-sensitive liposomes did not reduce the leakage of calcein in response to lowering the pH. Surprisingly, the substitution of dioleoyl PC for dioleoyl PE destabilized liposomes also containing CHEMS and PEG-PE ($T_{1/2}$=1 h). Substitution of Chol for CHEMS in PE/PEG-PE liposomes increased their stability. Leakage of calcein from the liposomes decreased with increasing gel-liquid crystalline phase transition temperature of the PE component. Increasing the percentage of PEG-PE and the PEG chain length decreased leakage slightly. The inclusion of 5% PEG-PE in CHEMS/PE liposomes did not appreciably decrease their uptake by, or the delivery of their contents into, differentiated monocytic THP-1 cells, as determined by fluorescence microscopy and FACS analysis.

Tu-Pos454

MECHANICAL MEASUREMENT OF INTERLAYER FRICTION AND TRANSBILAYER MOVEMENT OF PHOSPHOLIPID MOLECULES IN GIANT VESICLES. ((Robert M. Raphael and Richard E. Waugh)) Dept. of Biophysics, U. Rochester, Sch. Medicine and Dentistry. Rochester, NY 14642

The application of an axial force on the order of 15 to 60 pN to a lipid vesicle results in the formation of a thin cylindrical strand of membrane, referred to as a tether. The mechanical equilibrium of this system has been previously used to determine the local and nonlocal bending stiffness of the membrane. When a perturbation is made in the force balance, growth of the tether is initiated and observed to follow a biphasic time course: an initial exponential increase is followed by a linear phase. The exponential phase is attributed to drag between the leaflets of the bilayer as they move into the tether region at different velocities. From the time constant of this process we calculate the coefficient of interfacial friction to be $2.7 \cdot 10^{10}$ N-s/m^3. After this exponential slip, the tether is expected to reach a new equilibrium length. However, we find that the tether exhibits continuous slow growth at a rate proportional to the magnitude of the change in the boundary tension. This behavior is explained by hypothesizing the movement of phospholipids from the inner to the outer leaflet to relax differential stress in the membrane. We calculate the coefficient of interlayer permeation to be $7 \cdot 10^5$ m/s/N. In addition, studies on vesicles containing 20% phosphatidylserine have revealed anomalous behavior which is currently under investigation. (Supported by NIH grant no. HL-31524.)

Tu-Pos455

EXCHANGE OF LYSOLIPIDS WITH VESICLE MEMBRANES STUDIED BY MICROPIPET MANIPULATION. ((Doncho V. Zhelev and David Needham)) Department of Mechanical Engineering and Materials Science, Duke University, Durham, NC 27708-0300

The exchange of lysolipids, is of particular interest, because of their relatively high solubility both in the membrane and in water solutions. When in the membrane, these lipids may promote formation of membrane defects (pores). The kinetics of exchange and the partitioning of lysoPC in a vesicle membrane is studied by using micropipet technique. The advantage of using this technique is that it allows to measure both the kinetics of lysoPC intercalation and its desorption from the membrane for a given vesicle, and to monitor the formation of pores.

The results show that the kinetics of intercalation and desorption are similar for lysoPC concentrations below the CMC, while for larger concentrations, the kinetics of intercalation is slower. Both kinetics depend on the unstirred layer that bounds the membrane. The intercalation of lysoPC above the CMC, includes both monomer association and micelle fusion while the desorption depends only on the monomer apparent "off" rate. The measured apparent rate of desorption is on the order of 0.3 s^{-1}. After its intercalation in the outside monolayer the lysolipid is transferred into the inside monolayer in a relatively slow process, with rate of interbilayer transfer on the order of 0.002 s^{-1}. The partitioning of lysoPC in the membrane at steady state conditions depends on its concentration in the bathing solution and for 5 µM lysoPC it is 30 mol%. Such a high molar concentration of the lysolipid promotes formation of pores. The size of these pores matches the size of the used solutes (on the order of 0.5 nm) and their line tension is on the order of 10^{-13} N. This is two orders of magnitude smaller than the line tension of giant electropores (Zhelev and Needham (1993) BBA: 1147:89).

This work is supported by grants GM 40162 and 5 RO1 HL23728 from NIH.

Tu-Pos456

EFFECT OF LIPID COMPOSITION ON THE PHASE BEHAVIOR OF SUSPENSIONS CONTAINING PEG-LIPID ((K.Hristova*[1], A.K.Kenworthy+[2], D.Needham* and T.J.McIntosh+)) *Dept. of Cell Biology, Duke University Medical Center, Durham, NC 27710 and +Dept. of Mechanical Engineering, Duke University, Durham, NC 27708. Present addresses: [1]Dept. of Physiology and Biophysics, University of California, Irvine, CA 92717 and [2]Dept. of Biology, Johns Hopkins University, Baltimore, MD 21218

Liposomes containing PEG-lipids (phospholipids with covalently attached polyethylene glycol) are currently being developed for in vivo drug delivery. We are interested in determining: (1) the amount of PEG-lipid that can be incorporated into liposomes and (2) the physical principles that determine the phase transition from bilayer to micellar phase. Using X-ray diffraction we measure the repulsive pressures between lipid bilayers containing PEG-lipids and the phase properties of phospholipid:cholesterol:PEG-lipid suspensions for a variety of phospholipids. We find that the maximum PEG-lipid concentration in the bilayer is nearly independent of: (1) bilayer phase (gel vs. liquid-crystalline), (2) number of double bonds in the phospholipid chains and (3) cholesterol content. However, the presence of lysolipids or a decrease in phospholipid hydrocarbon chain length, decreases the maximum concentration of PEG-lipids in the bilayer. These data are interpreted in terms of a theoretical treatment [1] that states that the maximum concentration of PEG-lipids in the bilayer is the concentration at which micelle formation becomes thermodynamically favorable over bilayer formation. That is why incorporation of lysolipids and reduction of phospholipid hydrocarbon chain length decreases the maximum concentration of PEG-lipids in the bilayer.

[1] Hristova, K. and Needham, D. Biophys. J., v.66 #2, A177.

Tu-Pos457

SPECTROSCOPIC AND KINETIC EVIDENCE THAT α-CHYMOTRYPSIN ACTIVITY IS MODULATED BY POSITIVELY CHARGED VESICLES. ((M.L. Bianconi[1], L. Barkas[2], F.C.L. Almeida[1], S. Schreier[1], and H. Chaimovich[1])) [1]Dept. of Biochemistry, Institute of Chemistry, Universidade de São Paulo, Brasil, [2]Facultad de Ciencias Exatas UNLP, Argentina. (Spon. by A.S. Ito)

We have examined the correlation between enzyme kinetics and changes in protein structure upon interaction of α-chymotrypsin (α-CT) and an interface. Km and Vmax of α-CT catalyzed hydrolysis of p-nitrophenyl acetate (NPA) were not significantly affected by phosphatidyl choline (PC) or PC:dihexadecyl phosphate (PC:DCP, 4:1) SUV. In contrast, there was an increase in both Km (up to 10x) and Vmax (up to 6x) in the presence of PC:Dioctadecyl-dimethylammoniun chloride (PC:DODAC, 4:1) SUV. α-CT conformational changes in the presence of PC:DODAC SUV were detected by electron spin resonance (ESR) and circular dichroism. The ESR spectra of spin labeled α-CT indicated that the label in the active site was considerably immobilized. The spectra did not change upon addition of PC or PC:DCP vesicles. However, line narrowing was observed in the presence of PC:DODAC, indicating higher mobility due to the protein at the interface. The more immobilized spectrum was recovered by addition of unlabeled α-CT. In conclusion, interfacial binding of α-CT causes protein conformational changes which, in turn, lead to increased catalytic efficiency.
Supported by: FAPESP, CNPq, Fundacion Andes

Tu-Pos458

BILAYER COMPACTION: A POSSIBLE ROLE FOR THE MYELIN PROTEOLIPID.(C. Nicot, R.Ober*, W. Urbach and M. Waks) Laboratoire d'Imagerie Paramétrique, URA1458 CNRS, Université Paris 6 and *Laboratoire de Physique de la Matière Condensée, URA 792 CNRS, Collège de France. Paris, France.

We have investigated the interactions of the Folch-Pi proteolipid (a protein-lipid complex) from myelin with a ternary system composed of tetraethylene glycol dodecyl ether, dodecane and water. The system exhibits at low water and surfactant concentrations, and at 20°C, a lamellar structure which may mirror some properties of the native multilamellar myelin membrane. We report that the system solubilizes substantial amounts of the transmembrane proteolipid in a stable conformation. After a lag period, we have observed the presence of a clear dodecane phase above the proteolipid-containing lamellae. Incorporation of other proteins under identical experimental conditions failed to induce a similar phenomenon. Small angle X-ray scattering measurements were carried out on the proteolipid-free and proteolipid-containing lamellar phases. The results demonstrate unambigously that interlamellar distances decrease as a function of protein concentration, reaching a plateau value. The specific interactions of the inserted proteolipid with the system are relevant to its role in the organization of the compact multilamellar myelin sheath and in its destruction in demyelinating diseases. Studies of the acoustic properties of the model system and their perturbation induced by incorporation of the membrane protein are under way in our laboratory.

Tu-Pos459

ANTIFREEZE GLYCOPROTEINS INHIBIT LEAKAGE FROM LIPOSOMES DURING THERMOTROPIC PHASE TRANSITIONS. ((L.M. Hays, R.E. Feeney†,L.M. Crowe, and J.H. Crowe)) Sect. of Cell. and Molec. Biol., †Dept. of Food Science and Technol., University of California, Davis, CA 95616.

Antifreeze glycoproteins found in the blood and tissues of polar fish at concentrations as high as 35 g/L are known to prevent ice crystal growth and depress the freezing temperature of the blood. Recently, Rubinsky *et al.* (1992. *Am. J. Physiol.*) provided evidence that antifreeze glycoproteins block ion fluxes across membranes during cooling; an effect that they ascribed to interactions with ion channels. We investigated the effects of antifreeze glycoproteins on the leakage from liposomes (dielaidoylphosphatidylcholine; with a transition temperature of 12°C) during chilling. As these liposomes are cooled through the transition temperature they leak approximately 60% of their contents. Addition of as little as 1 mg/ml of antifreeze glycoprotein prevents up to 100% of this leakage. Increasing the concentration of AFGP decreases liposome leakage further. To achieve this effect it is necessary to add the antifreeze glycoprotein above the transition temperature. If antifreeze glycoproteins are heated to 80°C, prevention of ice crystal growth is maintained but the capacity to inhibit leakage from liposomes is lost. Purified **non**glycosylated antifreeze proteins Type I and Type III (A/F Protein, Inc.) did not inhibit leakage. We conclude that AFGPs stabilize liposomes during thermotropic phase transitions and suggest that they may have similar effects on the lipid components of native membranes. (Supported by NSF IBN 93-08581 and ONR USN N00014-94-1).

Tu-Pos460

PLA_2 ACTIVITY IN DEHYDRATED SYSTEMS IS INFLUENCED BY THE PHYSICAL STATE OF THE LIPID BILAYER AND INHIBITED BY ARBUTIN. ((A.E. Oliver, L.M. Crowe and J.H. Crowe)) Section of Molecular and Cellular Biology, Univ. of California, Davis, CA, 95616.

It is well known that in hydrated systems, PLA_2 activity depends upon the physical characteristics of the lipid substrate. In order to determine if the physical state of the lipid bilayer is also important in partially dehydrated systems, liposomes of various charge, lipid composition, and level of hydration were compared for their effect on PLA_2 activity. Liposomes were freeze dried in the presence or absence of PLA_2 and rehydrated at controlled relative humidities. PLA_2 lipid hydrolysis was measured by the accumulation of free fatty acids in the liposomal membranes with analytical thin layer chromatography. It was found that PLA_2 activity increased with increasing hydration and negative charge of the bilayer, though the two were not necessarily correlated. PLA_2 was inactive in multilamellar vesicles, indicating that it was either excluded from or inhibited in the interlamellar spaces. Thus, the physical state of the lipid substrate seems important for PLA_2 activity in systems with low water availability as in those with excess water. Arbutin, a compound found in high concentrations in certain plants able to withstand prolonged dehydration, inhibits PLA_2 lipid hydrolysis only in dehydrated liposomes. This finding provides a possible function for arbutin in these organisms. This study was supported by NSF grant IBN 93-08581.

Tu-Pos461

THE INFLUENCE OF STEROLS ON THE SENSITIVITY OF LIPID BILAYERS TO MELITTIN ((Alexander M. Feigin, John H. Teeter, and Joseph G. Brand)) Monell Chemical Senses Ctr., Philadelphia, PA 19104

The sensitivity of planar lipid bilayers formed from neutral and negatively charged phospholipids to the permeabalizing effect of melittin was evaluated when sterols of varying structure were incorporated into the membrane. The addition of cholesterol to a bilayer containing negatively charged phospholipids strongly decreased the sensitivity of these membranes to melittin; however, cholesterol was not effective in membranes formed from zwitterionic lipids. Using a number of sterols with different structures (cholesterol, 7-dehydrocholesterol, stigmasterol, ergosterol, and lanosterol) the present study also demonstrated that neither the presence nor absence of the 5,7-dien system in the sterol molecule, nor the branching of the sterol side chain, influenced sterols' ability to decrease membrane sensitivity to melittin. The presence of three additional methyl groups (compared with cholesterol) in the tetracyclic nucleus (lanosterol) completely eliminated the ability of this sterol to influence membrane sensitivity to melittin. The dependence of the sterol effect on the presence of negatively charged lipids in the bilayer suggests that this effect results not only from the sterol being able to influence membrane fluidity but also from the sterol being able to influence the interaction of melittin with polar and charged groups on the surface of the bilayer.

Tu-Pos462

BIOPHYSICAL MODELS OF THE FIRST CELLS: MEMBRANE PERMEABILITY TO AMINO ACIDS AND SMALL PEPTIDES ((A.C. Chakrabarti, P.R. Cullis* and D.W. Deamer)) Dept. of Chemistry and Biochemistry, Univ. of California, Santa Cruz 95064. * Dept. of Biochemistry, Univ. of British Columbia, Vancouver, B.C. (Spon. by A. Chakrabarti)

A central problem in the origin of cellular life concerns the manner in which ionized or polar substrates were transported to support complex reactions, such as amino acid polymerization, prior to the evolution of membrane transport proteins. One possible mechanism involves the translocation of the neutral species of nutrients. Zwitterionic molecules (e.g. amino acids) can be chemically modified to create weak bases, which become neutral species at high pH. The neutral forms of amino acids and peptides that have their carboxyl termini modified permeate membranes up to 10^{10} times faster than charged forms. A transmembrane pH gradient can produce high rates of net unidirectional transport. Such pH gradients have been generated in membrane systems used to model protocells that preceded and were presumably ancestral to early forms of life. In response to pH gradients, amino acids and short peptides (2-3 amino acids in length) can be accumulated to higher concentrations (about 50-fold) than that of the external medium. Short peptides (composed of tryptophan and lysine) that have their basic functions sequestered at one end of the molecule exhibited dramatically improved abilities to translocate across membranes. These short peptides may serve as a starting point for modeling the origin and evolution of translocation mechanisms for membrane-spanning proteins and signal sequences. This work was supported by grants from the MRC of Canada, NASA Exobiology and NSCORT Exobiology.

Tu-Pos463

THE ROLE OF LIPID LATERAL HETEROGENEITY IN PROTEIN KINASE C ACTIVATION ((A.R.G. Dibble, Y.A. Shen, J.J. Sando and R.L. Biltonen)) Department of Pharmacology, University of Virginia, Charlottesville, VA 22908.

To test the hypothesis that the activation of protein kinase C (PKC) is strongly influenced by the dynamic structural state of the lipid bilayer, we analyzed the thermotropic phase behavior of the ternary lipid mixture dimyristoylphosphatidylcholine (DMPC)/dimyristoylphosphatidylserine (DMPS)/dioleoylglycerol (DO). We used differential scanning calorimetry to measure the enthalpy change (ΔH) associated with the gel-to-liquid crystalline phase transition as a function of composition. ΔH decreased with increasing DO content with ternary mixtures and with DMPS/DO binary mixtures, but not with DMPC/DO binary mixtures. In addition, Fourier transform infrared spectroscopy was used to monitor the temperature dependence of the conformational disorder of the acyl chains of DO, perdeuterated DMPC, and perdeuterated DMPS separately, within ternary mixtures. Increasing DO content perturbed the conformational disorder of DMPS more than that of DMPC. The results are consistent with DMPS/DO interactions being more favorable than DMPC/DO interactions in the ternary mixtures. These data, as well as PKC activity measurements using DMPC/DMPS/DO as the lipid activator, suggest that the formation of DMPS/DO-rich domains is associated with PKC activation.
(Supported by NIH grants DK07320, GM31184, and GM37658.)

Tu-Pos464

VESICLE MORPHOLOGY MODULATES PHOSPHOLIPASE A_2 ACTIVITY ((T.E.R. Hønger, A.R.G. Dibble, W.R. Burack, M.M. Allietta and R.L. Biltonen)) Departments of Pharmacology and Pathology, University of Virginia, Charlottesville, VA 22908.

The hydrolysis of dipalmitoylphosphatidylcholine (DPPC) large unilamellar vesicles (LUV) by phospholipase A_2 (PLA_2) proceeds in a complex manner: a period of slow product accumulation (the lag) ends with a sudden increase in rate (the burst). Previous work from this laboratory has shown that there is a profound change in vesicular structure which is concomitant with the burst [Burack, W.R., A. Dibble, M. Allietta, T. Hønger, and R.L. Biltonen. 1994. *Biophys. J.* 66:A58]. Here, we further characterize the lipid morphological changes which take place during PLA_2-catalyzed hydrolysis of DPPC LUV. ^{31}P and ^{13}C nuclear magnetic resonance spectroscopies were used to monitor changes in lipid composition and organization during hydrolysis. In addition, electron microscopy was used to visualize the lipid at various stages of the hydrolytic process. The morphological transformation at the burst is attributed to curvature instability in the bilayer arising from sufficient product accumulation during the lag period of PLA_2-catalyzed hydrolysis. This phenomenon is rationalized as a coupling between lateral compositional heterogeneity and local bilayer curvature. (Supported by grants from NIH.)

Tu-Pos465

The biophysical theory of lateral patterns of the neuron membrane proteins on the surface.

(L.Savtchenko & S. Korogod)
Lab of biophysics & bioelectronics, State Univ., 320625, Dniepropetrovsk, Ukraine.

Self-organization processes were investigated in the simulated neuronal cylinder-shaped cells with the membrane containing mobile ion channels and the pumps. The ions (Na^+, Ca^{2+}, K^+) moved across the membrane by the currents through corresponding channels along electrochemical gradients and by the pumps against these gradients. Local submembrane concentrations of the ions changed by several mechanisms, including transmembrane flux, diffusion and exchange with the deeper cytoplasm and the depots. Molecules of the channels had electrophoretic charge exposed to intracellular space and were subject to lateral electrodiffusion and to voltage-dependent conformational transitions between open and closed states. Steady-state non-uniform lateral distributions of the channels and related distributions of the voltages and ion concentration occurred in these systems. The following mechanisms responsible for that were found: 1) Ca^{2+} release from the depots induced by intracellular free Ca^{2+}; 2) sensitivity of the transmembrane flux to submembrane concentrations Na^+, K^+ and Ca^{2+}; 3) lateral electrodiffusion of the channels. The spatial and time scales of the pattern formation depended on principal contributing mechanism. If that was the submembrane ion concentration then average distance between "hot" and "cool" domains of the patterns was about 10-30 μm, and time of formation was about 100 s. If mobile channels dynamics dominated then the above spatial and temporal parameters were about 1-50 μm and 10^4 s, respectively. This approach considering self-organization as stochastic non-linear thermodynamic process is an alternative to that of "positional information", which assumes genetical predetermination of the patterning. It could be useful in many applications, including problems of neuron differentiation and development, cell-cell contact formation, myelination, signal transduction etc.

Tu-Pos466

STUDY OF THE SYNERGISTIC ACTION OF PHOSPHOLIPASE A2 AND MELITTIN IN THE HYDROLYSIS OF PHOSPHOLIPID MONOLAYERS.
((M. Grandbois, J. Dufourcq* and C. Salesse)) Centre de recherche en photobiophysique, Université du Québec à Trois-Rivières, Québec, Canada. *CRPP/CNRS, Université de Bordeaux, Pessac, France.

Phospholipase A2 (PLA2) is a small water soluble enzyme that catalyses hydrolysis of sn 2 acyl ester linkages of glycero phospholipids. Melittin (ML) is an amphiphilic peptide of 26 amino acids which binds phospholipid membranes and leads to the lysis of the cells. In the membranes, this peptide is well known to have an alpha helical conformation with a hydrophilic part including 6 positive charges. PLA2 and ML are two common constituents of numerous venoms and are known to show a marked synergism in their action on cell membrane. To investigate this synergistic mechanism, different ML analogs bearing various numbers of positive charges were used. The speed of hydrolysis of different phopholipid monolayers by PLA2 in the presence and absence of ML analogs was determined by measuring the variation of molecular area and surface potential at constant surface pressure. The results show that the speed of monolayer hydrolysis increases with the number of charges on the analogs. Moreover, epifluorescence microscopy has been used to visualize the effect of these analogs on the hydrolysis of dipalmitoylphosphatidylcholine (DPPC) monolayers in the phase transition. In the absence of ML analogs, the hydrolysis of DPPC monolayers occurs only from one single point at the border of the DPPC solid domains. However, when the analogs are present, the hydrolysis starts all around the DPPC solid domains. This result strongly suggests that the effet of ML is not only due to the presence of positive charges, but also to its ability to create defects in the phospholipid organization.

Tu-Pos467

CHARACTERIZATION OF LIPOSOMES CONTAINING TRANSMEMBRANE CD4. ((D. Alford, C. Larsen and C. Nicolau)) Center for Blood Research Labs, Harvard Medical School, 800 Huntington Ave., Boston, MA 02135.

CD4 is an integral membrane glycoprotein expressed predominantly on the surface of helper/inducer T-lymphocytes and on cells of monocyte/macrophage lineage. Under normal physiological circumstances, it functions as an accessory to the T-cell antigen receptor for major histocompatibility complex class II antigen and as a complex with $p56^{lck}$ to deliver intracellular activating signals. CD4 also functions as the high-affinity receptor for the HIV envelope glycoprotein gp120. We have produced liposomes containing a reconstituted purified recombinant form of CD4 (tmCD4, composed of the extracellular, transmembrane and truncated cytoplasmic domains). Several methods (including detergent dialysis, electroinsertion and passive insertion) were used to produce CD4-liposomes of various sizes. Unassociated tmCD4 was removed by flotation on a 0-10-15% dextran step gradient. Recovery of liposome-associated tmCD4 was determined by a flow cytometry assay, ELISA and SDS-PAGE. Liposome diameter and population size distribution were determined by dynamic light scattering and ultrastructural analysis using transmission electron microscopy. Liposomes contained the equivalent of more than 30 tmCD4 epitopes per 1 μm^2 surface area. The ability of CD4-liposomes to bind gp120 specifically was quantified by recombinant gp120 association in a flotation binding assay and by the ability of CD4-liposomes to bind specifically to cells expressing gp120 on their surface. CD4-liposomes will be useful for studying viral envelope glycoprotein conformational changes during the HIV fusion reaction.

Tu-Pos468

MODEL FOR ANTIBODY BINDING TO N-ETHYL-PHOSPHATIDYLETHANOLAMINE IN HEXAGONAL PHASE MICELLES. ((J. R. Trudell)) Department of Anesthesia, Stanford School of Medicine, Stanford, CA 94305-5117.

Several studies have shown that antigenic phospholipids have greatly enhanced antigenicity when they are exposed in a host of hexagonal phase micelles compared with a host of lamellar liposomes. However, most models of hexagonal phase micelles show only long tubes of inverted micelles with the antigenic headgroup exposed only to the inside of a long water-filled cylinder. Based on these models, it is difficult to explain binding of exogenously added antibodies to these headgroups. A possible explanation for the observed binding of antibodies to headgroups in hexagonal phase micelles is that the hexagonal tubes are covered on the outside by a very disorganized monolayer of phospholipids that are oriented with the headgroups facing outward. Molecular graphics techniques were used to draw this proposed outer monolayer in two and three dimensional arrays. The very large spacing between headgroups of N-ethyl-phosphatidylethanolamine in this outer monolayer may explain the increased ability of antibodies to bind to the haptenic site.

Tu-Pos469

SINGLE-PARTICLE TRACKING: HOW TO DETECT CORRALS. ((Michael J. Saxton)) Institute of Theoretical Dynamics, University of California, Davis, California 95616

Structural proteins of the membrane skeleton are thought to form "corrals" at the membrane surface, and these corrals may restrict lateral diffusion of membrane proteins. Recent experimental developments in single-particle tracking and laser trapping make it possible to examine the corral model in detail. We present techniques to interpret these experiments. First, we find the escape time of a diffusing particle from a corral for various corral sizes, shapes, and wall permeabilities. The permeability can then be obtained from the observed escape time in tracking experiments. From the permeability, size, and shape of the corral, we can predict the long-range diffusion coefficient, as measured by fluorescence photobleaching recovery. Second, we consider how to identify corrals in tracking experiments. The simplest way to identify corrals is by sight. If the walls are impermeable enough, a trajectory fills the corral before the diffusing particle escapes. For a random walk in a corral on a lattice, we find the number of distinct sites visited before escape for corrals of various sizes, shapes, and permeabilities, and we reduce these to a common curve. A test for confined motion proposed earlier is compared with identification purely by sight. (Supported by NIH grant GM38133.)

ELECTROSTATICS

Tu-Pos470

SURFACE CHARGES DETECTED WITH AN ELECTROSTATIC FORCE MICROSCOPE. ((Shaohua Xu and Morton F. Arnsdorf)), Department of Medicine, University of Chicago, Chicago, Ill 60637. (spon. Z. Zhou).

A variety of charged cantilever probes were developed which enabled scanning force microscope (SFM) to be used as an electrostatic force microscope (EFM). Surface electrostatic charges of samples in aqueous solution could be analyzed with the EFM on an nanometer scale. The EFM was used to image mica, DEAE-sephadex beads, 3-propyltriethoxysilane-treated-glass and lysozymes in water or phosphate buffer. When a charged probe and a specimen of opposite charge were used, an adhesion force was measured that was 10 to 30 times greater than when a bare probe was used. This dramatic increase of measured adhesion force can be attributed to the energy required to break the salt bridges formed between the charged probe and the specimen. The adhesion force was also found to be strongly dependent upon the ionic strength of the solution. Probes with densities as high as 1 charge per 1.2 square nanometers were prepared, and were stable over a broad pH range. A method of probe geometry determination reported earlier (Xu and Arnsdorf, 1994, J. Microscopy, 173(3), 199-210) will allow us to quantitatively analyze the surface electrostatic charges of biomembranes and proteins such as ribonucleases and lysozymes using this EFM.

Tu-Pos471

RAPID EVALUATION OF PH DEPENDENT EFFECTS IN PROTEINS. **((H. Oberoi and N. M. Allewell)) Department of Biochemistry, University of Minnesota, St Paul, MN 55108.**

Calculating accurate binding energies and modeling conformational changes in proteins require the evaluation of the energetics of charge-charge interactions. Since the energetics are closely linked to the ionization state of proteins, the pH dependent charge array of the protein needs to be determined accurately. We will describe a rapid technique for calculating the protonation state of the protein, based on a modified approach for evaluating the Boltzmann-weighted sum over all possible protonation states of ionizable groups in the protein. The implementation will be described in the framework of an object-oriented system for calculating electrostatic properties in proteins. The application of this technique in calculating the energetics of ligand binding and its dependence on the protonation state of the protein will be presented. Supported by NIH grant DK-17335 to NMA.

Tu-Pos472

MODELING THE ELECTROSTATIC EFFECTS OF LIGAND BINDING IN ASPARTATE TRANSCARBAMYLASE. **((H. Oberoi, X. Yuan, J. Trikha and N. M. Allewell)) Department of Biochemistry, University of Minnesota, St Paul, MN 55108.**

Aspartate transcarbamylase (ATCase) from *E. coli* has been widely studied as a model allosteric system. Although it is known that binding of substrate analogs causes ATCase to switch between two major conformational states, T and R, and that this allosteric transition is pH dependent [Pastra-Landis, *et al., J. Biol.Chem.* 253:426 (1978)], details of the coupling between pH and the allosteric transition at the molecular level remain elusive. We will describe the results of the application of the multigrid Poisson-Boltzmann (MGPB) approach to calculate electrostatic effects of ligand binding in ATCase and compare them with previous results obtained with the modified Tanford-Kirkwood (MTK) model. Agreement with experimental titration curves can be achieved with both MTK and MGPB, despite differences in individual pK values. The results of the MGPB calculations confirm the conclusion drawn previously from the Tanford-Kirkwood calculations, that ligand binding induces large changes in the $pK_{1/2}$ values of residues as much as 60 Å distant from the ligand binding site. It appears likely that long range electrostatic effects are involved in the transmission of allosteric signals in ATCase. Supported by NIH grant DK-17335 to NMA.

Tu-Pos473

ELECTROSTATICS IN ORGANIC SOLVENTS VIA CONTINUUM METHODS ((D. Sitkoff, N. Ben-Tal, K. A. Sharp, B. Marten, R. A. Friesner and B. Honig)) University of Pennsylvania, Phila., PA 19104 and Columbia University, NY, NY 10032 (Spon. by A. Palmer)

Continuum dielectric approaches have recently been shown to yield excellent results for solvation free energies, pK_a's and Stark effect shifts for groups in aqueous solution (see electrostatics review by Sharp, K.A. **Curr. Opin. Sruct. Biol.**, *4*, 234). Given the relevance of low dielectric environments to biological systems (e.g. membranes as barriers and as sites for bound proteins) we now evaluate the utility of the continuum method in computing energies in organic media. Transfer free energies from organic solvant (cyclohexane) to water are calculated and compared with experiment for 18 small molecules representing the amino acid side chains and related functional groups. Energies are calculated both via a classical and a quantum mechanical solute model. Results demonstrate that, particularly in the case of hydrogen bonding groups, the ability of the continuum method to obtain accurate solvation energies depends upon solvent-specific adjustment of the solute-solvent boundary. The adjustment sign and magnitude (~0.7 Å greater for solutes in organic solvent vs. water) are shown to be reasonable based on experimental atomic distances and quantum mechanical electron density contours. The newly adjusted method is used to evaluate the energy of burial of a hydrogen bond in a low dielectric medium, and implications to protein insertion into membranes are discussed.

Tu-Pos474

A FAST MOLECULAR SURFACING ALGORITHM WITH APPLICATIONS TO FINITE-DIFFERENCE ELECTROSTATIC CALCULATIONS ((S. Sridharan, A. Nicholls and B. Honig)) Dept. Biochemistry and Molecular Biophysics, Columbia University, New York, NY.10032

We describe a fast and accurate algorithm to calculate the Molecular Surface(MS) on a cubic grid. Analytic methods for calculating the MS are of limited use in applications such as graphical displays or electrostatic calculations. In contrast our algorithm renders the MS in a format that is directly usable in finite-difference electrostatic calculations. The errors are much smaller and the CPU times scale much better with grid size compared to traditional grid based methods. Volumetric rendering is possible with algorithms for triangulation of 3D-gridded data. We present applications in Finite-Difference electrostatic calculations, calculation of solvation forces in Molecular Mechanics/Dynamics simulations and in graphical display of surfaces.

Tu-Pos475

SMALL MOLECULE pKa PREDICTION WITH CONTINUUM ELECTROSTATICS CALCULATIONS*. ((M.J. Potter , M.K. Gilson , J.A. McCammon)) Dept. of Chemistry and Biochemistry, and Dept. of Pharmacology, University of California at San Diego, La Jolla, California 92093. CARB, NIST, 9600 Gudelsky Dr., Rockville, Maryland 20850.

Finite-difference solutions to the linearized Poisson-Boltzmann equation are used to calculate the pKas of a variety of diacid and diamino compounds. An initial pKa is assigned to each titratable group based on experimental data for a structurally similar monofunctional acid or amine. These initial pKas are adjusted for the electrostatic environment of the sites within the difunctional compounds and used along with the calculated electrostatic interaction energy between sites to predict the pKas. Ionization is modelled either as the addition of a unit positive or negative charge to a single atom, or through the use of partial charges appropriate for the group and its ionization state. Both models produce pKas in reasonable accord with the experimental values for the diamines, with the partial charges results slightly better. The ± 1 model results are poor for the diacids, though they improve with increasing inter-site distance. While the use of partial charges improves the calculated diacid pKas, large errors are still observed when sites are close together. Overall, the results provide confidence in similar approaches used in protein studies, where both through-bond and direct distances are relatively large, and indicate that it would be reasonable to extend the method to medium-sized organic molecules. MJP is a Howard Hughes Predoctoral Fellow. *Journal of the American Chemical Society, in press.

Tu-Pos476

ROLE OF ELECTROSTATICS IN HEN-EGG LYSOZYME/ANTIBODY ASSOCIATION. ((Stuart P. Slagle[1], Shawn McDonald[2], J. Andrew McCammon[2], & Shankar Subramaniam[1])) National Center for Supercomputing Applications, Beckman Institute, Center for Biophysics and Computational Biology, and Department of Physiology & Biophysics, University of Illinois, Urbana[1], IL 61801 & Department of Chemistry, University of Houston[2], Houston, TX 77204.

High resolution structures of several monoclonal antibodies raised against hen–egg lysozyme have been obtained in the complexed state by Davies and coworkers and Poljak and coworkers. Two of these antibodies share common epitope features, despite being different in their three dimensional structures. HyHEL–5 and D44.1, both contain two charged glutamate residues which form salt links with two arginine residues on the lysozyme. We use a multigrid–based Newton method, for solving the Poisson–Boltzmann equation, to investigate the role of electrostatics in the association of these two complexes. An important question that arises in such systems is the pKa values of ionizable residues and hence their state of protonation. Using thenewly developed method due to Antosiewicz, McCammon, and Gilson, we calculate pKa values of key interface residues in these complexes. pH dependence of the complexation and its implications for structure in these two antibody–antigen complexes are presented. [supported by funds from NSF, NIH, and Human Frontiers Science Program].

Tu-Pos477

DIRECT EVIDENCE FOR THE ROLE OF ANTIBODY STRUCTURE IN THE ELECTROSTATIC CONTROL OF ANTIGEN BINDING. ((D. Leckband, T. Kuhl, H.-K. Wang, W. Müller, J. Herron, and H. Ringsdorf)) SUNY at Buffalo, UC Santa Barbara, Univ. of Utah, J. Gutenberg Univ., Germany.

The forces between the binding surface of anti-fluorescyl monoclonal IgG Fab' and fluorescein presenting membranes were directly measured as a function of their intermolecular separation with the surface force apparatus. Measurements at different ionic strengths verified the electrostatic control of the long-range interactions between the protein and membrane surface. Despite the fact that the overall Fab' and membrane surface charges were net negative under the experimental conditions, the directly measured electrostatic potential of the Fab' surface was net positive. This behavior is consistent with the the ring of positive charge surrounding the binding site and with the calculated positive electrostatic potential near the binding site. The dependence of these forces on the folded Fab' structure was demonstrated by the change in the forces from overall attractive to repulsive upon Fab' denaturation. These results directly demonstrate that the electrostatic control of long-range fluorescein-Fab' interactions is directly determined by the details of the exterior protein surface.

Tu-Pos478

EFFECTS OF CONFORMATIONAL FLEXIBILITY ON ELECTROSTATIC FIELDS ((Malcolm E. Davis and William J. Metzler)) Bristol-Myers Squibb, P.O.Box 4000, Princeton, NJ 08543-4000.

Electrostatic interactions play an integral part in the molecular recognition process. Small changes in the electrostatic properties of a molecule can lead to dramatic gains or losses in binding affinity, thus a detailed understanding of the electrostatic component to binding will play an important role in drug discovery. Electrostatic analysis are typically performed on a single, static structure derived from either x-ray crystallography or NMR spectroscopy; however, proteins are mobile in solution, and the functional groups that most strongly contribute to the electrostatic potential (e.g. lysine amino groups or glutamic acid carboxylates) are generally the most poorly characterized from a structural perspective. To understand the effect that conformational flexibility has on the electrostatic fields surrounding a molecule requires knowledge of the magnitude of the electrostatic fluctuations and extent from the protein surface that their influence extends for realistic variations in conformation.

In this study we analyze the effect of conformational flexibility on electrostatic fields. We use the NMR-determined ensemble of solution structures of human profilin to represent the conformational variation that one sees in small globular proteins. The electrostatic fields are calculated using a continuum dielectric model. This model, a generalization of Tanford-Kirkwood theory, describes the protein as an irregularly shaped, low dielectric cavity immersed in a high dielectric solvent. The atomic partial charges are located as point charges at the atomic coordinates. A finite difference solver for the resulting Poisson- Boltzmann equation, determines the electrostatic field surrounding the protein. We then analyze the fields and their differences over surfaces at various distances from the molecular surface.

Results of the magnitude and extent studies will be presented along with investigations of the major contributors to these variations.

Tu-Pos479

TITRATION AND ELECTROSTATIC STUDIES OF IONIZABLE RESIDUES IN DHFR: IMPLICATIONS FOR THE CATALYTIC MECHANISM ((W. R. Cannon and S. J. Benkovic)) Dept. of Chemistry, Penn State Univer ty, University Park PA 16802

Dihydrofolate reductase (DHFR) catalyzes the reduction of dihydrofolate to tetrahydrofolate, a cofactor required for nucleotide biosynthesis. Considerable debate in the literature has arisen regarding a titration phenomenon of pKa = 6.5. Recent IR studies have suggested that this pKa is due to the protonation of dihydrofolate at the N5 site. However, previous studies have shown that this pKa is required for product release presumably due to the protonation of Asp 27. We are employing Poisson-Boltzmann techniques to determine the pKa of ionizable sites in the DHFR apoenzyme, the DHFR-NADPH binary complex and the DHFR-NADPH-dihydrolate ternary complex. The implications of these findings on the mechanism of DHFR and biological hydride-transfer reactions will be discussed.

Tu-Pos480

THE ELECTROSTATIC INTERACTIONS OF PLASTOCYANIN AND CYTOCHROME F. ((Douglas C. Pearson Jr. and Elizabeth L. Gross.)) Biophysics Program and Department of Biochemistry, The Ohio State University, Columbus, Ohio 43210. (Sponsored by J.Y. Cassim.)

The electrostatic interaction between two proteins involved in photosynthetic electron transport is studied. Plastocyanin (PC) is a 10 kDa copper protein, and cytochrome f (cyt f) is a 25 kDa protein and one of PC's reaction partners. Using the program GRASP, which solves the linearized Poisson-Boltzmann equation and displays the solution in the form of contours surrounding a molecule, it is possible to compute and observe the electrostatic potential about these two molecules. PC has two sizeable patches of negative electrostatic potential, one involving residues 42-44 and one in the region of residue 61 (residues 59-61 in most higher plants). Cyt f has a sizeable region of positive potential, generated by the heme at its center and reinforced by arginines 156 and 209 and lysine 187, among others. Based on the assumption that electrostatic attraction between the two molecules is responsible for the long-range alignment of the two molecules, two docking configurations are proposed; these docking configurations also take into account previous experiments describing the interactions between the two molecules. Possible residues through which electron transfer may take place are tyrosine 83 and histidine 87 on PC, both of which may be implicated with tyrosine 1 on cyt f. Hypotheses are proposed to attempt to explain the docking procedure, taking into account the electrostatic effects, possible short-range hydrophobic effects, and possible electrostatic steering involving lysine 77.

Tu-Pos481

HYDRATION AND ELECTROSTATIC INTERACTIONS DURING GENERATION OF COAGULATION FACTOR Xa ((Maria P. McGee and Hoa Teuschler)) Bowman Gray School of Medicine, Wake Forest University, Winston-Salem, NC 27157. (Spon. by R.L. Wykle)

The rate of factor Xa generation via the extrinsic coagulation pathway assembled in aqueous phase was previously shown to be increased by OS (osmotic stress). The purpose of the present study was to examine the contribution of electrostatic interactions to the energetics of the reaction proceeding under OS in aqueous phase and on phospholipid membranes (phopsphatidylcholine/phosphatidylserine). Reaction mixtures were assembled with purified human coagulation proteins, factors X, VIIa and tissue factor, and stressed osmotically with polyethylene glycol in aqueous univalent salt solutions of ionic strengths ranging from 0.03 to 0.7 M. Initial rates of factor Xa generation from factor X were measured with chromogenic substrates. In membrane-assembled reactions, the value of free energy of activation, ΔG^*, was unchanged by osmotic stress at low salt concentration but was decreased at high salt concentration, i.e.>0.15M. In aqueous phase reactions, ΔG^* increased linearly with salt concentration, [S], for NaCl, KCl, CsCl, and LiCl. The slope of $\Delta G^*/[S]$ regression lines did not vary significantly with either the type of ion or OS and had a value of 6.6 ± 0.5 and 6.5 ± 0.3 kcal/mol per M of salt, under OS and standard conditions respectively. Results are interpreted as indicating that for aqueous phase reactions, electrostatic and hydration-dehydration interactions are largely independent from one another. For reactions assembled on lipid membranes, high salt concentration appears to increase exposure of reactants to water.

Tu-Pos482

PHYSICAL MODELS OF MECHANISM OF ELECTROPORATION ((K. Cheng)) University of Miami School of Medicine, Miami FL 33136

In an electroporation system, a mechanical function is developed, based on Newton's Second Law, for a small patch with proteins and lipids, in a cell membrane and on the positive or the negative side. Two physical models of the critical potential deference $\Delta\Psi_0$ of electroporation are derived from the function. One is expressed in terms of the Law of the Conservation of Energy and another one is presented in terms of the Impulse-Momentum Principle. The two models elucidate that: $\Delta\Psi_0$ is proportional to the mass m, the thickness L and the departure velocity v of the patch and the electric attraction force f between the patch and the cell membrane; $\Delta\Psi_0$ is inversely proportional to the net charge q carried by the patch and the absolute temperature T of the system. A concept of work function ϕ_w of electroporation is proposed and ϕ_w is described as $\phi_w = q\,\Delta\Psi_0/2$ in the first model. The second model particularly indicates that $\Delta\Psi_0$ and the critical width τ_0 of the externally imposed electric pulse can compensate each other. Many previous experimental results can be qualitatively explained with the two models. The essential and sufficient conditions of electroporation occurrence for the patch are proposed too. The essential condition is $-q\,d\Psi/dx > f$ and the sufficient condition is $\tau > \tau_0$, where $-d\Psi/dx$ and τ are the electric field at the patch and the pulse width respectively.

Tu-Pos483

Abstract Withdrawn.

Tu-Pos484

THEORY OF GENERALIZED DIELECTROPHORESIS AND ITS APPLICATIONS. ((X-B. Wang, Y. Huang, F. F. Becker and P.R.C Gascoyne)) Box 89, UT M.D. Anderson Cancer Center, 1515 Holcombe Blvd., Houston TX 77030

We present a generalized theory that unifies the description and interpretation of conventional dielectrophoretic and travelling wave dielectrophoretic forces acting on particles in a standing non-uniform AC electric field and in a travelling electric field, respectively. We show that the generalized dielectrophoretic (gDEP) force experienced by particles in a field arises from the spatial non-uniformities of the magnitude and the phase of the field interacting, respectively, with the in-phase and out-of-phase components of the induced dipole moment.

We apply the gDEP theory, in conjunction with measured cell dielectric properties and numerically calculated electric field distributions for several experimental electrode configurations, to explain the translational effects that can be observed for particles exposed to standing, travelling and rotating fields. The good agreement found between these theoretical predictions and the experimental observations that we also present validate the theory. Finally, we illustrate the usefulness of the gDEP theory by employing it to derive an expression for the mutual dielectrophoretic forces acting on two neighboring particles that result from dipole-dipole interactions induced in an applied AC field. We conclude that the gDEP theory is of use not only for providing new insights into electrokinetic interactions between particles and applied electric fields but also for guiding the design of novel electrode geometries for use in particle characterization and manipulation applications.

Tu-Pos485

LOSS OF I_{to} AND Kv1.4 ARE COINCIDENT IN FELINE VENTRICULAR MYOCYTES KEPT IN CELL CULTURE.

((Christopher Hansen, Robert S. Decker and Robert E. Ten Eick)) Depts. of MPBC & CMB, Northwestern University, 320 Superior Street, Chicago, IL 60611

The density of the myocardial transient outward K^+ current (I_{to}) is affected by cardiac hypertrophy, failure and ischemia; all are conditions associated with an increased risk of sudden-death. Both increases and decreases have been reported. Comprehensive cellular electrophysiological studies have suggested that the other major components of the cellular membrane current are not much changed by these disease conditions. These findings suggest that an understanding of the regulation of I_{to} expression might be important for an improved understanding of the mechanism of sudden death associated with hypertrophy, failure and ischemia. One candidate gene for I_{to} is Kv1.4, a gene for which we created (PCR technique) a ~280 base-pair, cat-specific Kv1.4 cRNA probe that could be used in an RNase protection assay to quantify the cellular level of Kv1.4 mRNA. We recently documented that I_{to} slowly "disappears" in feline ventricular myocytes (VM) kept in cell culture for 11-14 days, with the first detectable loss appearing on day 7. When we examined the question "Does Kv1.4 also disappear in VM kept in culture?", we found that it did disappear and that the time courses of loss of Kv1.4 and of I_{to} were almost coincident, despite there being no change in the total mRNA content. This finding suggests that Kv1.4 is intimately involved with I_{to} in cat VM. At this time we do not know if other candidate genes for I_{to} undergo similar changes in their mRNA content during cell culture at the time when I_{to} expression is disappearing.

Tu-Pos486

SINGLE-CELL ANALYSIS OF DNA HELIX OPENINGS WITHIN EXTENDED AND CONDENSED CHROMATIN DURING GENE TRANSCRIPTION.

((J.H. Frenster)) Physicians' Educational Series, Atherton, CA 94027-5446.

DNA molecules are opened locally during active gene transcription, and these DNA helix openings can be detected within single intact cells by high-resolution probe electron microscopy (Ann. N.Y. Acad. Sci. 567, 334 (1989). Human bone marrow cells were aspirated and rapidly fixed in cold glutaraldehyde, followed by acridine orange probe insertion and DNase-I digestion. Probe sites were visualized as electron-dense reaction products only following digestion with DNase-I. DNA helix openings ranged in length from 25 to 700 nm, corresponding to 70-2000 base pairs in length of DNA. Probe sites were never found within condensed heterochromatin masses, and were found only within the extended euchromatin microfibrils of the cell nucleus, where they correlate most highly in location with sites of active gene transcription. Cell types known to have low rates of RNA synthesis were found to have low counts of probe sites per cell, and smaller probe sizes per site. Probe site numbers and sizes decreased through the course of cell division and cell differentiation. It is concluded that DNA helix openings correlate with active gene transcription, and are found only within extended euchromatin microfibrils.

Tu-Pos487

INVESTIGATIONS OF THE SINGLE STRAND DNA BINDING PROPERTIES OF TWO ASSOCIATED STRUCTURES OF RECA PROTEIN FROM *ESCHERICHIA COLI*.

((P.V Riccelli, A.P. Desai and A.S. Benight)) Department of Chemistry, University of Illinois, Chicago, IL. 60607. (Spon. by T.M. Paner)

Two aggregated structures of RecA protein with significantly different hydrodynamic properties (the large and small RecA structures) were prepared. Equilibrium binding of these RecA structures at 6 μM to 24 and 32 base oligomers, with homo purine or pyrimidine sequences, $d(py)_{32}$, $d(py)_{24}$, $d(pu)_{32}$ and $d(pu)_{24}$), at 0.6 μM bases in the presence or absence of 2 mM Mg-Acetate and increasing amounts of ATP-γS, was investigated. For the large and small RecA structures increased ATP-γS lead to diminished binding capacity of the protein for all DNA sequences. Influence of ATP-γS on binding varied with DNA length and sequence and was stronger for the small RecA structure. Effects of ATP-γS on binding were smaller in the presence of Mg-Acetate but the relative binding affinity for different DNA oligomers was unaffected. The large structure had a higher binding affinity for all DNAs examined and the binding was less sensitive to [ATP-γS]. For both RecA structures the relative binding affinity was conserved in the order $d(py)_{32}$ > $d(py)_{24}$ > $d(pu)_{32}$ >> $d(pu)_{24}$. Kinetic analysis of binding the RecA structures to a 77 base DNA single strand was performed. Results suggest the different hydrodynamic properties of the two RecA structures directly influence sequence dependent equilibrium binding and kinetics. (Supported by NSF)

Tu-Pos488

DNA STRUCTURE ANALYSIS OF MULTI-PROTEIN BINDING TO THE *Escherichia coli gal* OPERON.

((Dennise D. Dalma-Weiszhausz and Michael Brenowitz)) Albert Einstein College of Medicine, Bronx, NY 10461

The regulation of gene expression requires the binding of RNA polymerase (RNAP) as well as other regulatory proteins to specific DNA sequences. Upon binding, these proteins may interact with each other and alter the DNA structure. We are studying the changes in DNA conformation as a function of the simultaneous binding of RNAP and other known regulatory proteins. The *E. coli gal* operon is an ideal model system to study this since its regulation is conferred by two well characterized proteins, Gal repressor (GalR) and Catabolite Activator Protein (CAP). This promoter sequence contains two distal binding sites for GalR, a CAP binding site, and two partially overlapping RNAP binding sequences in a span of only 114 bp.

The use of alternate footprinting reagents allows for the determination of the DNA conformation upon multi protein binding. We have used 5'-phenyl 1-10 phenanthroline, hydroxyl radical and DNase I as probes for DNA structure changes when protein(s) bind. The different size, groove preference, and DNA structure sensitivity of these probes has been exploited to build a map of the DNA conformation when a combination of these three different proteins bind. We have also done parallel studies on a *chimeric gal* operon in which the GalR binding sites have been point mutated to Lac repressor (LacI) recognition sequences.

Our results show that RNAP binds to this promoter sequence and causes an extended DNase I footprint. This footprint is further extended in the presence of CAP. The CAP-induced DNase I hypersensitivity increases as a function of RNAP binding, suggesting that CAP and RNAP form a complex in which the DNA is tightly bent (Steitz and Crothers, Transcriptional activation by *Escherichia coli* CAP Protein. In: *Transcriptional Regulation*. Cold Spring Harbor Laboratory Press, New York 1992). Our results are mostly consistent with those of Lavigne *et al.* (*Biochemistry* 31, 9647-9656.1992), who have used this methodology to probe the interaction between CAP and RNAP. We further extended our studies to include the binding of GalR at one or two of its cognate operators.

Tu-Pos489

MULTIPLE CYTR DIMERS BIND TO *E. COLI* DEOP2 AND INTERACT BOTH COOPERATIVELY AND COMPETITIVELY WITH THE CAMP-CAP COMPLEX.

((D.F. Senear, E.A. Doherty & L. Perini)) Dept. of Molecular Biology & Biochemistry, University of California, Irvine 92717.

Binding of CAP and CytR mediates both positive and negative control of transcription from *E. coli* deoP2. Transcription is activated by cAMP-CAP. A multi-protein (cAMP-CAP)-CytR-(cAMP-CAP) complex that is stabilized by cooperative interactions between CytR and CAP represses transcription. Similar interactions at the other transcriptional units of the CytR regulon coordinate expression of the transport proteins and enzymes required for nucleoside catabolism. We have studied the site specific, cooperative protein-DNA interactions of CAP and CytR, to understand this combinatorial control of gene expression. Footprint analysis of CytR binding demonstrates interactions with the CAP binding sites (CRP1 & CRP2) as well as with the previously recognized CytR site flanked by CRP1 & CRP2. The CytR concentration dependence differs for binding to these three contiguous DNA sequences, indicating multiple binding events. This suggests competition between CytR and cAMP-CAP for CRP1 & 2, a previously unknown feature of regulation. CAP and CytR binding to every combination of active and inactive sites were studied using reduced valency operator mutants. Data analysis yielded precise estimates of the Gibbs free energy changes for intrinsic binding to every site and for all cooperative (and competitive) interactions. CytR binding to CRP1 & 2 is weakly specific and non-cooperative. Cytidine induces transcription by binding to CytR and eliminating cooperative interaction with cAMP-CAP. As our model predicts, cytidine liganded CytR is a strict competitive inhibitor of cAMP-CAP binding. Supported by NIH grant GM41465.

Tu-Pos490

THE CONTRIBUTION OF BIDENTATE INTERACTIONS TO THE RATE OF ASSOCIATION OF THE *E. coli* LAC REPRESSOR TETRAMER FOR OPERATOR.

((M. Hsieh and M. Brenowitz)) Department of Biochemistry, Albert Einstein College of Medicine, Bronx, NY 10461.

The control of transcriptional initiation requires the binding of regulatory proteins to specific DNA amidst a large background of nonspecific DNA. Protein association to a specific site is thought to occur by a multi-step process involving initial nonspecific DNA binding followed by one or more translocation steps [O.G. Berg, R.B. Winter & P.H. von Hippel, *Biochemistry 20*, 6929-6948, 1981]. Facilitated translocation has been used to account for the apparent ability of some DNA-binding proteins to locate a specific DNA target at rates faster than a free-diffusion would allow. Lac repressor (LacI) was originally noted to exhibit large rate enhancement as measured by filter binding studies [A. D. Riggs, S. Bourgeoise, & M. Cohn, *J. Mol. Biol. 53*, 401-417, 1970]. Recent kinetics studies using LacI and its dimeric mutant have provided some evidence for translocation mechanisms but with conflicting results. [T. Ruusala & D.M. Crothers, *PNAS 89*, 4903-4907, 1992; R. Fickert & B. Müller-Hill, *J. Mol. Biol. 226*, 59-68, 1992]. The nature of the rate enhancement remains unclear.

We have performed association kinetics studies of LacI, a dimeric mutant ($LacI^{ad}$) and the dimeric *E. coli* Gal repressor (GalR) by quantitative DNase I footprinting using a quench-flow apparatus. Use of the quench flow apparatus provided the time resolution necessary to allow experiments to be conducted at protein concentrations under which their oligomerization state is unequivocally known. Under the range of salt concentrations studied (25 mM - 200 mM), the dimeric, monodentate proteins, GalR and $LacI^{ad}$, exhibited comparable association rate constants and similar salt dependence of the rate constants. In contrast, the tetrameric, bidentate LacI exhibited rate constants an order of magnitude greater with a less pronounced salt dependence. (Supported by NIH grants GM39929 and F31-GM13850.)

Tu-Pos491

LINKAGE OF PROTEIN FOLDING AND FUNCTION IN THE TRP REPRESSOR OF *E. COLI*

((Ross J. Reedstrom* and Catherine A. Royer)) University of Wisconsin - Madison, Cell & Molecular Biology and School of Pharmacy, Madison, WI 53706

The fine-control of gene expression in the trp repressor system is achieved through the thermodynamic linkage of protein folding to binding interactions involving the *trp* repressor protein (TR), tryptophan and DNA. Studies of super-repressor mutant proteins are useful for dissecting the various thermodynamic contributions to the *trp* repressor function. While all other tested super-repressors have shown *in vitro* differences from wild-type repressor by various assays, including operator and ligand affinity and DNA binding stoichiometry, purified AV77 has been indistinguishable from wild-type TR . We have demonstrated that AV77 differs from wild-type TR in the folded state of the unliganded, apo-repressor form of the protein. AV77 has a lower affinity for 1,8-ANS, indicating reduced solvent access to hydrophobic regions of the protein. CD spectroscopy shows the apo-repressor form of AV77 to be significantly more structured than that of wild-type repressor. When monitored by intrinsic tryptophan fluorescence, AV77 is 2 kilocalories more stable to urea denaturation than wild-type TR. In addition, the effect of tryptophan on protein • protein interactions observed with wild-type TR is abolished in AV77. These data are consistent with NMR solution structural models of TR and calorimetric data, that indicate that the DNA binding domains are not rigidly structured in the wild-type apo-repressor. These binding domains also form part of the tryptophan binding pocket. These results implicate folding of the DNA binding domains in the allosteric linkage of the ligand binding and protein • protein interactions to the DNA binding function of the *trp* repressor.

Tu-Pos492

INTERACTIONS OF GRDBD WITH DNA MONITORED BY FLUORESCENCE ANISOTROPY

((John J. Hill and Catherine A. Royer)) University of Wisconsin-Madison, School of Pharmacy

The interactions of the DNA binding domain of the glucocorticoid receptor, (GRDBD) amino-acids 407-556, with a variety of DNA target sequences was monitored by the anisotropy of emission of a fluorescence probe covalently bound to the 5'-end of the target DNA sequences. The stoichiometry and apparent cooperativity of binding depended on the target DNA sequence and the salt concentration used. At 100 mM salt, the intrinsic affinity of the monomer for the 3S-GRE half site was found to be quite low ($K_d \approx 200$ nM), although due to the high degree of cooperativity the apparent affinity for full dimer/DNA complexation was near 30 nM At low salt, 2:1 dimer/DNA complexes formed with high cooperativity, indicating that specific DNA is not required to induce dimerization. Cooperativity could be abolished by changing the half site spacing or by mutations at the dimer interface. Squelching mutants exhibited both higher affinity and cooperativity in binding, implicating a DNA-induced conformational change in their altered function. Non-cooperative, high affinity (10 nM) binding was observed for WT GRDBD at high salt to a composite GRE sequence derived from the control region upstream of the proliferin gene (plfG), consistent with its altered functional properties at that site.

Tu-Pos493

A SPECTROSCOPIC CHARACTERIZATION OF THE BINDING OF WHEAT GERM INITIATION FACTORS TO mRNA.

((M.L. Balasta and D.J. Goss)) Chem. Dept., Hunter College (CUNY) New York, NY 10021.

Direct fluorescence titration methods were used to study the formation of binary and ternary complexes involving wheat germ eukaryotic initiation factors, eIF-4F, -4A and -4B, mRNA, and ATP. These three initiation factors are involved in the formation of the 48S initiation complex: eIF-4F recognizes the cap structure (m^7G) of RNA; eIF-4A has RNA-dependent ATPase and ATP-dependent helicase activities; and eIF-4B stimulates these activities. A characterization of the binding of these proteins to capped oligoribonucleotides using fluorescence spectroscopic techniques will lead to a better understanding of the mechanism of initiation complex formation.

Equilibrium binding constants (K_{eq}) calculated for the binary and ternary interactions show that initial formation of the eIF-4F:oligo complex enhances the subsequent binding of eIF-4B or eIF-4A to form the ternary complexes. Formation of the latter appear to be ATP dependent, an effect which is more prominent in the case of the eIF-4A interactions (approximately a 15-fold increase from 0 to 20 μM ATP). On the other hand, the eIF-4B interactions with eIF-4F in the presence of the oligo is characterized by high binding constants but these values exhibit a much lower ATP effect. A close look at these interactions can therefore aid us in elucidating the roles of these initiation factors with respect to binding to mRNA in the presence of ATP.

Tu-Pos494

HELICASE ACTIVITY OF WHEAT GERM PROTEIN SYNTHESIS INITIATION FACTORS eIF-4A AND eIF-(iso)4F

((J.Ren and D.J. Goss)) Chem. Dept., Hunter College (CUNY) New York, NY 10021.

In order for a ribosome to scan mRNA, double stranded regions must become single stranded. This is most likely accomplished by initiation factors.

The interaction of two eukaryotic protein synthesis initiation factors from wheat germ with mRNA has been examined. Eukaryotic initiation factor eIF-(iso)4F is an isoenzyme of the cap binding protein eIF-4F. Two oligonucleotides (34 mer and 14 mer) were transcribed from DNA templates and annealed to form a partially double stranded RNA. It was found that eIF-4A and eIF-(iso)4F could unwind the double stranded RNA. ATP and Mg^{2+} were required for this reaction. The reaction was cap-dependent and required a single stranded region. These studies combined with binding affinity studies suggest that the cap-binding subunit of eIF-(iso)4F forms a complex with mRNA. Subsequently in the presence of ATP, eIF-4A is bound. Hydrolysis of ATP provides energy for the protein complex to process along the mRNA and unwind double stranded regions.

Tu-Pos495

PH-DEPENDENT CONFORMATION OF AN EUCARYOTIC PROTEIN INITIATION FACTOR, EIF-(ISO)4F AND ITS TWO SUBUNITS

((Yahong Wang#, Wu Yun Ren$, Ann van Heerdon&, Karen S. Browning&, Diana Friedland# and Dixie J. Goss#)) #Dept. of Chem., Hunter College of CUNY, NY 10021, $Sloan-Kettering Institute for Cancer Research, NY, NY 10021, &Dept. of Chem. & Biochem., Univ. of Texas at Austin, TX 78712

The structural features of wheat germ protein synthesis initiation factor eIF-(iso)4F, one of the cap binding proteins, are unknown. In this study, circular dichroism (CD) spectra and secondary structure prediction were obtained for eIF-(iso)4F and its two subunits, p28 and p86, as a function of pH. The CD spectra indicate that there were significant conformational changes with pH. Analysis of CD data using the SELCON program yielded estimates of the content of secondary structural elements. The result shows α-helix content changes dramatically with pH. The CD spectra of the two subunits, p28 and p86 were also measured and analyzed. The PEPTIDESTRUCTURE program in the GCG sequence analysis software package was applied to the amino acid sequences of these two subunits. The predicted estimates of α-helix has in good agreement with values derived from the CD spectra analysis. The pH dependence of the conformational change and functional properties suggest binding may involve β-sheet interactions between the protein and RNA. The surface profile implies the cap binding site may reside within amino acid residues 83-103.

Tu-Pos496

FUNCTIONAL PROPERTIES OF WHEAT GERM PROTEIN SYNTHESIS INITIATION FACTOR eIF-(iso)4F, AND THE SEPARATED P28 AND P86 SUBUNITS.

((Ma Sha#, Ann van Heerdon*, Karen S. Browning*, and Dixie J. Goss#)) #Dept. of Chem., Hunter College of CUNY, New York, NY 10021. *Dept. of Chem. & Biochem., Univ. of Texas at Austin, TX 78712.

Initiation of protein synthesis in eucaryotes is a complex process involving at least ten initiation factors. In higher plants, one of the initiation factors, eIF-4F, exists in an isozyme form (eIF-(iso)4F). eIF-(iso)4F contains two subunits, p86 and an m^7G cap-binding protein, p28. In order to study the interaction and role(s) of the subunits of this protein we have analyzed the structural and functional properties of the separate subunits and the native protein. Neither subunit alone functions in polypeptide synthesis. However, when combined the resulting protein has full activity. The binding of p28, p86 and eIF-(iso)4F with m^7GTP and oligonucleotides was measured and compared. From these studies it appears that cap recognition resides in the p28 subunit. However, p86 enhances the interaction with capped oligonucleotides and probably is involved in protein:protein interactions as well.

Tu-Pos497

TRANSLATED AND UNTRANSLATED FORMS OF THE mRNA IN A WHEAT GERM CELL-FREE SYSTEM. ((S.V.Matveev, T.N.Tsalkova*, L.M.Vinokurov, Yu.B.Alakhov)) Branch of the Shemyakin and Ovchinnikov Institute of Bioorganic Chemistry,*Institute of Protein Research, Russian Academy of Sciences, 142292 Pushchino, Moscow Region, Russia.

A sensitive experimental approach is suggested for investigating the fate of mRNA during its translation in a wheat germ cell-free system. The basis of the approach is that the mRNA of apoobelin is used as "test" template.The product of the translation represents a Ca2+-dependent photoprotein, which can be detected up to 2.5E-14 M owing to its high luminescent activity.Different forms of the mRNA in the translation solution were separated by centrifuging on a sucrose gradient. It has been shown that only part of the mRNA (~20%) added to the translation system migrates with 80S ribosomes in the sucrose gradient. Another part did not connect with ribosomes and had the same mobility as pure mRNA.The sucrose gradient was fractionate and the aliquot from each fraction was added to fresh translation system as a source of the template. We used two different translation systems: one containing no exogenic mRNA and another already containing the loading template encoded DHFR at the moment of the addition of sample mRNA. We found that the mRNA of obelin that migrated with 80S ribosomes was translated in both systems ten times more effectively than a control deproteinased mRNA. The mRNA of obelin that did not complex with ribosomes was translated in the first system as a control deproteinased mRNA of obelin. The same mRNA was translated two hundred times less effectively than a control in the second system of translation. We conclude that there are some factors making part of the mRNA unable to be translated.

CHEMOSENSORY TRANSDUCTION AND CHEMOTAXIS

Tu-Pos498

QUANTAL-LIKE CURRENT FLUCTUATIONS INDUCED BY ODORANTS IN OLFACTORY RECEPTOR NEURONS. ((A. Menini*, C. Picco* and S. Firestein+)) *Istituto di Cibernetica e Biofisica, C.N.R., Genova, Italy and +Department of Biological Sciences, Columbia University, NY, NY 10027.

Many sensory systems have evolved signal detection capabilities that are limited only by the physical attributes of the stimulus. Most notable is the detection of single photons by both invertebrate and vertebrate photoreceptors. The olfactory stimulus also has a quantal unit, the single odorant molecule. We have used high gain recordings to measure the current in response to low odorant concentrations in isolated olfactory receptor neurons from the salamander. Under whole-cell voltage-clamp conditions bell shaped fluctuations with amplitudes ranging from 0.3 to 1 pA were measured both in the presence of long steady exposures to low odorant concentrations and after application of short pulses of odorants. These small responses are likely to be triggered by the binding of a single odorant molecule. Occasionally larger fluctuations of 1 to 10 pA amplitude were also observed, presumably originating from multiple binding events. These fluctuations are likely to play an important role in determing the threshold of these cells for odorant detection.

Tu-Pos499

Structural Studies of a Recombinant Odorant Binding Protein

((*G. Bains, #H. Monaco, *L. M. Amzel))
*The Johns Hopkins School of Medicine, Baltimore, MD 21205
#Dept. of Organic Chemistry, University of Padova, Italy

Odorant binding proteins (OBPs) are secreted into the nasal epithelium and bind over 50 different compounds perceived in olfaction with affinities which appear to correlate with sensory perception. The cloning and overexpression of bovine OBP has been accomplished in E. Coli as a fusion protein with the maltose binding protein. Recombinant OBP has been obtained in high quantities from the fusion protein through cleavage at a thrombin-specific site to yield a product which is 99% pure. CD spectroscopy confirms that the protein is primarily β sheet as predicted by its sequence homology to β - lactoglobulin and the retinol binding protein. Additionally, a pH-induced transition between pH 4 and pH 5 is observed with fluorescence spectroscopy which may be attributed to the separation of the physiological dimer into monomers at low pH. Two crystal forms have been obtained of recombinant OBP in solutions of 78% $(NH_4)_2SO_4$ in 50 mM Tris, pH 8.5 (form I), and 45% $(NH_4)_2SO_4$ in 50 mM NaAcetate, pH 3.75 (form II). Reflections are observed out to 2.7 Å when crystal form I is subjected to X-ray diffraction. An analysis of these diffraction data reveals that the recombinant protein in form I is crystallized in the orthorhombic space group $p2_12_12_1$ with unit cell parameters a=67.7 Å, b=43.5 Å, c=121.5 Å. These results are comparable to data previously obtained from crystals (form I) of nonrecombinant OBP. (Supported by GM#44692).

Tu-Pos500

EVIDENCE FOR THE PARTICIPATION OF A Ca^{2+}-ACTIVATED K^+-CHANNEL IN THE INHIBITORY RESPONSE INDUCED BY ODORANTS IN OLFACTORY NEURONS. ((B. Morales, G. Ugarte, R. Madrid, P. Labarca and J. Bacigalupo)). Dpto. de Biología, Fac. de Ciencias, Universidad de Chile y Centro de Estudios Científicos de Santiago.

Olfactory neurons respond with an increase in action potential firing upon stimulation with odorants that activate the cAMP-cascade in olfactory cilia. Recently, we reported that these neurons respond with a decrement in action potential firing when stimulated with an odorant mixture (M-I) that do not activate the cAMP-cascade (Morales et al., Proc. R. Soc. Lond, In Press). This inhibition is due to membrane hyperpolarization, caused by the activation of a K^+-outward current. In this work we show evidence for the participation of a Ca^{2+}-activated K^+ channel in the inhibitory response induced by odorants in isolated olfactory neurons from the toad *Caudiverbera caudiverbera*.

Electrical recording were obtained using a patch-clamp in the whole-cell mode. The odorant mixture was applied with a miltibarreled pipette (2 μm each) connected to a picospritzer. The I-V relation of the current induced by M-I develops at ~-50 mV, presents a maximum near +30 mV, decaying at higher voltages. This shape of the I-V curve suggests a Ca^{2+}-activated K^+-conductance. The outward current induced by M-I was reversibly abolished by 10 nM charibdotoxin (CTX; n=5), which blocks maxi Ca^{2+}-activated K^+-channels. On the other hand, CTX did not effect the voltage activated K^+-currents. Under current-clamp, the hyperpolarization induced by M-I was blocked by 10 nM CTX. Focal application of the chemical stimulus was most effective when directed to the olfactory cilia, having a much weaker effect when applied onto the cell body, indicating that transduction to M-I odorants takes place in the olfactory cilia. This results are consistent with the participation of a ciliary Ca^{2+}-activated K^+ conductance in the inhibitory response to odorants.

FONDECYT 1930859 and 2930018.

Tu-Pos501

Possible participation of a cAMP regulated K^+ channel detected in planar bilayers in the speract-induced repolarization of sea urchin spermatozoa. ((Labarca, P., Santi, C., Morales, E., Zapata, O., Beltrán, C., Liévano, A., and Darszon, A)).* *Centro de Estudios Científicos de Santiago y Universidad de Chile, Chile Departamento de Genética y Fisiología Molecular, Instituto de Biotecnología-UNAM, Cuernavaca Mor. México.*

In sea urchin spermatozoa K^+ and Ca^{2+} channels are involved in quimotaxis and in the acrosome reaction. During both events cyclic nucleotides, which are known to modulate ion channels, increase several fold. Here, we describe a cAMP regulated K^+-selective channel from sea urchin flagellar sperm plasma membranes fused into planar bilayers. Its single channel conductance in 100 mM KCl is 103 pS. In biionic experiments, the channel displayed a K^+/Na^+ permeability ratio (P_{K^+}/P_{Na^+}) of ~5. Thus, in sea water its reversal potential would be -13 mV and channel opening would depolarize sperm. The channel has low open probability (Po=0.8 % at 0 mV applied voltage) and weak voltage dependence. Channel activity is reversibly up-regulated by *cis* cAMP, but not by cGMP. This modulation is dose dependent (Kd of 200 μM); at this concentration the channel open probability at 0 mV increases ~11 fold. TEA^+ blocks the channel only from *trans*. Ba^{2+} in *trans* also blocks the channel in a voltage dependent manner. We explored if this channel could participate in the depolarization induced by speract in sea urchin spermatozoa. This decapeptide isolated from *S. purpuratus* egg-jelly, influences sperm motility, elevates [cGMP], [cAMP], intracellular Ca^{2+}, induces an alkalinization, and a hyperpolarization followed by a depolarization. Here we show that in spermatozoa, the speract induced depolarization depends on external $[Na^+]$ independently of intracellular pH, is stimulated by papaverin, a phosphodiestresase inhibitor, and blocked by TEA^+ and Ba^{2+}. These results would be consistent with the participation of the cAMP-regulated K^+ channel identified in bilayers in the . speract induced depolarization in sea urchin spermatozoa.

This work was supported by grants from Howard Hughes Medical Institute, DGAPA and CONACyT.

Tu-Pos502

DOPAMINE INCREASES INTERNAL CA^{+2} IN SQUID OLFACTORY RECEPTOR NEURONS. ((M. Lucero, D. Piper. and *W. Gilly)) Univ. of Utah, Salt Lake City, UT 84108, *H. M. S., Stanford Univ., Pacific Grove, CA 93950.

Squid olfactory receptor neurons (ORNs) respond to dopamine (an aversive odorant) with a hyperpolarization that inhibits the firing of action potentials [1]. This hyperpolarization can be mimicked by including IP_3 in the patch pipette [2]. In catfish ORNs, IP_3 increases $[Ca^{+2}]_i$ via an IP_3 receptor located in the ciliary membrane [3]. We wanted to test whether the dopamine hyperpolarization in squid ORNs involved changes in $[Ca^{+2}]_i$, and if so, whether Ca^{+2} increases were the result of influx through the ciliary membrane, release from intracellular stores, or both. Using the Ca^{+2} indicator dye fura-2-am we find that dopamine dramatically and reversibly increases $[Ca^{+2}]_i$ in squid ORNs. The rise in $[Ca^{+2}]_i$ is faster and larger in the ciliary region suggesting that dopamine's initial site of transduction is at the cilia. Three lines of evidence indicate that unlike vertebrate ORNs, Ca^{+2} is released from internal stores in squid ORNs: 1) Shortly after changing to a zero Ca^{+2} + 10 mM EGTA bath (<90s), dopamine increases internal Ca^{+2}; 2) Responses to dopamine in zero external Ca^{+2} are approximately the same size as in normal (10 mM) external Ca^{+2}; 3) Dopamine induced increases in $[Ca^{+2}]_i$ are blocked when internal Ca^{+2} stores are depleted by extended incubation in zero Ca^{+2} + 10 mM EGTA bath, however responses return when stores are replenished.

1. Lucero, M. T., Horrigan, F. T. & Gilly, W. F. *J. Exp. Biol.* **162**, 231-249 (1992).
2. Lucero, M. T. & Piper, D. R. *Chem. Senses* **19(5)**, 593 (1994).
3. Kalinoski, D. L., Aldinger, S. B., et al. *Biochem. J.* **281**, 449-456 (1992).

Tu-Pos503

PHYSICAL ASPECTS OF CELL MIGRATION ((H. Gruler)) Chaire scientifique Roger Seydoux de la Fondation de France, Centre d'Écologie Cellulaire, Hôpital de la Salpétrière, F 75651 Paris Cedex 13, France. Permanent address: Abteilung Biophysik, Universität Ulm, D 89081 Ulm, Germany

The amoeboid movement of cells like granulocytes, fibroblasts, neural crest cells, etc., can be characterized by two independent variables: v and φ. A steerer (=controller without feedback) is responsible for the speed: The force to move is produced by a speed-dependent, cellular linear motor supplied by the amplified (=linear chemical amplifier) primary cellular signal (=the receptor occupancy, monopole of the spatial receptor distribution). An automatic controller (= controller with feedback) is responsible for the angle of migration: The torque to rotate is induced by a deterministic cellular signal (=dipole of the spatial distribution of the occupied receptors) and a stochastic cellular signal. The distribution function of the angle of migration is in analogy to the Boltzmann statistics. Migrating cells and condensated state: Two conditions are necessary to build up a condensated state: (i) interaction between cells and (ii) motion. Attractive cell-cell interaction (granulocytes) is switched on at low calcium concentrations (<nM). The migrating cells form a liquid crystal phase. Disturbed cell migration: Viruses like ECHO 9 can disturb the deterministic cellular signal of the automatic controller. The cells become blind and loose their ability to detect an extracellular polar guiding field.

Tu-Pos504

CAUSES AND CONSEQUENCES OF THE $[Ca^{2+}]_i$ GRADIENT IN LEUKOCYTES REVEALED BY NP-EGTA. ((S.H. Gilbert*, G.C.R. Ellis-Davies†, J.H. Kaplan† & F.S. Fay*)) *Biomed. Im. Group, UMMC, Worcester MA 01605 and †Dept. of Biochem. & Mol. Biol., Oregon Health Sciences Univ., Portland OR 97209.

In migrating leukocytes, $[Ca^{2+}]_i$ is higher in the rear than in the front. This pattern could result from regional differences in the density of Ca^{2+} stores, low-mobility Ca^{2+} buffers and sites of Ca^{2+} extrusion. Ca^{2+} changes after full-field photolysis of caged $InsP_3$ show that Ca^{2+} stores are clustered in the rear. To determine whether buffers and Ca^{2+} pumps are concentrated in the front, we monitored changes in $[Ca^{2+}]_i$ in response to uniform photolysis of NP-EGTA (nitrophenyl-EGTA, injected into newt eosinophils at 0.5-1 mM with 70 kDa calcium-green-dextran at 12.5 μM). $[Ca^{2+}]_i$ increased within 10 msec to twice the levels that occur in active cells (0.2-0.5 μM), and the rate of decline was spatially uniform. Responses to local photolysis (5-μm spot) in different regions had similar magnitudes and kinetics. $[Ca^{2+}]$ also declined without spreading. Changes in morphology and locomotion after localized photolysis varied with location. Increased $[Ca^{2+}]$ near lamellipods caused withdrawal, in the uropod region increased speed, and near the MTOC caused changes in direction or loss of directional persistence. We conclude that the Ca^{2+} gradient results principally from the distribution of Ca^{2+} stores and that Ca^{2+} acts as a local messenger. Furthermore, the spatial pattern of Ca^{2+} is critical to its role as an intracellular messenger.

Tu-Pos505

LEUKOCYTE STIFFENING: ANALYSIS OF LIGAND-INDUCED CYTOSKELETAL MODIFICATIONS. ((Ralph Nossal)), Physical Sciences Laboratory, DCRT, National Institutes of Health, Bethesda, MD 20892.

Leukocytes become resistant to mechanical deformation when immersed in a medium containing various amounts of chemoattractants and certain other cytokines [1,2]. Data obtained when neutrophils are reacted with the chemotactic peptide N-formyl-methionyl-leucyl-phenylalanine (FMLP) provide measures of the development of rigidity in such activated cells [1,2]. We present a physico-chemical theory of polymer network formation that has been developed to enable one to understand how ligand binding at a cell surface influences the cytoskeletal transformations that give rise to cell rigidity. This theory is used to examine the experimental relationship between cellular actin polymerization and cell rigidification, and we thereby quantitatively affirm that cell stiffening derives from changes in the amount of matrix-incorporated actin. We also use the theory to distinguish between different steps of the transduction process and to obtain insight into underlying molecular processes.

[1] Worthen, G. S., *et al.*, 1989, *Science*, **245**:183-186.
[2] Pecsvarady, Z. *et al.*, 1992. *Blood Cells*, **18**:333-352.

Tu-Pos506

A NOVEL INTERMOLECULAR ZINC BINDING SITE MODULATES INTERACTIONS BETWEEN A REGULATORY PROTEIN AND ONE OF ITS COGNATE TARGET PROTEINS. ((D.W. Pettigrew[1], M.J. Feese[2], S.J. Remington[2], N.D. Meadow[3], and S. Roseman[3])) [1]Dept. of Biochem. & Biophys., Texas A&M Univ., College Station, TX 77843, [2]Institute of Molecular Biology, Univ. of Oregon, Eugene, OR 97403, [3]Dept. of Biology, The Johns Hopkins Univ., Baltimore, MD 21218. (Spon. by T. Baldwin)

E. coli glycerol kinase is an element in a signal transduction pathway that modulates gene expression in response to carbon source availability. Its activity in this pathway is controlled by IIIglc, a regulatory protein of the phosphotransferase system. Recent X-ray crystallographic determinations of the structure of the complex of these two proteins identified a novel intermolecular Zn(II) binding site that is formed upon their association. Enzyme kinetics studies show that Zn(II) binding enhances the free energy of complex formation about 2 kcal/mol, decreasing the apparent dissociation constant from 10μM to 0.3μM at pH 7, 25°C. The affinity of the site is much higher for Zn(II) than for Co(II) or Cd(II). Replacement of the Zn(II) ligands contributed by IIIglc has different effects on the complex; H75Q abolishes only Zn(II) binding while H90Q completely abolishes complex formation. Replacement of the Zn(II) ligand contributed by glycerol kinase, E478Q, abolishes Zn(II) binding while other mutations, E478D, E478H, E478C, have little effect on Zn(II) binding. (Supported by grants from NIH: GM49992 (DWP), GM42618 (SJR), GM38759 (SR)).

Tu-Pos507

SIMULATION OF THE EFFECT OF KINEMATICS ON THE DETACHMENT OF MACROMOLECULARLY-BOUND PARTICLES FROM SURFACES. ((Kai-Chien Chang and Daniel A. Hammer)), School of Chemical Engineering, Cornell University, Ithaca, NY 14853.

In adhesion experiments, cells are allowed to attach to ligand-coated substrata, and forces, such as centrifugation or shear forces, are used to remove cells. The magnitude of the force at which the cell relents is quoted as the strength of adhesion. However, different strengths of adhesion may be reported for the same cells, owing to the kinematics (character or direction) of the force applied in different adhesion assays. We demonstrate this principle by simulating the detachment of receptor-coated hard spheres from ligand-coated surfaces using normal, tangential and shear forces after the particles are allowed to bind to steady state. Depending on the properties and distribution of the molecules, tangential forces can be up to 50 times or more disruptive than normal forces in removing cells from surfaces. The increased sensitivity to tangential forces is because only the bonds at the back edge of contact see the applied load, and because the particle may "detach" even if there is continued receptor-ligand binding. Hydrodynamic shear, with its associated torque, is only slightly more disruptive than forces applied tangentially. There is a critical angle, close to normal to the surface, at which a force becomes ten times more effective than a normal force at detaching a cell. The ratio of normal and tangential forces required for detachment decreases as the reactive compliance of the bonds decreases, suggesting that experiments comparing the normal and tangential forces to detach a particle can be used to infer the mechanical properties of the adhesion molecules themselves. The result of our simulations provide a rational means for comparing the results between different adhesion assays. (Supported by NIH HL18208).

Tu-Pos508

A MECHANICAL ANALYSIS OF CELL-CELL ADHESION FOR THE MICROPIPETTE EXPERIMENT. ((C. Zhu, T.E. Williams and D. Xia)) School of Mechanical Engineering, Georgia Institute of Technology, Atlanta, GA 30332-0405.

The physics of cell adhesion can be separately analyzed at two different length scales. Such separate treatment is possible because spatial variations of key physical quantities occur very rapidly within a thin zone at the edge of the adhesion area but relatively slowly outside. Therefore, the structure of the governing equations resembles that of the boundary layer problem. At the scale of the cell body, the analysis is based on the continuum mechanics of the bulk cellular deformation; while at the scale of the thickness of the boundary layer at the contact edge, the analysis is based on the molecular dynamics of the adhesive receptors. We present a detailed mechanical analysis of cellular deformations due to cell-cell adhesion and due to separation by externally applied forces. The models were applied to the analysis of the dual micropipette experiment in which individual pairs of cells were manipulated by two micropipettes through aspiration to adhere to one another and to be detached from one another after conjugation had been formed. The objective was to evaluate the histories of adhesion force and energy during the entire processes of conjugation and detachment. The cell itself was used as a mechanical transducer to measure the adhesion force and energy from the observed cellular deformation under the controlled applied loading. A scheme was developed to simultaneously evaluate the adhesive properties and the mechanical properties (transducer parameters) based on the cortical shell-liquid core model for the cell. The goal was to determine the minimal mechanical property model for the cell required for accurate prediction of the adhesive properties. Quasi-static equilibrium was assumed to obtain a zeroth-order model, which yielded a simple analytical expression for the cell shape that compared extremely well with the experimentally measured cell outline. Cytoplasmic flow was accounted for in the first-order model, which yielded reasonable estimates of the apparent cortical tension and cytoplasmic viscosity. Both the apparent cortical tension and cytoplasmic viscosity were found to be insensitive to the cell elongation but strongly dependent of the aspiration pressure applied by the pipette. By contrast, the adhesion force resultant and the surface adhesion energy density were insensitive to the aspiration pressure and were strongly dependent of the cell elongation. These results provide the "outer solution" to be matched by the "inner solution" from the boundary layer analysis of the behavior of the cell adhesion molecules.

Tu-Pos509

SELECTIVE DYE AND IONIC PERMEABILITY OF CHICK AND RAT CONNEXIN43 GAP JUNCTION CHANNELS. ((Hong-Zhan Wang, Sridhar R. Goli, and Richard D. Veenstra)) Dept. of Pharmacology, SUNY Health Science Center at Syracuse, Syracuse, NY 13210.

Ion substitution and fluorescein-derivative dye transfer experiments have been performed on chick or rat connexin 43 (cCx43 or rCx43) gap junction channels to determine the relative anion/cation permeability ratio and dye permeability of these connexin-specific channels. Two major unitary channel conductances (γ_j) of 56 pS and 166 pS were observed in 120 mM Kglutamate internal pipette solution#2 (IPS#2). In 120 mM KCl (IPS#3), the cCx43 channel has three γ_j states(56, 120 and 200 pS). rCx43 exhibited multiple γ_j states of 30, 57, and 80 pS in IPS#2 and 80 and 108 pS in IPS#3. The increases in γ_j of the cCx43 166 pS state and the rCx43 56 pS state were 23% and 40%, respectively. These conductance increases correspond to respective anion/cation permeability ratios of 0.50 and 1.15. The cCx43 single channel open probability (P_O) was symmetrically distributed about 0 mV and quantitatively described by a two-state Boltzmann distribution with a $V_0 = \pm$ 33 mV. cCx43 gap junction channels are permeable to 2 mM 2',7'-dichloro-fluorescein (diCl-F) and 6-carboxyfluorescein (6-CF) dye, but the minimum junctional conductance for dye transfer was 20 times higher for 6-CF than diCl-F (0.2 nS for diCl-F and 4 nS for 6-CF). rCx43 was 100% permeable to both dyes. These observations support the hypothesis that there is a fixed negative charge associated with the cCx43 channel which dramatically reduces pore permeability to anions which is absent in the rCx43 channel. The presence of three distinct unitary channel conductances confers multiple open state configurations of the cCx43 channel. Supported by grants HL-45466, HL-42220.

Tu-Pos510

REMODELING OF Cx43 IN PRIMARY CULTURES OF VASCULAR SMOOTH MUSCLE CELLS.
((X-D. Huang and M. L. Pressler)) Krannert Institute of Cardiology, Indiana University & Roudebush VAMC, Indianapolis, IN

We have previously reported changes in localization and expression of the gap junctional protein connexin43 (Cx43) during the cell cycle of cultured bovine aortic smooth muscle (BASM) cells. We now describe that activation of protein kinase C (PK-C) may modulate Cx43 trafficking in proliferating BASM cells. Quantity and distribution of Cx43 were analyzed using a confocal microscope. BASM cells ($\leq$ 7 passages) were examined 72 hrs after plating $\pm$ stimulation by 1 μM phorbol dibutyrate (PDB $\times$ 0, 1, 2, 24 hrs). Transient (1-2 hrs) exposure to PDB resulted in marked (87%) reduction of immunoreactive Cx43 in proliferating cells ($n=9$; $P<0.01$). Studies of Lucifer Yellow dye transfer showed coincident changes in intercellular communication: dye coupling was reduced from 85% (control) to 18% (PDB $\times$ 2 hrs; $P<0.02$). Western blots showed a similar reduction in Cx43 (to 40% of control) after 2 hrs PDB. After prolonged (24 hr) PDB exposure, immunoreactive Cx43 and coupling returned to control values. Biochemical assays showed that >90% of PK-C activity was depleted after 24-hr exposure to 1 μM PDB. The results suggest that activation of PK-C reduces intercellular communication in BASM cells by downregulation of Cx43. Studies are in progress to determine if the localization of PK-C is altered during the above noted changes in Cx43.

Tu-Pos511

POTENTIAL ROLE OF CALCINEURIN IN GAP JUNCTION CHANNEL GATING ((C. Peracchia, X.G. Wang, A. Lazrak and L.L.Peracchia)) Department of Physiology, University of Rochester, Rochester, NY.

Evidence for channel gating sensitivity to physiological $[Ca^{2+}]_i$ in crayfish axons (Peracchia, J. Membr. Biol. 113, 75, 1990) and in Novikoff hepatoma cells (Lazrak and Peracchia, Biophys. J. 65, 2002, 1993; Lazrak et al., Biophys. J. 67, 1052, 1994), and data for the ability of calmodulin (CaM) inhibitors to prevent uncoupling, suggested that channel gating may involve a CaM-dependent mechanism (Peracchia and Girsch, Am. J. Physiol. 248, H765, 1985). This was confirmed in *Xenopus* oocyte pairs injected with oligonucleotides antisense to CaM mRNA to knock-out CaM gene expression, a method shown to completely degrade CaM mRNA in oocytes in ~5 hr (Dash et al., P.N.A.S. 84, 7896, 1987). With 3 min exposure to 100% CO_2, junctional conductance (G_j), measured by double voltage clamp, decreased by ~94% (n=12) in controls, by ~35% (n=19) 24 h post-injection, by ~18% (n=11) 48 h post-injection, and by ~2% (n=9) 72 h post-injection. CaM injection into oocytes previously injected (72 h earlier) with oligonucleotides antisense to CaM caused 35% recovery of uncoupling efficiency. CaM could act directly on gap junction proteins (connexins) or via activation of kinases or phosphatases. To test the possible participation of calcineurin, a Ca-CaM dependent phosphatase 2B, *Xenopus* oocytes expressing the native connexin (Cx38) were injected with calcineurin (intracellular conc. =~300 nM). With 3 min superfusion of solutions bubbled with 100% CO_2, calcineurin injected oocytes uncoupled much faster than controls, the max. rate of decrease in G_j being 11%/min (n=12) in controls and 34.5%/min (n=3) in calcineurin-injected oocytes. Calcineurin inhibitor, genetic knock-out and overexpression protocols are being tested. An involvement of calcineurin could point to an uncoupling mechanism based on Ca-CaM mediated dephosphorylation of connexins, likely to be reversed by cAMP-dependent rephosphorylation. Supported by NIH GM20113.

Tu-Pos512

MECHANISM OF THE AUGMENTATION OF ERYTHROCYTE AGGLUTINATION IN AN ULTRASOUND FIELD ((E. Pohl, P. Pohl, E. Rosenfeld, R. Millner)) Dept. of Medical Physics and Biophysics, Martin-Luther-University, 06097 Halle, Germany

Recent investigations have shown that human erythrocytes of different blood groups were induced to form more agglutinates and aggregates at a sound pressure of 70-240 kPa *in vitro* than the control erythrocytes. Heating and acoustic cavitation are not responsible for this effect. The dependence of the phenomenon on sound pressure, sound frequency and geometry of the sound beam lead to the conclusion that acoustical macro-streaming (quarzwind) is the underlying mechanism. The streaming of another origin (magnet stirring or pump) produced similar results under definite conditions. The ultrasound effect can be explained both with the reduction of the surface charge due to alterations of the ion concentration within the unstirred layer near the erythrocytes and with an increasing frequency of cell collisions. In the light of the fact that the aggregation and agglutination behaviour of the erythrocytes has to be regarded as an integral parameter of cell surface properties the acoustical macrostreaming becomes significant for therapeutical and pharmacological applications of ultrasound.

Tu-Pos513

SUBSTATE PERMEABILITY OF CONNEXIN37 (Cx37) GAP JUNCTION CHANNELS STABLY EXPRESSED IN N_2A CELLS. ((M.W. Waltzman and D.C. Spray)) Dept. of Neuroscience, Albert Einstein College of Medicine, Bronx, New York 10461.

All gap junction channels are sensitive to transjunctional voltage (V_j) such that increasing V_j decreases junctional conductance, g_j. However, for almost all gap junctions, this voltage dependent uncoupling is incomplete; even at high V_j, residual g_j remains (g_{min}). We have previously found that for junctional channels formed by Cx37 or by other connexins, g_{min} is due to a channel substate with greatly reduced unitary conductance. We addressed the issue of whether permeability of this substate differs markedly from that of the fully open state by substituting cations or anions in internal solutions and quantitating both single channel conductance and macroscopic g_j. Surprisingly, substitution of KCl or CsCl with TMACl or TEACl revealed little or no anion permeability of this gap junction channel. Both main state and substate conductances were profoundly reduced by these substitutions, but the ratio of g_{min}/g_{max} was not radically changed. We conclude that fully open and substate permeabilities for Cx37 gap junction channels are similar. Furthermore, the g_{min}/g_{max} ratio usefully reports these relative permeabilities, because the mainstate predominates at low V_j and the substate at higher potentials.

Tu-Pos514

ASYMMETRICAL CALCIUM CURRENTS OF VENTRICULAR CELL PAIRS DURING ACTION POTENTIAL CONDUCTION. ((Rajiv Kumar and Ronald W. Joyner)) Department of Pediatrics, Emory University, Atlanta, GA, 30322

We studied the L-type Ca^{2+} current that occurs during action potential (AP) conduction between a pair of guinea pig ventricular cells. We recorded APs, in normal Tyrode's solution at physiological temperature, from the leading cell (stimulated cell, cell 1) and the follower cell (non-stimulated cell, cell 2) with a coupling resistance between the cells supplied by a coupling clamp circuit (Tan and Joyner, Circ. Res. 67:1071-81;1990). We then applied these recorded APs as command potential waveforms for cells studied in the voltage clamp mode in which we used internal and external solutions which isolated the L-type Ca^{2+} current. The AP waveform of the leading cell had a rapid upstroke and then a partial repolarization during the conduction delay before activation of the follower cell. The Ca^{2+} current occurred with a large magnitude during the conduction delay for the leading cell but not for the following cell. This leads to an asymmetry of Ca^{2+} current for the two cells, with greater peak Ca^{2+} current (8.88 $\pm$ 0.96 pA/pF) for the leading cell than for the following cell (5.93 $\pm$ 0.77 pA/pF). When we reversed the direction of conduction for cell 1 and cell 2 by stimulating cell 2, we found that application of these recorded waveforms for the APs for cell 1 and cell 2 to the voltage clamped cells also reversed the asymmetry of the magnitude of the Ca^{2+} current. We conclude that discontinuous conduction in cardiac tissue is associated with a directionally determined asymmetry in the magnitude of the Ca^{2+} current, with the leading cell experiencing a greater peak Ca^{2+} current than the follower cell, which may be significant in determining the success or failure of conduction and may also represent an increased Ca^{2+} load for cells experiencing discontinuous conduction.

Tu-Pos515

EFFECTS OF CELL SIZE ON ACTION POTENTIAL CONDUCTION FOR A CARDIAC CELL PAIR. ((R.W. Joyner, R. Kumar, R. Wilders, E.E. Verheijck, H.J. Jongsma and W.N. Goolsby)). Dept. of Pediatrics, Emory Univ., Atlanta, GA and Dept. of Medical Physiology and Sports Medicine, Utrecht University, Utrecht, The Netherlands.

Action potential (AP) conduction in ischemic regions of the heart becomes discontinuous with conduction between specific groups of cells which are partly uncoupled from each other. We used a mathematical model of the guinea pig ventricular cell ("LR Cell", Luo and Rudy, *Circ. Res.* 74:1071-96;1994) electrically coupled to a real isolated guinea pig ventricular cell to investigate the effects of the relative size of the leader cell (stimulated directly) to that of the follower cell (not stimulated directly) regarding the critical value of intercellular conductance (g_j) for AP conduction and the maximum conduction delay. By scaling the coupling current, we effectively increased or decreased the size of either the LR cell or the real cell. On normalizing the real cell size to that of the LR cell, the g_j for propagation was greater for conduction from real cell to LR cell (7.02 $\pm$ 0.17 nS, n=8) (mean $\pm$ SEM) and from LR cell to real cell (8.27 $\pm$ 0.55 nS, n=8) than between two LR cells (5.4 nS). Partial repolarization of the AP of the leader cell during conduction was significantly greater for real cells than for LR cells even when real cell size was normalized to be equal to LR cell size. On doubling the follower cell size, the g_j for conduction was dramatically increased, and this increase was greatest for conduction from real cells to LR cells, less for LR cells to real cells, and least between two LR cells. Similar results occurred when the leader cell size was halved. For all three conduction conditions (LR cell to LR cell, real cell to LR cell, LR cell to real cell) g_j for conduction was greater for changes in the follower size compared to changes in the leader size, and maximal conduction delay was increased or decreased with the respective changes in the ratio of leader to follower size. Anatomical features of the surviving cell groups in the ischemic zone may play a decisive role in discontinuous conduction and conduction delays.

INTRACELLULAR SIGNALLING

Tu-Pos516

CHOLINERGIC AGONISTS MODULATE CALCIUM MOBILIZATION IN HUMAN T LYMPHOCYTES. ((A. Rivera, D. Bloom and A. Lorenzo)) Universidad Interamericana, San Juan, PR 00919-1293. (Spon. by V. Eterović)

Lymphocyte activation is dependent on calcium and potassium fluxes, and lymphocytes are exposed to a variety of neural transmitters and hormones which appear to modulate the immune response. A possible mechanism by which neural substances modulate lymphocyte function is by acting on membrane channels and ionic currents. To explore this idea, we have first studied the effects of some transmitters and hormones on calcium mobilization. We used a human lymphoblastoid cell line (CEM, ATCC CCL 119), incubated in RPMI 1640 at 37°C in 5% CO_2. Intracellular calcium was estimated using the fluorescent Ca indicator dye fura-2. Cells were loaded with 1 μM fura-2 AM for 25 min at 37°C in the dark, washed and resuspended in RPMI. Fluorescence measurements were made with cells in suspension (10^6 cells/ml) using a Perkin Elmer spectrofluorimeter. Our results indicate a baseline calcium level of 105 ± 12 nM (n = 11). Addition of acetylcholine (0.01 mM) caused a fast, variable increase in [Ca]i, from 50 to 300% of the baseline value (n = 9). This effect was reduced after addition of TEA (10 mM), which could mean modulatory effects of acetylcholine on T cell potassium channels. Nicotine (0.01 mM) and muscarine (0.01 mM) were also tested, and produced small increments in [Ca]i. Among other compounds tested, db-cAMP (100 μM) and progesterone (100 μM) had no effect on basal calcium levels (n = 4), however, preliminary results suggest progesterone modifies the acetylcholine-induced increase in [Ca]i. These results suggest that neurotransmitters and hormones may modulate immune function by acting on levels of intracellular calcium in T cells.
Supported by NIH grant GM08159.

Tu-Pos517

CALMODULIN BINDING PEPTIDES AS INHIBITORS OF CALMODULIN ACTIVATION OF SMOOTH MUSCLE MYOSIN LIGHT CHAIN KINASE. ((K. Török and D.R. Trentham)) UCL, Gower Street, London, WC2E 6BT, UK and National Institute for Medical Research, Mill Hill, London, NW7 1AA, UK (Supported by NIH Grant HLB 15833 to PMI and MRC, UK).

The dissociation constant K_d of the 17-residue peptide, Ac-R-R-K-W-Q-K-T-G-H-A-V-R-A-I-G-R-L-$CONH_2$ (Trp peptide) to calmodulin from pig brain has been estimated to be 6 (± 2 s.d.) pM in 100 μM $CaCl_2$ at ionic strength 0.15 M, pH 7.0 and 21°C [Török and Trentham (1994) Biochemistry **33**, in press]. This value is two orders of magnitude less than the K_d estimate of a related peptide, RS 20, to calmodulin [Lukas et al (1986) Biochemistry **25**, 1458-1464], and so has been checked in an independent assay. Trp peptide inhibited the calmodulin activation of smooth muscle myosin light chain kinase - catalyzed regulatory light chain (MLC) phosphorylation. The rate of production of one of the reaction products, ADP, was measured in a coupled enzymic assay by continuous fluorimetric monitoring of NADH removal. The solution was similar to that used above plus MLC and other components of the enzyme assay. The K_m value of calmodulin was 3.5 nM and the inhibition constant K_i of Trp peptide was 8.6 (± 1.4 s.d.) pM confirming the original K_d measurement. The K_d and K_i values of a peptide related to that of Lukas et al (1986) were one to two orders of magnitude greater. This peptide, kindly provided by Dr. M. Ikebe, had the sequence: A-R-R-K-W-Q-K-T-G-H-A-V-R-A-I-G-R-L-S-S. Trp peptide is effective in arresting presumed calmodulin activated processes in the cell division cycle of sea urchin embryo. [Török et al (1995) Biophys. J. Abstracts (this meeting)].

Tu-Pos518

CALMODULIN LOCALISATION AND ACTIVATION IN THE CELL DIVISION CYCLE OF SEA URCHIN EMBRYO. ((K. Török. M. Wilding, R. Patel and M.J. Whitaker)) *UCL, Gower St WC2E 6BT, UK (Supported by Wellcome Trust Grant 042284/PMG/VW)*

We used TA-calmodulin[1], DTAF-calmodulin (calmodulin labelled with 5-(4,6-dichlorotriazinyl)aminofluorescein) and the calmodulin binding Trp peptide[1] to investigate the role of calcium and calmodulin in the control of cell cycle transitions. The fluorescence intensity of TA-calmodulin rises 10-fold on calcium and target protein binding[1], whereas the fluorescence of DTAF-calmodulin is relatively insensitive. DTAF-calmodulin provides information on localisation. Ratio changes of TA-calmodulin and DTAF-calmodulin fluorescence show calmodulin activation. DTAF-calmodulin and TA-calmodulin were microinjected into sea urchin eggs and their fluorescence was observed during mitosis by confocal microscopy. DTAF-calmodulin localised to the nucleus and the mitotic apparatus during cell cycle. Calmodulin activation transients were detected in association with nuclear envelope breakdown (NEB), anaphase and cleavage. TA-calmodulin activation lagged the fertilisation calcium wave by 10 s at 16°C. Trp peptide injected prior to fertilisation blocked NEB and when injected post-NEB, impaired the metaphase-anaphase transition. Our observations suggest that calcium-calmodulin dependent processes are required for mitotic transitions.

Reference 1: Török & Trentham (1994) *Biochemistry* 33 IN PRESS.

Tu-Pos519

SEQUESTRATION OF PHOSPHORUS AND CATIONS IN YEAST CELL GRANULES AS REVEALED *IN SITU* BY ELECTRON MICROPROBE ANALYSIS

((Radek Pelc*, Zdeněk Žižka* & Branislav Uhrík**)) *Inst. Microbiol., Czech Acad. Sci., Vídeňská 1083, 14220 Praha 4, Czech Republic; **Inst. Molec. Physiol. & Genet., Slovak Acad. Sci., Vlárska 5, 83334 Bratislava, Slovakia.

Various cations, namely Mg^{2+}, K^+, Ca^{2+} and Zn^{2+}, are often found sequestered together with phosphorus in cytosolic electron-dense granules of numerous plant and animal cells (ion binding). These granules are believed to serve as intracellular stores/buffers for cations. In yeasts, they also sequester polyphosphates [1]. Our aim was to find out which ions are concentrated in these phosphorus-rich granules and determine whether granules are confined only to cytoplasm, in *Candida boidinii*, a biotechnologically important yeast species. We employed an energy-dispersive X-ray spectrometer under electron microscope control and analysed individual granules directly *in situ* on ultrathin frozen-dried cryosections of cells. In granules of *C. boidinii*, we detected higher concentrations of P, Na, Mg, K and Zn than either in vacuoles or cytoplasm while only P, Mg and Ca were reported to be sequestered in granules of *Saccharomyces cerevisiae* [1]. We found granules not only in cytoplasm but in vacuoles as well. This raises the possibility of communication between vacuolar and granular polyphosphates which have so far only been observed separately in vacuoles [2] and cytosolic granules of vacuoles-free cells [1].

[1] Roomans G. (1980) *Physiol. Plant.* **48**: 47-50
[2] Urech K. *et al.* (1978) *Arch. Microbiol.* **116**: 275-278

Tu-Pos520

THE EXCLUSION-VOLUME EFFECT OF POLYMERS ON GTP-DEPENDENT FUSION OF ENDOPLASMIC RETICULUM MEMBRANES ((A.V.Sokoloff and S.P.Radko)) NICHD, NIH, Bethesda, MD 20892

Post-mitotic restoration and the maintainance of spatial organization of the endoplasmic reticulum (ER) in the cell involves fusion of ER membranes locally concentrated through their interaction with cytoskeleton elements. It is known that GTP-dependent fusion of ER membranes in vitro is markedly promoted by aggregation of membranes induced by the inclusion of high-molecular weight polyethyleneglycol (PEG) in the incubation mixture. This raises the interesting possibility that the aggregation substitutes, to a certain extent, for the juxtaposition of fusing membranes in vivo provided that PEG does not promote fusion due to direct interactions with the membranes. Here we show that promotion of fusion is non-specific in regard to the nature of polymer. Thus, fusion is highly stimulated by dextrans, branched linear polymers unrelated to PEG. Membrane aggregation and fusion increase with an increase in the molecular weight of polymers. Both aggregation and fusion of membranes show low sensitivity to the concentration of membranes and composition of the medium. These results strongly suggest that polymers promote membrane fusion by thermodynamically favorable formation of a membrane "phase" caused by the competition of membranes and polymers for the occupied volume, without direct interactions between polymers and membranes. Thus, polymer-promoted fusion of ER membranes appears to be a simple model for "template"-driven fusion of cytoskeleton-associated ER membranes in vivo.

Tu-Pos521

EFFECT OF DIFFERENTIATION ON CALCIUM SIGNALLING AND ION CHANNEL ACTIVITY IN U937 CELLS TRIGGERED BY ANTIBODY CROSS-LINKING OF HUMAN HIGH AFFINITY IgG RECEPTOR, FcγRI.((R.A.Floto, B.Somasundaram, J.M.Allen & M.P.Mahaut-Smith)) Physiological Laboratory, Cambridge,U.K.CB2 3EG. (Spon. by T.Tiffert)

FcγRI, the high affinity receptor for IgG, has a central role in mediating endocytosis, phagocytosis and macrophage activation. We are investigating early steps in FcγRI-linked signal transduction events using the human monocytic cell line, U937, which can be differentiated into a more functional macrophage-like cell type by treatment with dibutyryl cAMP (dbcAMP). Using confocal ratio imaging of cells co-loaded (by AM-ester incubation) with two Ca^{2+} indicators, Fluo3 and Fura-Red, we found 81% of all cells responded to cross-linking IgG-occupied FcγRI (with goat anti human IgG (0.5 mg/ml))with a rise in $[Ca^{2+}]_i$. Undifferentiated cells showed a simple spike lasting 34-63s whereas 44% of dbcAMP-treated cells gave Ca^{2+} oscillations (mean period 19.5s, mean duration 73s). Experiments using Fura2-loaded U937 cells gave similar results but indicated serious limitations of this two dye ratio method. Patch clamp experiments showed FcγRI-triggered activation of a non-selective cation channel in both undifferentiated and differentiated cells but only the latter showed a Ca^{2+} selective current, activated by Ca^{2+} store depletion (I_{crac}), which is required for the maintainance of IP_3-sensitive stores at rest and also for prolonged Ca^{2+} oscillations. Our results indicate fundamental modulations in the Ca^{2+} signalling of U937 cells upon differentiation into a more macrophage-like state.

Tu-Pos522

ISOLATION OF MULTIPLE REGULATORS OF XENOPUS OOCYTE $[CA^{2+}]_i$ FROM THAPSIGARGIN-ACTIVATED MAMMALIAN CELLS. ((H.Y.Kim, D.Thomas, N. Sasakawa, and M. Hanley)) Dept. of Biological Chemistry, UCD School of Medicine, Davis CA 95616-8635.

Depletion of calcium stores in Jurkat T-lymphocytes has been reported to generate a novel messenger, Calcium Influx Factor, with' *extracellular* activity in stimulating calcium entry (Randriamampita & Tsien, Nature 364, 809 (1993)), but communication between calcium stores and activation of calcium entry predicts an *intracellular* mediator. *Xenopus laevis* oocytes have been microinjected with extracts from resting and activated Jurkat cells to test for intracellular regulators of cytosolic $[Ca^{2+}]$ using currents under voltage-clamp. *Xenopus* oocytes are uniquely suited to this purpose because they do not generate a positive calcium signal in response to thapsigargin (TG); a SERCA pump inhibitor giving sustained depletion of calcium stores. Acid extracts of TG-activated Jurkat cells revealed both an intracellular and extracellular activity stimulating $[Ca^{2+}]$-dependent currents. The factors responsible for these activities could be distinguished in that intracellular activity was abolished by alkaline phosphatase treatment, and extracellular activity was not. Partially purified fractions revealed unexpected complexity on gel filtration. At least three fractions have been identified activating $[Ca^{2+}]$-dependent Cl^- currents- 1: a protein fraction ; 2: a fraction (approx. 700 daltons) active both intracellularly and extracellularly; and 3: a fraction (approx. 400 daltons) active only intracellularly. The intracellular activity of Fraction 2 is absent from resting cells and elevated by TG treatment whereas Fraction 3 is present at the same levels in resting and TG-treated cells.

Tu-Pos523

REVERSAL OF GTP-INDUCED Ca^{2+} TRANSLOCATION BY LONG-CHAIN FATTY ACYL CoA ESTERS: EVIDENCE FOR A GTP-ACTIVATED PREFUSION EVENT. ((K.E. Rys-Sikora and D.L. Gill)) Department of Biological Chemistry, University of Maryland School of Medicine, Baltimore, MD 21201.

A specific and sensitive GTP-activated translocation process mediates transfer of Ca^{2+} between $InsP_3$-releasable and $InsP_3$-insensitive Ca^{2+} pools. The actions of CoA and fatty-acyl CoA derivatives on GTP-mediated Ca^{2+} translocation were investigated since fatty acylation can modify G protein-mediated events. Palmitoyl-CoA (PCoA) completely blocked GTP-mediated Ca^{2+} release from ER within permeabilized DDT$_1$MF-2 smooth muscle cells, Ca^{2+} pump-loaded with $^{45}Ca^{2+}$. The EC_{50} PCoA was 0.5 μM. Palmitoyl- and myristoyl-CoA were equally effective; longer and shorter length fatty-acyl CoA molecules were less effective, acetyl-CoA was without effect. CoA itself inhibited GTP-mediated Ca^{2+} release; the ATP-dependence of this effect revealed it required acylation via fatty acyl-CoA synthetase. This was confirmed by the lack of effect of desulfo-of CoA. The nonhydrolyzable myristoyl-CoA analog, *S*-(2-oxopentadecyl)-CoA, blocked the GTP effect identically to myristoyl- and palmitoyl-CoA (IC_{50} = 0.5 μM); thus, fatty acyl transfer is not required indicating that blockade is due to a direct allosteric modification of a component of the GTP-activated process by acyl-CoA esters. Palmitoyl-CoA not only inhibited but completely *reversed* GTP-activated Ca^{2+} release resulting in the released Ca^{2+} being taken back up into pools. In the presence of oxalate, GTP-activated Ca^{2+} transfer results in a substantial increase in Ca^{2+} accumulation; palmitoyl-CoA also completely reversed this effect resulting in rapid termination of Ca^{2+} uptake. This reversal provides strong evidence that GTP-activated Ca^{2+} translocation does not reflect a membrane fusion event. Instead, it likely represents formation of a reversible junction or pore between organelles which may be a required prefusion event. Interestingly, palmitic acid in the 10-100 μM itself had a major effect on Ca^{2+} accumulation, but only in the presence of GTP. This effect appears similar to that of oxalate and may indicate passage of palmitate into a anion-permeable Ca^{2+} subpool wherein an insoluble Ca^{2+}-palmitate complex is formed. This effect may reflect a major physiological role for fatty acids in stabilizing Ca^{2+} within the lumen of Ca^{2+} pools. (NIH grant NS19304; NSF grant DCB 9307746).

Tu-Pos524

GABA RHO$_1$-SUBUNIT REGULATED BY INTRACELLULAR SIGNALLING SYSTEM IN *XENOPUS* OOCYTES

(Yunfei Huang & Luo Lu) Department of Physiology & Biophysics, Wright state university school of medicine, Dayton, OH 45435

Protein phosphorylation is regarded as a primary mechanism for modulation of neuronal function. There are multiple putative consensus sites for protein phosphorylation by cAMP-dependent protein kinase (PKA) or protein kinase C (PKC) in the major intracellular domain in GABA receptor/channels. Phosphorylation induced by PKC results in down-modulation of $GABA_A$ receptor and several specific amino acid residues were found to be involved in phosphorylation in some subunits. We have characterized the GABA ρ_1-subunit, isolated from human retina cDNA library by PCR and subcloned in PCR-3 vector, at single channel level expressed in *Xenopus* oocytes. Single channel conductance was 34.0±0.50 pS, which differs from $GABA_C$ receptor (7 pS) reported from rat retina. Single channel current was activated by trans-aminocrontonic acid and blocked by picrotoxin, and was insensitive to bicuculline. Our results are consistent with its pharmacological profile at whole-cell level. We further studied the regulation of the ρ_1-subunit by intracellular second messenger systems. Whole-cell currents evoked by 5 μM GABA were recorded before and after exposure to 50 nM PMA (*4β-phorbol 12-myristate 13-acetate*), an activator of PKC. Time course of GABA-mediated current revealed that suppression of current amplitude was observed 10 min after application of PMA, which occurred gradually following increases of exposure time. The total current was suppressed to 13.3± 54% and 44.4±4.3% at 10 min and 30 min, respectively. Effects of PMA was a slow processing and irreversible, which indicates that a complicated intracellular signaling system involves the regulation of the receptor/channel.

Tu-Pos525

Nicotinic Acid Adenine Dinucleotide Phosphate: A novel calcium release messenger in sea urchin eggs. ((E.Chini[1], C.Perez[2], K.Beers[1], D.E.Clapham[2] and T.P. Dousa[1])).[1]Department of Physiology and [2]Department of Pharmacology, Mayo Clinic and Mayo Foundation, Rochester, MN, 55904.

Release of calcium (Ca^{2+}) from intracellular stores is an important component in several signalling pathways, including egg fertilization. In sea urchin eggs, we found that in addition to the inositol 1,4,5-trisphosphate ($InsP_3$) and cyclic ADP-ribose (cADPr)-induced Ca^{2+} release, a third mechanism for Ca^{2+}-release was regulated by nicotinic acid adenine dinucleotide phosphate (NAADP). In sea urchin egg homogenates, NAADP elicited Ca^{2+} release in a dose dependent manner(EC_{50}=20 nM). NAADP-induced Ca^{2+} was not inhibited by heparin, (a competitive inhibitor of $InsP_3$), by ruthenium red, spermine, blockers of ryanodine-induced Ca^{2+} release, or by 8-NH_2-cADPr a competitive inhibitor of cADPR. Confocal laser scanning microscopy in fluo-3 loaded eggs showed that the microinjection of NAADP produced a rapid rise in intracellular Ca^{2+} that spread from the site of injection to the rest of the cell. NAADP-induced Ca^{2+} release may represent a novel Ca^{2+} release mechanism in some cells.

Tu-Pos526

INFERENCES ABOUT SUBMEMBRANE CA^{2+} CHANGES USING ANALYSIS OF CA^{2+} DEPENDENT K^+ CURRENTS IN ADRENAL CHROMAFFIN CELLS. ((M. Prakriya, C.R. Solaro, and C.J. Lingle)) Department of Anesthesiology, Washington University School of Medicine, St. Louis, MO 63110.

Theoretical arguments predict that $[Ca^{2+}]_i$ may briefly reach tens or even hundreds of micromolar near Ca^{2+} channels during Ca^{2+} influx. Evidence for this view remains limited due to limitations in the spatial and dynamic ranges of methods used to monitor free $[Ca^{2+}]_i$. Here, we have used large conductance Ca^{2+}-dependent potassium (BK) channels in rat adrenal chromaffin cells to assay changes in submembrane $[Ca^{2+}]$. We compared the fractional activation and inactivation rates of BK currents recorded in perforated, patch-clamped cells with those measured at defined $[Ca^{2+}]_i$ both in single channel and dialyzed cell recordings. Ca^{2+} influx during short depolarizing steps caused submembrane $[Ca^{2+}]$ to reach 10 - 20 μM. With longer depolarizing steps (≥ 200 msec), submembrane $[Ca^{2+}]$ usually stayed above 1 μM for hundreds of milliseconds after termination of the step (and influx). Increases in extracellular Ca^{2+} exaggerated elevations in submembrane $[Ca^{2+}]$, while introduction of exogenous internal Ca^{2+} buffers dramatically attenuated and prolonged submembrane $[Ca^{2+}]$ elevations. Our results do not suggest strong coupling of BK and Ca^{2+} channels. In addition, the findings are consistent with previous reports suggesting that Ca^{2+}-indicator buffers such as fura-2 markedly misrepresent both the true $[Ca^{2+}]_i$ and the time courses of change in $[Ca^{2+}]_i$.

Tu-Pos527

PURINOCEPTOR-MEDIATED Ca^{2+}-SIGNALLING IN HUMAN B-LYMPHOCYTES ((M. Löhn and F. Markwardt)) Julius Bernstein Institute for Physiology, Martin Luther University Halle, Germany

ATP-induced membrane currents and intracellular calcium ion concentration (Ca^{2+}_i) were measured simultaneously in Epstein-Barr-Virus-transformed human B-lymphocytes by means of the tight-seal voltage-clamp- und FLUO-3/FURA-red-fluorescence-technique. During bath application of ATP, the membrane conductance of the B-cells was increased within less than 100 ms to a level which was constant for at least 1 min. Blockade of G-proteins by intracellular GDP-ß-S was without effect on the ATP-induced membrane permeabilization. The dose-response-relationships for ATP^{4-}- and ADP^{3-}-elicited membrane currents (I_P) revealed the involvement of P_{2Z}-purinoceptors in the observed effects. The permeability sequence for I_P carrying cations is $P_{Ca}:P_K:P_{Cs}:P_{Na}:P_{TRIS}$ = 35:2:1.2:1:0.1 as calculated by the Goldmann-Hodgkin-Katz current equation. The increase in Ca^{2+}_i after ATP-application was small in physiological extracellular solutions but obvious if extracellular Na^+ was replaced by $choline^+$. This may reflect the involvement of a Na-Ca-exchange mechanism rapidly extruding Ca^{2+} after ATP-induced Ca^{2+}-influx. (Supported by Fritz-Thyssen-Stiftung, 9.26/90 and DFG, Ma 1581/2-1).

Tu-Pos528

ELEVATION OF INTRACELLULAR CALCIUM BY GROWTH HORMONE RELEASING HORMONE (GRF) IN ANTERIOR PITUITARY CELLS. ((L. Polo-Parada and S. J. Korn)) Physiology and Neurobiology, Univ. Connecticut, Storrs, CT 06269

Stimulation of growth hormone secretion from pituitary somatotrophs by GRF is accompanied by elevation of intracellular calcium concentration ([Ca]). [Ca] elevation appears to occur primarily due to influx of extracellular Ca through the plasma membrane. Our present studies are directed at understanding the mechanism by which GRF elevates [Ca]. Anterior pituitary cells were isolated from 125-200 g rats and used 4 hours to 1 week after dissociation. Cells were loaded with Fura-2 for detection of changes in [Ca], and placed in a bathing solution containing 10 mM Ca. Application of GRF for 1-2 min to this heterogenious cell population resulted in [Ca] elevation in 17% of cells. Application for 2-5 min resulted in [Ca] elevation in 43% of cells. Of these, 58% responded to the first application. 42% of responders did not respond to the first application but responded to subsequent applications. Once a cell responded, it responded to subsequent applications. GRF produced 3 types of Ca elevation response. In 28% of cells, [Ca] rose and fell during the GRF application. In 58% of cells, GRF produced a biphasic response; [Ca] rose in a sharp peak and then leveled off to a plateau level for the duration of GRF application. In 14% of cells, [Ca] rose to a plateau with no evidence of an early peak. The effects of GRF were examined on voltage-gated Ca channel currents with standard whole cell patch clamp recordings. In thoroughly dialyzed cells, GRF potentiated Ca currents, which suggests that GRF action did not require a soluble second messenger. *Supported in part by NSF, the Whitaker Found., the UCONN Res. Found. and the Pharmaceutical Manufacturers Assoc. Found.*

Tu-Pos529

CALCIUM DIFFUSION COEFFICIENT IN *MYXICOLA* AXOPLASM ((N. F. Al-Baldawi and R. F. Abercrombie)) Department of Physiology, Emory University, Atlanta, GA 30322.

The Ca diffusion coefficient was measured in *Myxicola* axoplasm by two techniques, one using ^{45}Ca and the other using Ca-specific mini-electrodes. A coefficient of ~ 0.1 x 10^{-6} cm^2s^{-1} was obtained by the electrode technique in axoplasm with Ca-sequestering organelles intact. A slightly higher coefficient (0.4 x 0^{-6} cm^2s^{-1}) found for the same condition with the ^{45}Ca technique was attributed to possible active migration of the ^{45}Ca-sequestering organelles. Free Ca averaged 0.7 ± 0.4 μM for both techniques. With ATP-depleted axoplasm, diffusion coefficients of 0.4 to 1 x 10^{-6} cm^2s^{-1} were obtained by isotope and electrode techniques (Ca^{2+} = 0.8 μM). In organelle-free axoplasm with a protein concentration roughly half that in the intact axoplasm, diffusion coefficients of 1.4 to 3 x 10^{-6} cm^2s^{-1} were measured at 0.7 μM Ca^{2+} and 7 x 10^{-6} cm^2s^{-1} at 3-5 μM Ca^{2+}. Comparing the free Ca diffusion coefficient of 8 x 10^{-6} cm^2s^{-1} to the values of 0.4 to 1 x 10^{-6} cm^2s^{-1} in ATP-depleted axoplasm and the axoplasmic buffering capacity (Δ bound Ca/Δ free Ca ~ 50) previously measured (*Biophys. J.* 66: 55a) under the same conditions, leads to the conclusion that some of the calcium buffer capacity must be located on mobile Ca binding sites. Supported by NIH NS-19194.

Tu-Pos530

INVOLVEMENT OF MITOCHONDRIA IN INTRACELLULAR CALCIUM SEQUESTERING IN RAT GONADOTROPES. ((S. Hehl, A. Golard, B. Hille)), Dept. of Physiology & Biophysics, Univ. of Washington, Seattle, WA 98195
(Spons. by A.M. Gordon)

We used the whole-cell patch-clamp technique in conjunction with indo-1 photometry to study calcium dynamics in rat gonadotropes identified with the reverse hemolytic plaque assay. The cells were dialyzed with 100 μM indo-1 in the patch-pipette, held at -80 mV and depolarized to +10 mV for 0.5 - 5 s to impose a Ca^{2+} load . Extracellular application of the mitochondrial uncoupler CCCP (2 μM) produced a reversible rise in the resting Ca^{2+} concentration by 54 ± 16 % (mean ± S.E.M., n=9). Furthermore CCCP reversibly increased the amplitude of the depolarization-induced Ca^{2+} transients by 30 ± 19 % (n=9). CCCP had little effect on the kinetics of small Ca^{2+} transients (< 150 nM, n=5). However, the decay of larger transients was slowed (n=4). In comparison to rat adrenal cromaffin cells the contribution of mitochondria in the intracellular Ca^{2+} dynamics in rat gonadotropes seems to be smaller. However our data indicate that mitochondria do play a role in Ca^{2+} homeostasis during large Ca^{2+} transients similar to those induced by GnRH in these cells.

Supported by NIH (HD 12629), Deutsche Forschungsgemeinschaft (He 2345/1-1 to S.H.) and Mellon Foundation (to A.G.) .

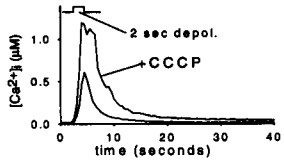

Tu-Pos531

DOMINANT ROLE OF MITOCHONDRIA IN CALCIUM CLEARANCE FROM RAT ADRENAL CHROMAFFIN CELLS. ((J. Herrington, Y.B. Park, D.F. Babcock and B. Hille)) Dept. Physiology & Biophysics, Univ. of Washington, Seattle, WA 98195.
(Spon. by M.S. Shapiro).

Mechanisms of intracellular calcium (Ca^{2+}_i) clearance of rat chromaffin cells (CCs) were studied with fluorescence photometry of CCs loaded with indo-1 (100 μM) through the whole-cell recording pipette. Rates of Ca^{2+}_i clearance at -80 mV were extracted from the decay of Ca^{2+}_i transients produced by Ca^{2+} influx during 0.1-2 sec depolarizations to +10 mV in 10 mM external Ca^{2+}. We expected at least four mechanisms could contribute to Ca^{2+}_i clearance: extrusion from the cell by plasma membrane Na/Ca exchange (NCE) and the Ca^{2+}-ATPase (PMCA) and uptake by endoplasmic reticular stores (SERCA) and mitochondria (MITO). Rates were measured by isolating each mechanism using combinations of the following agents, with their expected targets: Na^+ substitution with Li^+ or TEA (NCE), La^{3+} (1 mM) applied after the depolarization (NCE and PMCA), thapsigargin (1 μM) (SERCA) and CCCP (2 μM) (MITO). Using this approach, we did not detect a significant contribution by SERCA uptake. Assuming first-order kinetics, the measured rate constants (κ) and the $[Ca^{2+}]_i$ where the rate equals zero (0 κ $[Ca^{2+}]_i$) for the three other mechanisms are:

	κ (sec^{-1}) (± SE)	0 κ $[Ca^{2+}]_i$ (nM)
MITO	0.70 ± 0.12 (n = 8)	368 ± 23
PMCA	0.12 ± 0.01 (10)	131 ± 21
NCE	0.08 ± 0.01 (12)	197 ± 42

Overall, we conclude that mitochondria play a dominant role in determining the time course of Ca^{2+}_i transients in rat CCs when Ca^{2+}_i rises above ~400 nM.

Supported by AR 17803 and the W. M. Keck Foundation.

Tu-Pos532

CALCIUM HOMEOSTASIS IN RAT ADRENAL CHROMAFFIN CELLS. ((Y.B. Park, J. Herrington and B. Hille)), Dept. of Physiology & Biophysics, U. of Washington, Seattle, WA 98195.

We studied $[Ca^{2+}]_i$ clearance mechanisms of rat adrenal chromaffin cells, measuring slow tail currents through small-conductance Ca^{2+}-activated K^+ (SK) channels and $[Ca^{2+}]_i$ transients using indo-1 photometry following depolarization-induced Ca^{2+} entry. The time course of K^+ tail currents was little affected by removal of external Na^+. External La^{3+} or eosin slowed the decay of tail currents and rapid perfusion of alkaline bath solution (pH 8.0) following depolarization had little effect on the initial decay of tail currents, but the late phase was much slowed, indicating contribution of plasma membrane Ca^{2+}-ATPase. Thapsigargin and BHQ had little effect on $[Ca^{2+}]_i$ transients. In the presence of the mitochondrial uncoupler CCCP (2 μM), the decay of tail currents and $[Ca^{2+}]_i$ transients following large Ca^{2+} loads (0.2-2 s depolarizations) was dramatically slowed and antimycin and oligomycin had similar effects. These mitochondrial inhibitors had little effect with small Ca^{2+} loads. Intracellular ruthenium red (20 μM) had similar slowing effects on Ca^{2+} clearance and CCCP was much less effective with ruthenium red in the pipette. In the presence of CCCP, removal of external Na^+ slowed the decay of $[Ca^{2+}]_i$ transients. These data suggest mitochondria are important in clearing physiological Ca^{2+} loads in rat chromaffin cells, and Na/Ca exchange and plasma membrane Ca^{2+}-ATPase are also involved in the removal of Ca^{2+}_i.

Supported by AR 17803, NS 08174, and W.M.Keck Foundation.

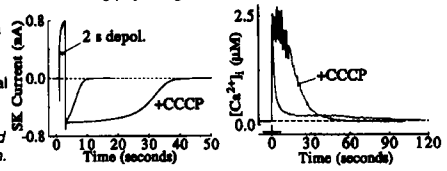

Tu-Pos533

MITOCHONDRIAL CA^{2+} UPTAKE DURING HORMONAL STIMULATION IN INTACT LIVER CELLS AND ITS IMPLICATION FOR THE MITOCHONDRIAL PERMEABILITY TRANSITION. ((J.B. Hoek and X. Wang)) Department of Anatomy, Pathology and Cell Biology, Thomas Jefferson University, Philadelphia, PA. 19107.

Hormones that elevate cytosolic $[Ca^{2+}]$ often use Ca^{2+} to activate intramitochondrial processes. Mitochondrial Ca^{2+} uptake also activates the mitochondrial permeability transition (MPT), the formation of a high conductance pore across the inner and outer membrane. We used isolated hepatocytes to study how elevation of $[Ca^{2+}]_c$ affects mitochondrial Ca^{2+} content ($[Ca^{2+}]_m$) and their susceptibility to undergo the MPT. Cells were treated with vasopressin, glucagon, or thapsigargin prior to permeabilization with digitonin. $[Ca^{2+}]_m$ was determined from the ionomycin-induced Ca^{2+} release in permeabilized cells and the MPT was measured as the cyclosporin A-sensitive light scattering change induced by phenylarsenoxide and rotenone. Agents that elevated $[Ca^{2+}]_c$ promoted mitochondrial Ca^{2+} uptake. A marked $[Ca^{2+}]_m$ increase (> 10-fold over basal) was caused by a combination of vasopressin and glucagon or in thapsigargin-treated cells. These conditions also induced a marked increase in rotenone-induced mitochondrial swelling. However, vasopressin alone did not enhance mitochondrial swelling, but instead partly suppressed swelling even in thapsigargin-treated cells. These effects were mimicked by phorbol ester, suggesting a role for protein kinase C. Thus, an increase in $[Ca^{2+}]_m$ following $[Ca^{2+}]_c$ elevation enhances the susceptibility to the MPT. However, hormones also activate protective responses in the cell that suppress the MPT.

Tu-Pos534

MITOCHONDRIA CONTRIBUTE TO Ca^{2+} REMOVAL IN SMOOTH MUSCLE CELLS ((R.M. Drummond, J.V. Walsh Jr., and F.S. Fay)) Department of Physiology, Univ. Massachusetts Med. Center, Worcester, MA01605.

There is increasing evidence that mitochondria are capable of sequestering significant amounts of Ca^{2+} during physiological levels of stimulation. We have examined the effect of mitochondrial inhibitors on the ability of cells to recover from the increase in cytosolic $[Ca^{2+}]$ ($[Ca^{2+}]_i$) induced by either a short or more prolonged period of stimulation. Freshly isolated smooth muscle cells from the stomach of *Bufo marinus* were loaded with the ratiometric Ca^{2+} indicator Fura-2 and then studied using tight-seal, whole cell recording. $[Ca^{2+}]_i$ was increased either by a single 300 msec depolarizing pulse to +10 mV or a 7.5 sec train of depolarizations (-110 mV to +10 mV; 2 pulses sec^{-1}) and Ca^{2+} removal was then examined following repolarization to the holding potential of -110 mV. In control cells, the rate of Ca^{2+} removal following the train of depolarizations was enhanced by approximately 30%, compared to the rates observed after the single pulse (Science 244; 211-214). When cells were treated with the mitochondrial uncoupler FCCP, rates of Ca^{2+} removal following the single pulse were slightly reduced compared to controls, whilst following the train the increased rate of Ca^{2+} removal normally observed was prevented. Similar results were obtained with the respiratory chain inhibitors cyanide and azide. Since the pipette solution contained 3.6 mM ATP, it seems unlikely that ATP production is the rate limiting process. Rather, we propose that mitochondria sequester Ca^{2+} from the cytosol, thereby influencing restoration of the $[Ca^{2+}]_i$ following stimulation. Since mitochondria are not believed to function as long term storage sites for Ca^{2+}, the Ca^{2+} which they accumulate must be extruded during periods of cellular quiescence. In an attempt to determine where this Ca^{2+} goes to, we have examined the subcellular distribution of mitochondria using antibodies directed against an inner membrane epitope. Mitochondria are primarily located around the periphery of the cell, in close proximity to the sarcoplasmic reticulum which may serve as the long term storage site for Ca^{2+} taken up by mitochondria following stimulation. Supported by an AHA Fellowship (RMD) and NIH HL14523 and HL 47530 (FSF).